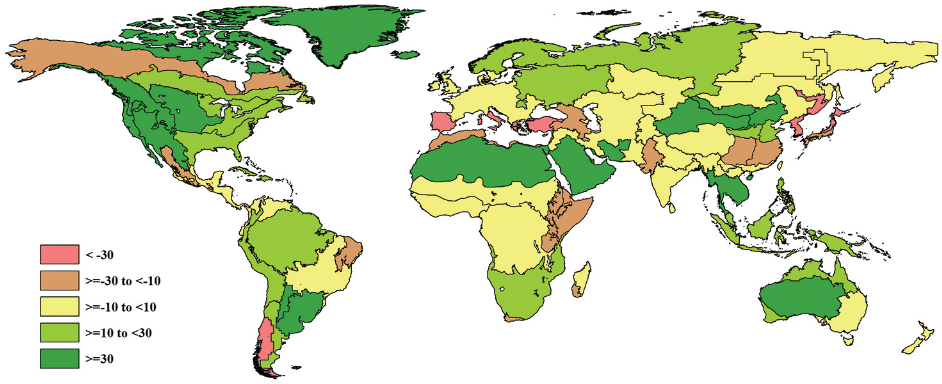

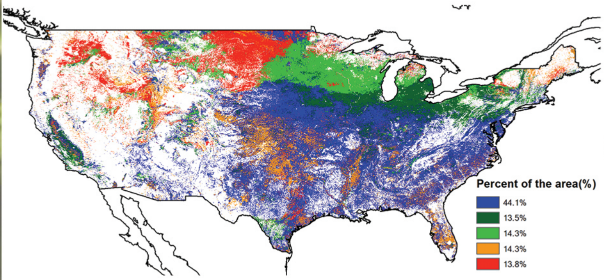

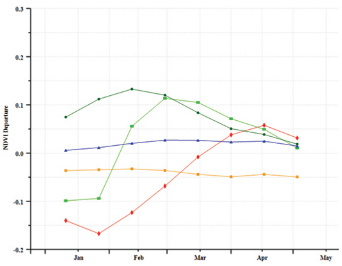

CropWatch bulletin

QUARTERLY REPORT ON GLOBAL CROP PRODUCTION

Monitoring Period: January - April 2017

May 31, 2017

Volume 17, No. 2 (Total No. 105)

Institute of Remote Sensing and Digital Earth (RADI)
Chinese Academy of Sciences (CAS)

May 2017

Institute of Remote Sensing and Digital Earth (RADI), Chinese Academy of Sciences
P.O. Box 9718-29, Olympic Village Science Park
West Beichen Road, Chaoyang
Beijing 100101, China

This bulletin is produced by the CropWatch research team at the Digital Agriculture Division, Institute of Remote Sensing and Digital Earth (RADI), Chinese Academy of Sciences, under the overall guidance of Professor Bingfang Wu.

Contributors are Jose Bofana, Sheng Chang, Bulgan Davdai, Mohammed Ahmed El-Shirbeny, René Gommes, Zhaoxin He, Mingyong Li, Olipa Lungu, Zonghan Ma, Elijah Phiri, Battestseg Tuvdendorj, Shen Tan, Fuyou Tian, Linjiang Wang, Meiling Wang, Bingfang Wu, Qiang Xing, Jiaming Xu, Nana Yan, Mingzhao Yu, Hongwei Zeng, Miao Zhang, Xin Zhang, Dan Zhao, Xinfeng Zhao, Liang Zhu and Weiwei Zhu.

Thematic contributors for this bulletin include: Wenjiang Huang (huangwj@radi.ac.cn) and Yingying Dong (dongyy@radi.ac.cn) for the section on pest and diseases monitoring; and Fengying Nie (niefengying@sohu.com) and Xuebiao Zhang (zhangxuebiao@caas.cn) for the section on food import and export outlook for 2017. English version editing was provided by Anna van der Heijden.

Corresponding author: Professor Bingfang Wu
Institute of Remote Sensing and Digital Earth, Chinese Academy of Sciences
Fax: +8610-64858721, E-mail: **cropwatch@radi.ac.cn**, **wubf@radi.ac.cn**

CropWatch Online Resources: This bulletin along with additional resources is also available on the CropWatch Website at http://www.cropwatch.com.cn.

Contents

Ⓘ *Note:* CropWatch resources, background materials and additional data are available online at www.cropwatch.com.cn.

LIST OF TABLES

LIST OF FIGURES

Abbreviations

5YA	Five-year average, the average for the four-month period for January-April from 2012 to 2016; one of the standard reference periods.
15YA	Fifteen-year average, the average for the four-month period from January-April from 2002 to 2016; one of the standard reference periods and typically referred to as “average.”
BIOMSS	CropWatch agroclimatic indicator for biomass production potential
BOM	Australian Bureau of Meteorology
CALF	Cropped Arable Land Fraction
CAS	Chinese Academy of Sciences
CWAI	CropWatch Agroclimatic Indicator
CWSU	CropWatch Spatial Units
DM	Dry matter
EC/JRC	European Commission Joint Research Centre
ENSO	El Niño Southern Oscillation
FAO	Food and Agriculture Organization of the United Nations
GAUL	Global Administrative Units Layer
GVG	GPS, Video, and GIS data
ha	hectare
kcal	kilocalorie
MPZ	Major Production Zone
MRU	Monitoring and Reporting Unit
NDVI	Normalized Difference Vegetation Index
OISST	Optimum Interpolation Sea Surface Temperature
PAR	Photosynthetically active radiation
PET	Potential Evapotranspiration
RADI	CAS Institute of Remote Sensing and Digital Earth
RADPAR	CropWatch PAR agroclimatic indicator
RAIN	CropWatch rainfall agroclimatic indicator
SOI	Southern Oscillation Index
TEMP	CropWatch air temperature agroclimatic indicator
Ton	Thousand kilograms
VCIx	CropWatch maximum Vegetation Condition Index
VHI	CropWatch Vegetation Health Index
VHIn	CropWatch minimum Vegetation Health Index
W/m^2	Watt per square meter

Bulletin overview and reporting period

This CropWatch bulletin presents a global overview of crop stage and condition between January and April 2017, a period referred to in this bulletin as the JFMA (January, March, April, May) period or just the "reporting period." The bulletin is the 105th such publication issued by the CropWatch group at the Institute of Remote Sensing and Digital Earth (RADI) at the Chinese Academy of Sciences, Beijing.

CropWatch analyses and indicators

CropWatch analyses are based mostly on several standard as well as new ground-based and remote sensing indicators, following a hierarchical approach. The analyses cover large global zones; major producing countries of maize, rice, wheat, and soybean; and detailed assessments for 30 major agricultural countries and Chinese regions. In parallel to an increasing spatial precision of the analyses, indicators become more focused on agriculture as the analyses zoom in to smaller spatial units.

CropWatch uses two sets of indicators: (i) agroclimatic indicators—RAIN, TEMP, and RADPAR, which describe weather factors; and (ii) agronomic indicators—BIOMSS, VHIn, CALF, and VCIx, describing crop condition and development. Importantly, the indicators RAIN, TEMP, RADPAR, and BIOMSS do not directly describe the weather variables rain, temperature, radiation, or biomass, but rather they are spatial averages over agricultural areas, which are weighted according to the local crop production potential. For each reporting period, the bulletin reports on the *departures* for all seven indicators, which (with the exception of TEMP) are expressed in relative terms as a percentage change compared to the average value for that indicator for the last five or fifteen years (depending on the indicator). For more details on the CropWatch indicators and spatial units used for the analysis, please see the quick reference guide in Annex C, as well as online resources and publications posted at www.cropwatch.com.cn.

This bulletin is organized as follows:

Chapter	Spatial coverage	Key indicators
Chapter 1	World, using Monitoring and Reporting Units (MRU), 65 large, agro-ecologically homogeneous units covering the globe	RAIN, TEMP, RADPAR, BIOMSS
Chapter 2	Major Production Zones (MPZ), six regions that contribute most to global food production	As above, plus CALF, VCIx, and VHIn
Chapter 3	30 key countries (main producers and exporters)	As above plus NDVI and GVG survey
Chapter 4	China	As above plus high resolution images; information on pests and diseases; and food import/export outlook
Chapter 5	Production outlook, disaster events, and an update on El Niño.	

Regular updates and online resources

The bulletin is released quarterly in both English and Chinese. To sign up for the mailing list, please e-mail cropwatch@radi.ac.cn or visit CropWatch online at www.cropwatch.com.cn. Visit the CropWatch Website for additional resources and background materials about methodology, country agricultural profiles, and country long-term trends.

Executive summary

The current CropWatch bulletin is based mainly on remotely sensed data. It focuses on crops that were either growing or harvested between January and April 2017. The bulletin covers prevailing weather conditions, including extreme factors, as well as crop condition and size of cultivated areas, paying special attention to the major worldwide producers of maize, rice, wheat, and soybean. The bulletin also describes the current crop condition and prospects in China and presents a first global production estimate for crops to be harvested throughout 2017. The estimated production is based on partial data and will be updated in the next two CropWatch 2017 bulletins.

Global agroclimatic conditions

Compared with previous CropWatch bulletins, the current reporting period does not identify very large (continent-wide) anomalies, and their intensity is mostly not very severe. There were, nevertheless, some areas with abnormal conditions that affect several contiguous MRUs (Mapping and Reporting Units, the largest CropWatch monitoring units), starting with below average rainfall in the winter crop areas in Eastern Asia and in the Mediterranean basin (where the biomass production potential fell 20 to 30%). In East Africa, the El Niño induced drought persisted in some areas that had not recovered yet from the 2016 drought, a situation exacerbated by a refugee crisis stemming from a combination of environmental stress and conflict.

Excess precipitation is reported from (i) northern China and Mongolia and adjacent areas, (ii) continental Southeast Asia to parts of Australia across maritime Southeast Asia, (iii) much of North America and, especially, from the two areas of (iv) South Africa, mostly in Zimbabwe and Mozambique, and (v) north-western South America (Ecuador, Colombia, and Peru) where excess precipitation started in December 2016, lasting for months and severely affecting millions of people with damage amounting to billions of US dollars.

Much of North America also recorded above average temperature and below average sunshine in major agricultural areas. At the time of reporting, the CropWatch indicator for cropped arable land fraction (CALF) reaches 47% for this region, which is 5 percentage points above the average of the previous five years, while the maximum Vegetation Condition Index (VCIx) is also satisfactory (0.85). VCIx is lowest in central Europe and western Russia (0.65) where, in addition, CALF dropped to 72%, 8 percentage points below the five-year average. The largest VCIx drop occurred in West Africa (-13%).

Production outlook

The final outcome of the 2017 season will depend on agroclimatic conditions up to the end of the year. It is, therefore, crucial to note that the occurrence of another El Niño during 2017, the likelihood of which is currently put at 50%, may dramatically alter the current outlook in South America, South and Southeast Asia, and the Horn of Africa, which are some of the areas directly under the influence of El Niño.

The current global production estimates for 2017 of the major commodities amount to 730 million tons of wheat (representing a 1% drop below 2016 production), 761 million tons of rice (up 3%), 305 million tons of soybeans (down 3%), and 1056 million tons of maize (up 5% over 2016). The major producers—defined as the countries that together produce 80% of the various commodities—contribute 622 million tons of wheat (-1%), 685 million tons of rice (+3%), 282 million tons of soybeans (-4%), and 936 million tons of maize (+6% compared to 2016). The share of the “minor producers” to the global production is 8% (soybean) to 15% (maize), and about 10% for rice and wheat.

For wheat production, in agreement with the above-mentioned agroclimatic and agronomic indicators for Russia, wheat production is currently put 18% below last year’s output. Relative production drops are also listed for Iran, Kazakhstan, Romania, and Turkey (in a range from -26% to -11%), as well as the United States with a smaller drop of 4%.

For rice production, most important Asian rice producers are also expected to do well, with the Philippines being the only major producer in the region that undergoes a decrease (-5%). The country is one of the major rice importers.

For soybean production, Argentina remains at the level of 2016 and Brazil is up 5%. For the global output, which is trend-based for all other countries, production drops among most minor producers, continuing a trend that has lasted for several years now. If it should continue in the future, it would exacerbate the current situation of “three producers and one buyer.”

Finally, for maize, CropWatch puts China at 212 million tons (+6%) and the United States at 383 million tons (+4%). In the southern hemisphere, both Brazil and Argentina did well with outputs of 79 million tons (+13%) and 30 million tons (+16%), respectively.

China

Winter wheat yield is up 2.2% over 2016, with a production forecast at 116 million tons, an increase of just under 2 million tons, equivalent to +1.7%, even if the cropped area dropped 2%, mostly in parts of Anhui and Jiangsu. The largest production increases are observed in Hebei (+4.0%), Shanxi (+5.7%), Shandong (+3.3%), and Henan (+3.9%). The area under rapeseed dropped about 1%, resulting in an overall increase of winter crops production by 1.3%.

In China, positive rainfall anomalies were largest in Inner Mongolia (+60%, accompanied by above-average temperature), while southwest China (-17%), Lower Yangtze (-21%), and southern China (-7%) all recorded a deficit and a reduction in sunshine. CALF was low in the Loess region (-7%) and crop/vegetation condition as assesses by VCIx was just fair or even rather low in Inner Mongolia (0.41). In terms of production, in addition to the already mentioned 6% increase in maize production to reach 212 million tons, rice and wheat (winter and summer crops) are up 2% (to 205 and 121 million tons, respectively), and soybean is down 3%. Since all estimates are trend-based, it is possible that soybean output will increase again, as it did in 2016 for the first time in a decade.

The present bulletin also includes a note on pests and diseases, the impact of which was relatively severe in mid-May 2017 in the main wheat producing regions.

Chapter 1. Global agroclimatic patterns

Chapter 1 describes the CropWatch agroclimatic indicators (CWAIs) for rainfall (RAIN), temperature (TEMP), and radiation (RADPAR), along with the agronomic indicator for potential biomass (BIOMSS) for sixty-five global Monitoring and Reporting Units (MRU). Rainfall, temperature, and radiation indicators are compared to their average value for the same period over the last fifteen years (called the "average"), while BIOMSS is compared to the indicator's average of the recent five years. Indicator values for all MRUs are included in Annex A table A.1. For more information about the MRUs and indicators, please see Annex C and online CropWatch resources at www.cropwatch.com.cn.

1.1 Overview

Connections between variables

A statistical analysis of table A.1 (CWAIs by CropWatch MRU) illustrates the fact that climatic variables and their spatial variations are interconnected. Alongside the climatologically expected correlations such as RAIN-TEMP (more rainfall in tropical areas, r=0.425, N=65) and TEMP-RADPAR (temperature is higher in high sunshine areas), the current reporting period is also characterized by some associations that can be used to add some coherence to the patterns observed in figures 1.1 to 1.4. They include a weak but positive correlation between rainfall departure from average and temperatures departures; that is, excess rainfall is linked to above-average temperature (r=0.339), an observation that has been made repeatedly in the semi-arid tropics and which is consistent with climate change projections. Since we also have a correlation (albeit negative) between TEMP and TEMP anomaly (-0.680), the current period was characterized by major temperature departures in the temperate areas. The same observation was made based on the January-April 2016 data. Finally, with the CropWatch biomass production potential (BIOMSS) being based on rainfall and temperature, a clear association also exists between BIOMSS departures and the departures in RAIN and TEMP, with RAIN variability accounting for just under 90% of the BIOMSS variability, and even more so at low rainfall values. It is also stressed that the reference period for CWAIs is the recent fifteen years, while for BIOMSS it is five.

Figure 1.1. Global map of January-April 2017 rainfall anomaly (as indicated by the RAIN indicator) by MRU, departure from 15YA (percentage)

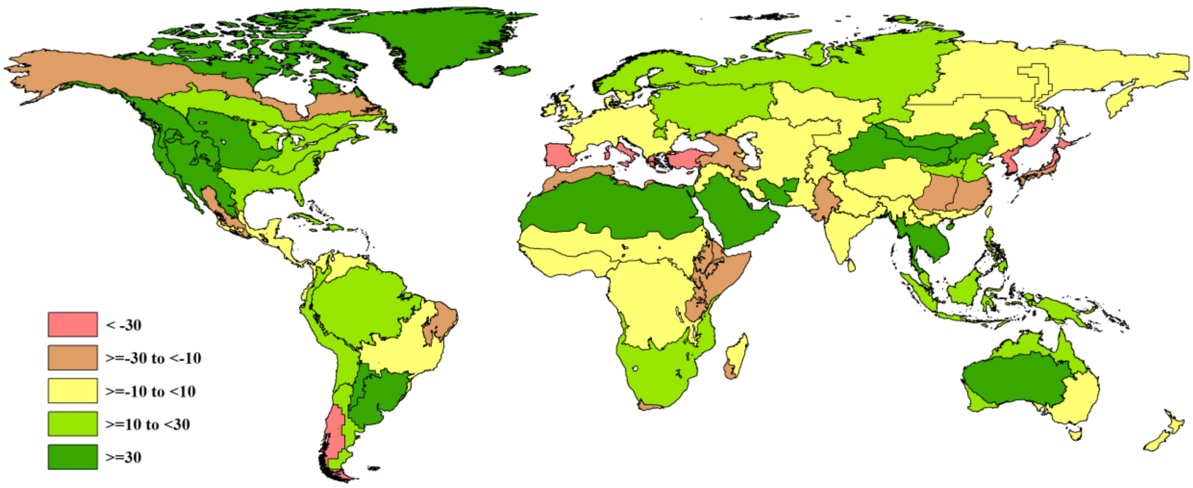

Figure 1.2. Global map of January-April 2017 biomass accumulation (BIOMSS) by MRU, departure from 5YA (percentage)

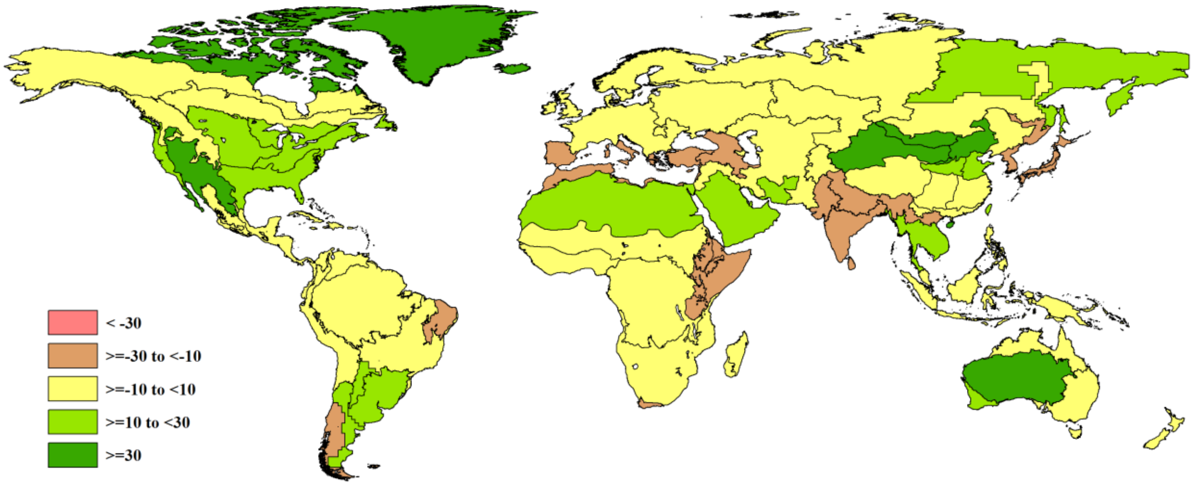

Rainfall and BIOMSS anomalies

Since rainfall and biomass are very directly connected, the BIOMSS anomalies are mentioned where appropriate in this section arranged according to rainfall anomalies. Figures 1.1 and 1.2 present the global maps showing the rainfall (1.1) and BIOMSS (1.2) anomalies over the reporting period.

Last year's May bulletin had identified some typical El Niño-related patterns, some of which persist into the current year and may be related to normal climate persistence (inertia) or to the possibility that 2017 may be another El Niño year (refer to section 5.4 on El Niño). Depending on prevailing climate conditions and the amounts of rainfall actually recorded, the anomalies do not always qualify as "drought" or "floods" as the impact on agriculture also varies as a function of the status of the local crop phenology. Typically, drought during the dormancy phase of winter crops is not immediately threatening crop production if adequate rainfall becomes available at the time when growth starts in spring. The "rainfall history" of the various MRUs also plays a part, of which two typical examples would be (i) abundant rainfall before the reporting period (which would have ensured that sufficient moisture had been stored in the soil before the dry spell) and (ii) even a minor deficit following another deficit period, which can result in disastrous conditions. Such situations are mentioned below.

Negative rainfall anomalies

The largest negative rainfall anomalies (RAIN shortage below -20%) all affect several MRUs and can be grouped into eight clusters. They are characterized by temperature values close to average in the range from -0.7°C (Horn of Africa, MRU-04 and the Caucasus, MRU-29) to +0.9°C (Brazilian Nordeste, MRU-22) or +1.0°C (Eastern Asia, MRU-43).

- *Eastern Asia.* In eastern Asia, where the largest MRU anomalies occurred, areas include the following: East Asia (MRU-43) with just 103 mm of rainfall, corresponding to a -43% deficit (BIOMSS: -18%), Southern Japan (MRU-46, 283 mm or -27%; BIOMSS, -11%), and the Lower Yangtze region in China (MRU-37) where the recorded amount (349 mm) is 21% below average (BIOMSS, -61%). These are winter crop areas where the situation needs close monitoring, which applies as well to summer crops planted now or to be planted, as they may suffer initial soil moisture stress.
- *Mediterranean basin.* The Mediterranean basin includes two MRUs. In the first, Mediterranean Europe and Turkey (MRU-59), 170 mm of rainfall were recorded (RAIN, -34%; BIOMSS: -26%); in the second, North Africa (MRU-07), rainfall was 20% below the average with just 126 mm

(BIOMSS, -17%). In particular the southern Mediterranean has recently experienced drought, as was reported in section 5.2 of the August 2016 bulletin.[1]. For the current season, the driest country in the area was Tunisia.

- *East Africa.* This area covers the Horn of Africa (MRU-04) where RAIN deficits amount to -30% (253 mm) and the East African highlands (MRU-02, 165 mm or -27%). BIOMSS departures are large as well (-22% and -18%, respectively). Some areas, especially pastoral lowlands, were affected by the 2016 El Niño drought and thus suffered a second deficit season at a time when the sequels of the previous drought had not been dispelled yet. The area receives detailed attention in the section on disasters (section 5.2).

The remaining areas are single MRUs, but they often border other deficit areas that may not be immediately apparent because of the large size of the MRUs:

- *Punjab to Gujarat* (MRU-48; RAIN, -19% or 43 mm; BIOMSS: -12%). Although rainfall appears to be "average" at the scale of the MRUs, BIOMSS, due to the shorter and more recent reference period of just five years, appears as below average area, which is probably closer to the actual situation than the situation described by rainfall alone. The MRU is bordered on the east by two large areas with a smaller rainfall deficit, namely the Southern Himalayas (MRU-44; RAIN, -6%) and Southern Asia, which includes all of India (MRU-45; RAIN, -9%), but where BIOMSS decreased more significantly (BIOMSS, -14% and -28% respectively).
- *Caucasus* (MRU-29), which recorded 200 mm (RAIN, -28%; BIOMSS, -14%).
- *Western Cape area in South Africa* (MRU-10), RAIN down 30% with just 78 mm and a BIOMSS drop of 22%.
- *Western Patagonia* (MRU-27, 84 mm of rainfall and 39% below average). This is a mostly pastoral area, and the water shortage has affected summer grazing areas where BIOMSS is down 18%.
- *Brazilian Nordeste* (MRU-22), with a large RAIN deficit (-30%) that nevertheless corresponds to 328 mm. No serious agricultural impact is reported even if BIOMSS fell 21% below average.

Positive rainfall anomalies

Even the largest rainfall excesses were mostly moderate: the 95% percentile corresponds to a +69% anomaly. The four areas listed below are those where the precipitation anomaly exceeds 30%, which is not very significant in low rainfall areas, as even a minor amount of rainfall can easily constitute a doubling. The largest positive departures occur in Asia.

- *Northern China, Mongolia and adjacent areas.* The largest positive departure (RAIN, +309%) occurred in MRU-47 (Southern Mongolia). The total rainfall amount, however, is 109 mm, so that the large excess corresponds to an average rainfall in the order of just 25 mm. The two other MRUs in this group are the two Chinese regions of Inner Mongolia (MRU-35; RAIN, +60%) and Gansu-Xinjiang (MRU-32; +78%). All recorded above average (but still freezing) temperatures (+2.1°C above average in Southern Mongolia). The biomass production potential, which will be brought about by stored soil moisture once low temperatures turn positive, varies between +48% to doubling (+209%) in southern Mongolia where water is normally the dominant limiting factor.
- *Southeast Asia to Australia.* A large region from mainland Southeast Asia (MRU-50; 228 mm and +49%) and Hainan (MRU-33; 206 mm or +52%) across maritime Southeast Asia (where excesses are moderate) to the Australian desert (MRU-63; +39% to reach 134 mm) experienced positive

[1] http://123.56.103.213/htm/en/files/eng16-3-6.pdf.

rainfall anomalies. Temperature was generally below average, while BIOMSS variations (all positive) vary from +18% (MRU-55) to +55% (MRU-33).

- *North America.* On this continent, the area with positive rainfall anomalies includes, from east to west, the Northern Great Plains (MRU-12; RAIN, +37%), British Columbia to Colorado (MRU-11, +38%), Southwest United States and North Mexican highlands (MRU-18, +71%), and the West Coast (MRU-16, +43%). BIOMSS increases amount to +20%, +8%, +32%, and +22%, respectively for these four MRUs, with relatively low values (compared with RAIN) as a result of lower than average temperature, especially in MRU-16.
- *South America.* This area includes MRU-25 (central-north Argentina, with 679 mm of rainfall or +44% over average) and MRU-26 (the Pampas, 768 mm and +34%). BIOMSS increases are more moderate and amount to 15% to 20%.

Temperature and sunshine anomalies

Figures 1.3 and 1.4 present the global maps showing temperature (1.3) and radiation (142) anomalies over the reporting period.

Figure 1.3. Global map of January-April 2017 temperature anomaly (as indicated by the TEMP indicator) by MRU, departure from 15YA (degrees Celsius)

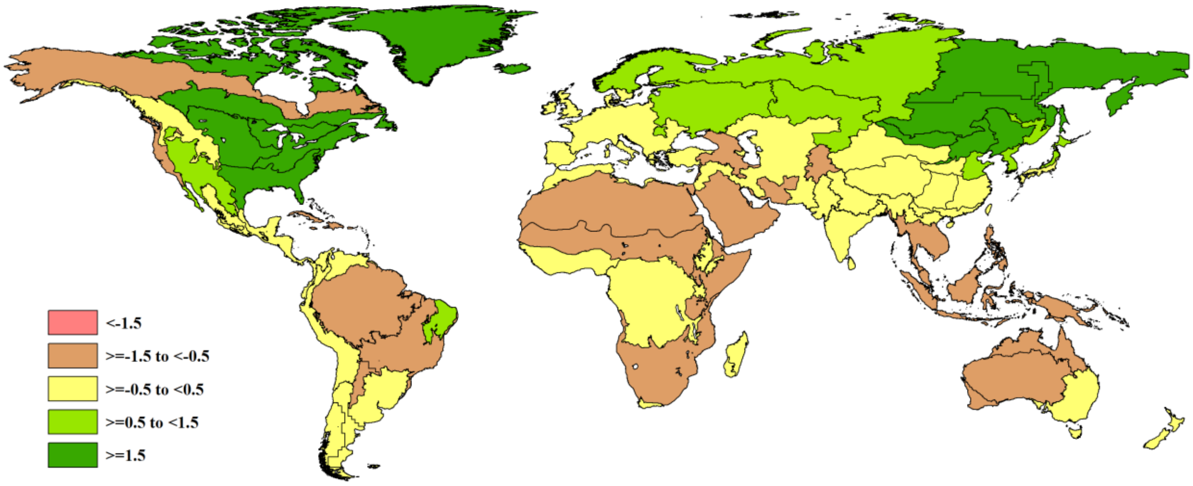

Figure 1.4. Global map of January-April 2017 PAR anomaly (as indicated by the RADPAR indicator) by MRU, departure from 15YA (percentage)

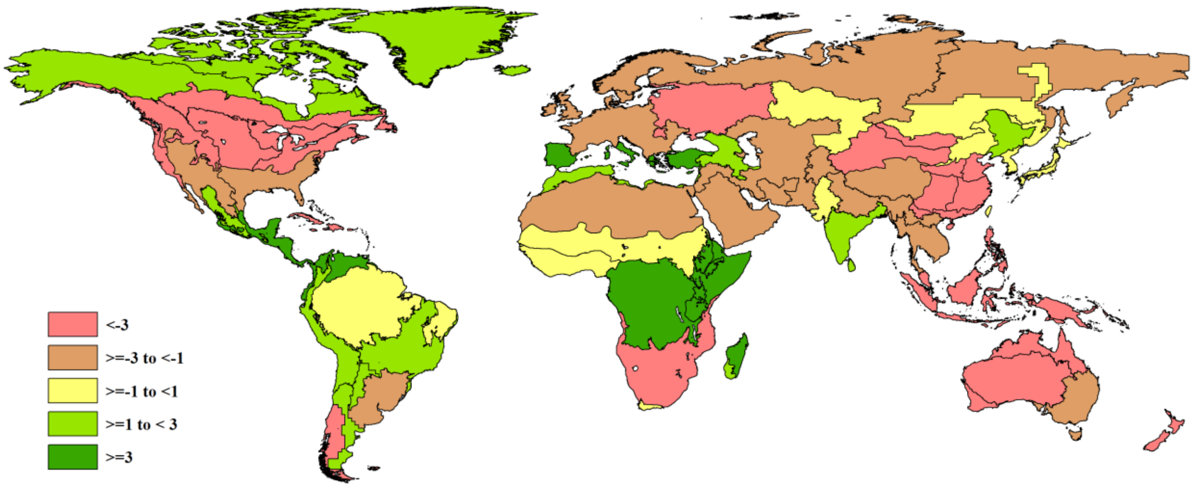

Few very large temperature anomalies occurred in important agricultural areas. The largest drop occurred in southern Africa (-1.2°C in MRU-09), which is now in its growing period of maize, the main crop in large parts of the area, in particular South Africa, Zimbabwe, and Zambia. The low temperature has contributed to a reduced crop water demand. The same mechanism may also have contributed to somewhat reduced water demand in the drought affected Horn of Africa (MRU-04) where, however, the temperature was just 0.7°C below average and RADAR increased (+4%). Southern Africa recorded a drop in sunshine (RADPAR, -3%).

Consistently higher than average TEMP was recorded in two areas starting on the eastern margins and extending land inwards of the Asian and North American continents. In America this was, paradoxically, accompanied by below average sunshine, sometimes markedly so, so that the temperature increase was brought about by cloudiness, which typically rises minimum temperature and reduces frost damage. This makes the qualitative assessment of crop condition difficult, as sunshine becomes the limiting factor once water requirements are covered. Values are TEMP, +1.7°C and RADPAR, -8% in the northern Great Plains (MRU-12), +2.2°C and -3% RADPAR in MRU-14, covering the area from the Cotton Belt to northeastern Mexico, and +2.3°C in the Corn Belt (MRU-13) where the lowest RADPAR was observed, reaching -9%. The MRUs adjacent to the ones mentioned also generally experienced warmer than average weather. In Asia, contrary to North America, high temperature was not correlated with any RADPAR pattern. Inner Mongolia (MRU-35) recorded a departure of 1.5°C with average RADPAR; in Northeast China (MRU-38), TEMP was up 1.9°C with +1% RADPAR; southern Mongolia (MRU-47) recorded +2.1°C in TEMP but a RADPAR drop (-4%), and, eventually, the largest absolute TEMP anomaly in eastern-central Asia (MRU-52; TEMP, +2.3°C) had close to average RADPAR (+1%).

Chapter 2. Crop and environmental conditions in major production zones

Chapter 2 presents the same indicators—RAIN, TEMP, RADPAR, and BIOMSS—used in Chapter 1, and combines them with the agronomic indicators—cropped arable land fraction (CALF), maximum vegetation condition index (VCIx), and minimum vegetation health index (VHIn)—to describe crop condition in six Major Production Zones (MPZ) across all continents. For more information about these zones and methodologies used, see the quick reference guide in Annex C as well as the CropWatch bulletin online resources at www.cropwatch.com.cn.

2.1 Overview

Tables 2.1 and 2.2 present an overview of the agroclimatic (table 2.1) and agronomic (table 2.2) indicators for each of the six MPZs, comparing the indicators to their fifteen and five-year averages.

Table 2.1. January-April 2017 agroclimatic indicators by Major Production Zone, current value and departure from 15YA

	RAIN		TEMP		RADPAR	
	Current (mm)	Departure (%)	Current (°C)	Departure (°C)	Current (MJ/m^2)	Departure (%)
West Africa	184	4	28.8	-0.3	1237	0
South America	745	10	23.9	-0.5	1130	0
North America	378	26	6.9	2.1	765	-6
South and SE Asia	126	2	24.6	-0.1	1168	0
Western Europe	168	-22	5.7	-0.3	581	-2
C. Europe and W. Russia	200	16	-0.4	0.5	507	-5

Note: Departures are expressed in relative terms (percentage) for all variables, except for temperature, for which absolute departure in degrees Celsius is given. Zero means no change from the average value; relative departures are calculated as (C-R)/R*100, with C=current value and R=reference value, which is the fifteen-year average (15YA) for the same period (January-April) for 2002-2016.

Table 2.2. January-April 2017 agronomic indicators by Major Production Zone, current season values and departure from 5YA

	BIOMSS (gDM/m^2)		CALF (Cropped arable land fraction)		Maximum VCI Intensity
	Current	Departure (%)	Current	Departure (% points)	Current
West Africa	557	-2	50	-13	0.67
South America	1802	6	100	0	0.89
North America	881	17	47	5	0.85
S. and SE Asia	348	-12	73	5	0.81
Western Europe	687	-16	94	0	0.84
Central Europe and W Russia	668	5	72	-8	0.65

Note: See note for table 2.1, with reference value R defined as the five-year average (5YA) for January-April 2012-2016.

2.2 West Africa

The previous (2016-2017) season has ended in the West Africa region, and the agricultural and food situations were generally described as satisfactory.

This reporting period marks yet another onset of the main growing season throughout the West African region for main crops (maize, sorghum, millet, and yams and cassava). It is also the beginning of the main long rainy season in West Africa, which will last till the end of April to mid-July in the south, and from July to September in the semi-arid Sahelian north.

For the MPZ as a whole, cumulative rainfall was recorded at 184 mm (4% above average), with positive departures in the coastal/southern parts of Nigeria, Togo, Gabon, and Ghana (representing 13.2% of West Africa). Both Togo and Côte d'Ivoire recorded abundant rainfall (+17% and +13%, respectively). In Sierra Leone, where rice is one of the major crops, the rainfall deficit was light (RAIN, -8%) but may nevertheless have affected planting of rice. Precipitation is currently building up, marking the transition from the "little" dry season into the main rainy season starting with the southern coastal areas. Average temperature of 28.8°C (-0.3°C departure) and sunshine (RADPAR: 1237 MJm-2) were experienced during this period. The largest departure for radiation occurred in Liberia (RADPAR, -7%).

A fraction of cropped arable land (CALF) of 50% (a decrease in 13 percentage points compared to average) and a biomass proportion of 557 gDM m-2 were also observed in the MPZ, much of which is the cropped land in the coastal area (BIOMSS, +20%), while the northern areas (BIOMSS departures <-20%) are still uncropped. This finding is supported by the VCIx map, an alternative measure of the relative vegetation health and crop condition and a proxy to detect potential drought; the maximum VCI intensity for the MPZ was 0.67 (range 0.5-0.8).

CropWatch indicators depict a stable and coherent climatic condition for the MPZ.

Figure 2.1. West Africa MPZ: Agroclimatic and agronomic indicators, January-April 2017

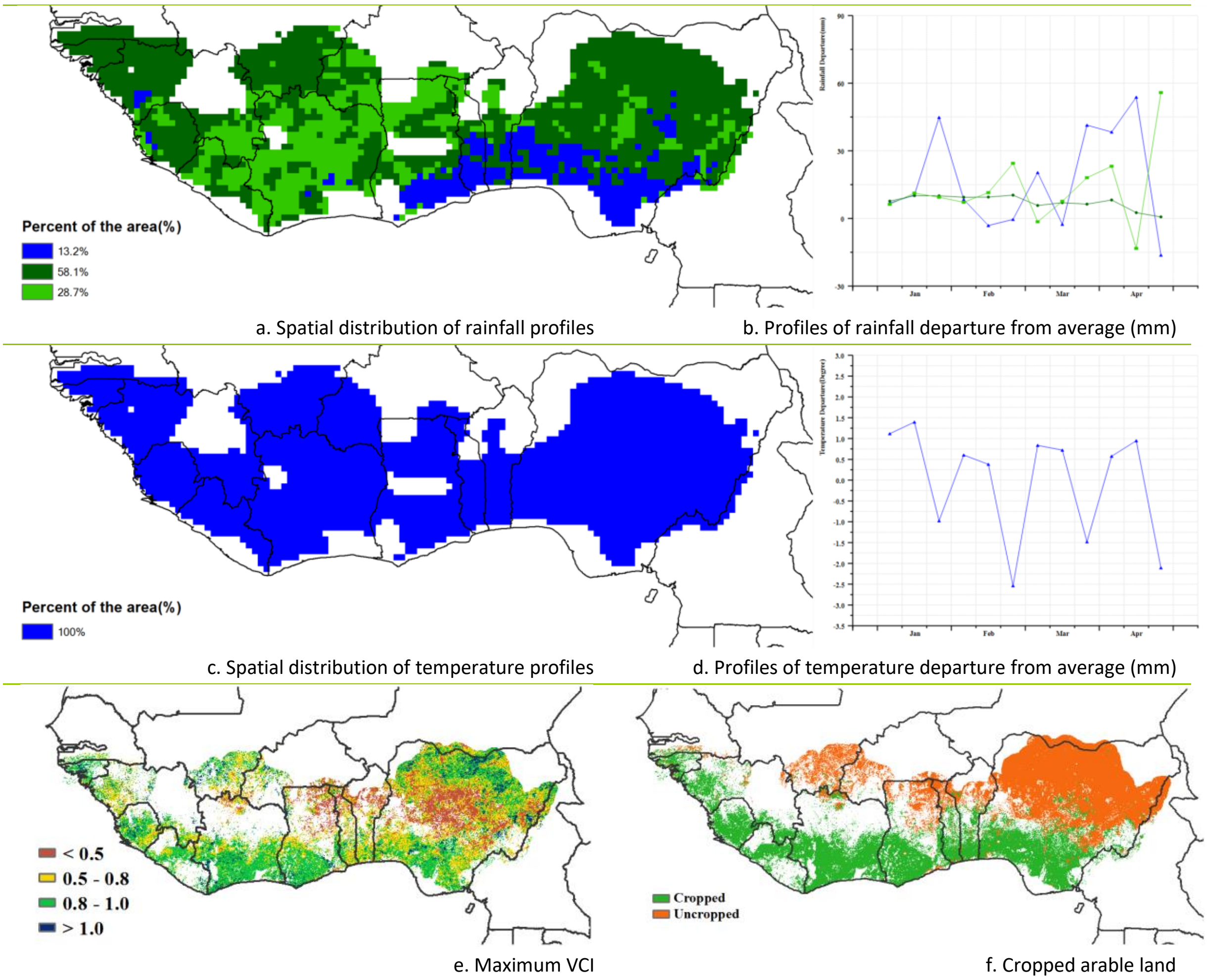

a. Spatial distribution of rainfall profiles

b. Profiles of rainfall departure from average (mm)

c. Spatial distribution of temperature profiles

d. Profiles of temperature departure from average (mm)

e. Maximum VCI

f. Cropped arable land

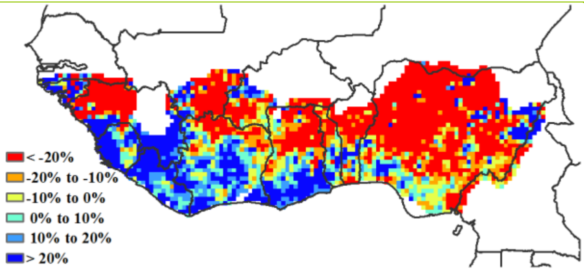

g. Biomass accumulation potential departure

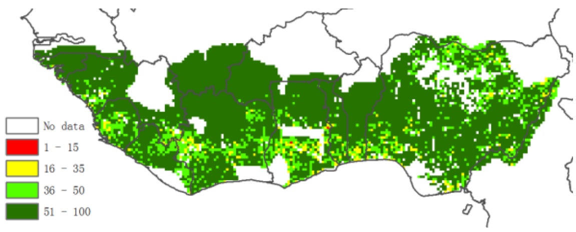

h. VHI minimum

Note: For more information about the indicators, see Annex C.

2.3 North America

The current monitoring period from January to April of 2017 covers the growth season of winter crops and planting season of summer crops in southern regions. CropWatch agroclimatic and agronomic indicators show above average crop condition in the North American MPZ (figure 2.2).

During the monitoring period, warm and humid weather prevailed in the MPZ, which was conducive to crop growth. The agroclimatic indicators show that RAIN was 26% above average, TEMP 2.1°C above, and RADPAR was significant below average (-6%), probably as a result of increased cloudiness associated with continuous precipitation. The extreme weather events that occurred in this reporting period include abnormally above average temperature in the late of January (+5 to +10°C) and February (+7 to +11°C), and 210 mm above average rainfall in the southern Corn Belt. Almost all major crop production regions recorded abundant rainfall, including Northern Plains (+RAIN, 56.5%), Corn Belt (+31.7%), California (+76.2%), Blue Grass (+17.4), and Canadian Prairies (+10.6%) which provided adequate soil water for the growth of winter crops. The impact of reduced sunshine on photosynthesis is probably not too relevant at this stage of crop development. Very few drought pockets are shown in the Minimum Vegetation Health Index map (VHIn).

Agronomic indicators confirm the generally above-average crop condition. Compared to the average of the past five years, accumulated biomass potential (BIOMSS) increased by 17%, with positive departure in almost all areas, for instance in the Northern Plains (BIOMSS, +33.8%) and the Corn Belt (+17.9%). Above average crop condition is confirmed by a high average VCIx value (0.85). However, a significant negative BIOMSS departure and below average VCIx value (<0.5) were observed in Eastern Colorado, Eastern Wyoming, and Western Nebraska due to heavy snow, resulting in unfavorable crop growth condition.

When considering these various agroclimatic and agronomic indicators together with the CropWatch indicator for cropped arable lands—which shows 47% of arable lands cropped; an increase of 5 percentage points over the five-year average, average or above average crop production can be expected for the North American MPZ.

Figure 2.2. North America MPZ: Agroclimatic and agronomic indicators, January-April 2017

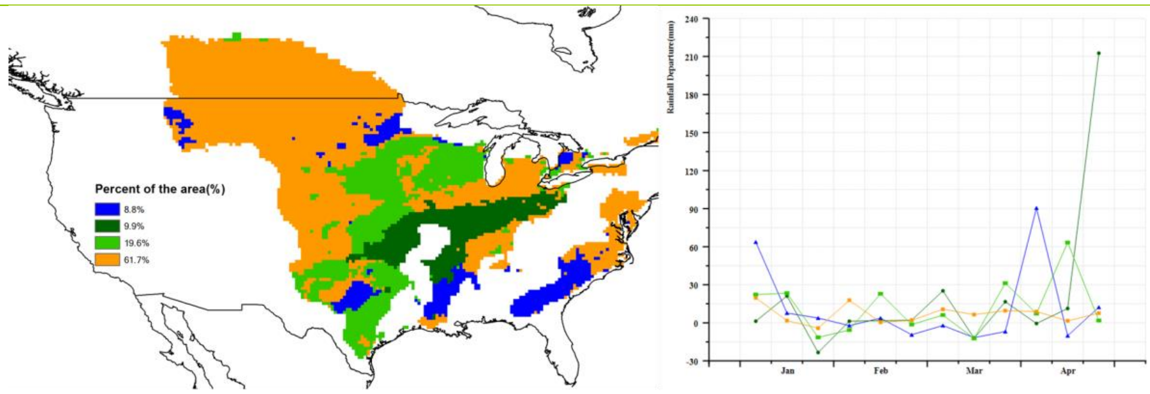

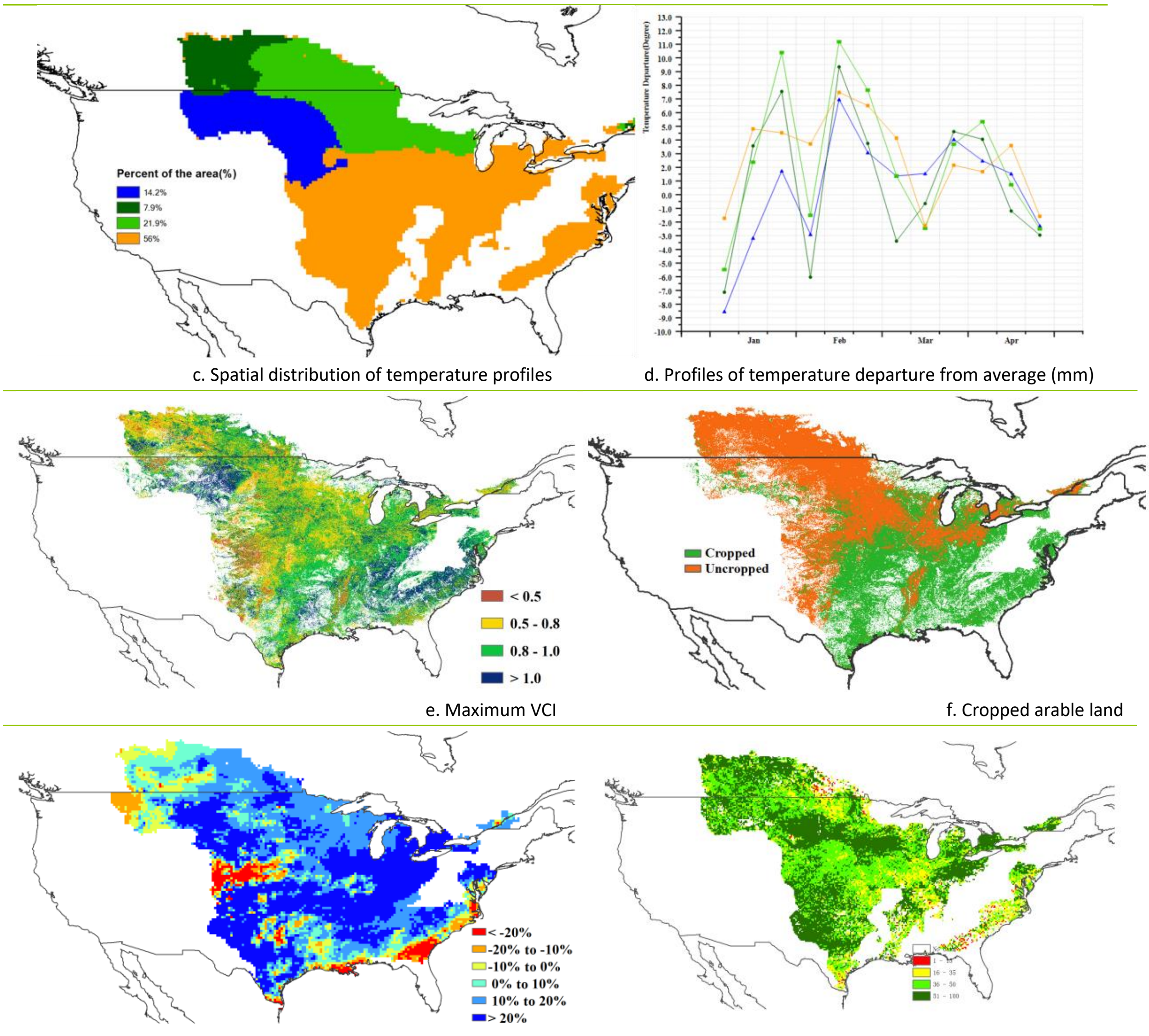

a. Spatial distribution of rainfall profiles

b. Profiles of rainfall departure from average (mm)

c. Spatial distribution of temperature profiles

d. Profiles of temperature departure from average (mm)

e. Maximum VCI

f. Cropped arable land

g. Biomass accumulation potential departure

h. VHI minimum

Note: For more information about the indicators, see Annex C.

2.4 South America

The current bulletin covers the main growing period of summer crops maize (main season), soybean, and rice in the South American MPZ (figure 2.3). Winter crops are currently not in their growing season.

Overall, conditions were favorable for crops during the monitoring period. Rainfall was 10% above average over the whole MPZ. According to the rainfall departure clustering analysis, extreme high precipitation (+100mm above average) occurred in early January and early April in Rio Grande do Sul (Brazil), Entre Rios and Santa Fe (Argentina) and in Uruguay. Most other places received normal rainfall (-30mm to +30mm from average) over the last four months. Average temperature was 23.9°C, about 0.5°C below average, but departures fluctuated between -2.5°C and +3.0°C. Favorable conditions resulted in a 6% above average BIOMSS, although the biomass accumulation potential departure map shows values of 20% or more below average in Cordoba in Argentina and in Santa Catarina and Minas Gerais in Brazil. The VHI map, however, does not show drought condition in those areas, indicating that the below average BIOMSS resulted from the combined effect of temperature and rainfall anomalies.

Favorable conditions together with the increase in maize planted area (as a result of strong export demand) led to almost 100% of arable land being cultivated during the last four months, with the only exception in an area around Bahia Blanca. Crops benefited from the good climatic conditions with an average VCIx for the whole MPZ of 0.89, a record level for this time of the year compared to the last five years. VCIx in Brazil was relatively higher than in Argentina, which might be caused by an early harvest of summer crops in Argentina.

In general, prospects are good for summer crop outputs in the South American MPZ.

Figure 2.3. South America MPZ: Agroclimatic and agronomic indicators, January-April 2017

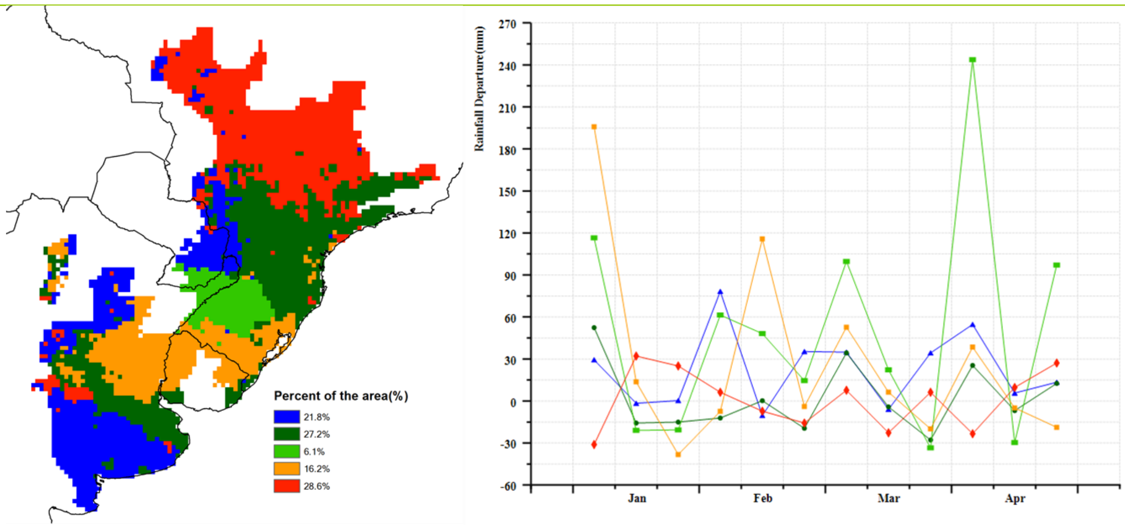

a. Spatial distribution of rainfall profiles
b. Profiles of rainfall departure from average (mm)

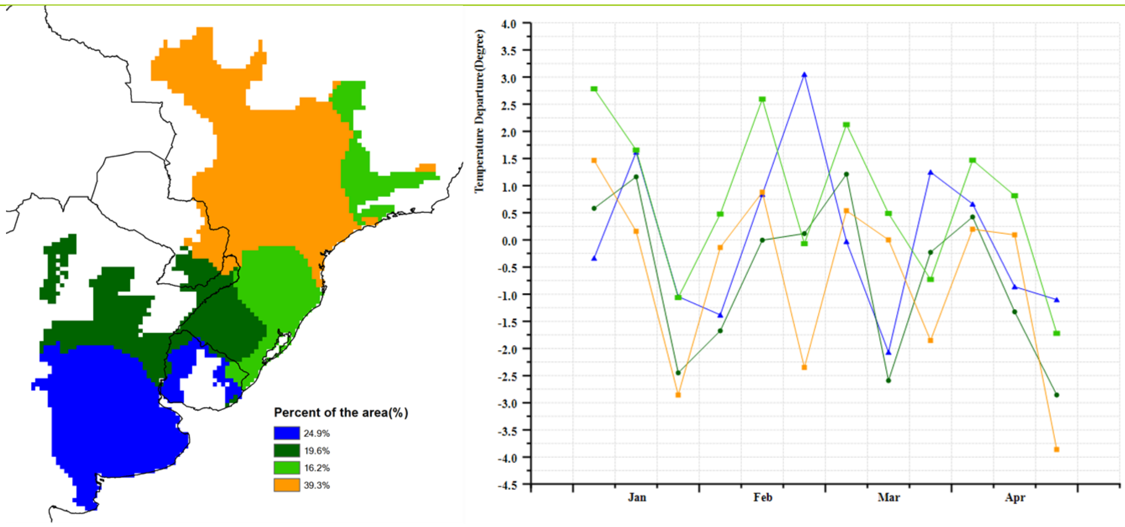

c. Spatial distribution of temperature profiles
d. Profiles of temperature departure from average (mm)

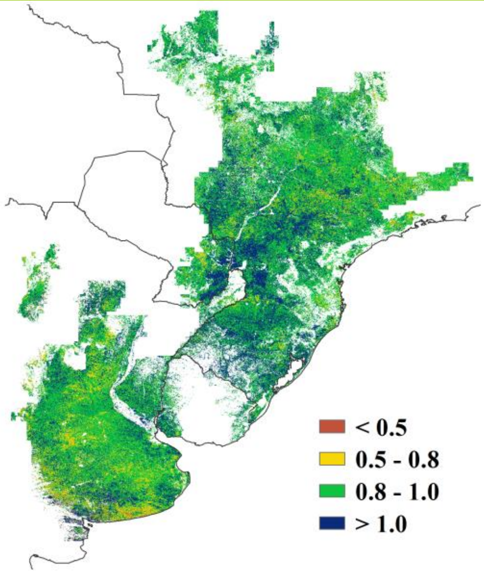

e. Maximum VCI

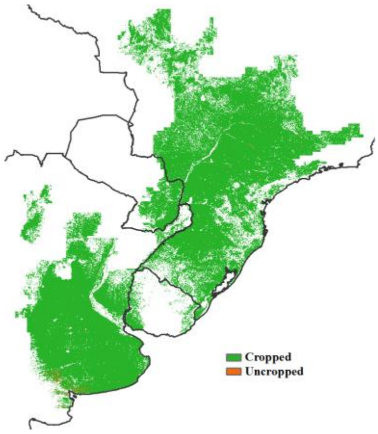

f. Cropped arable land

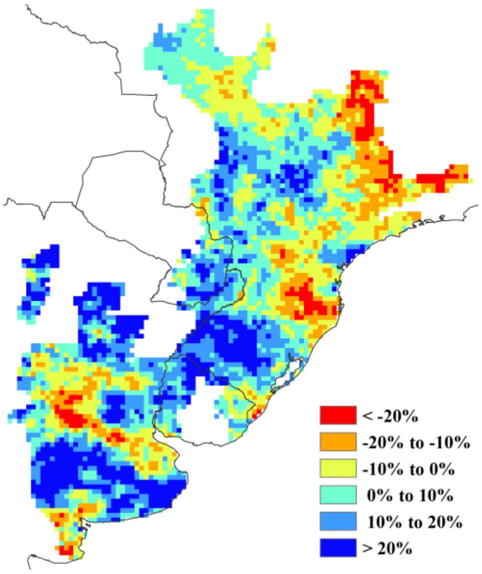

g. Biomass accumulation potential departure

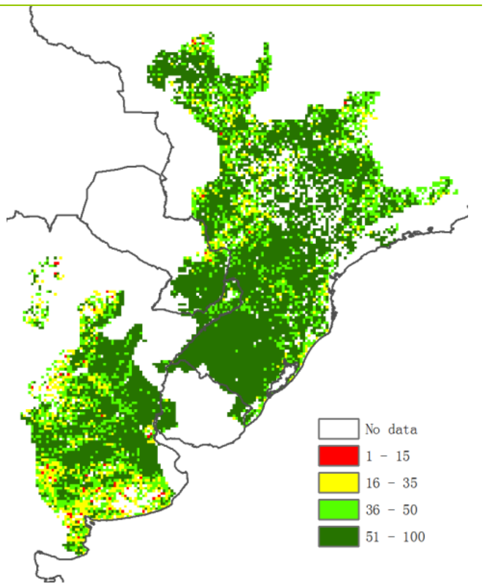

h. VHI minimum

Note: For more information about the indicators, see Annex C.

2.5 South and Southeast Asia

With large regional disparities, the crop condition was generally favorable in this MPZ (figure 2.4). The monitoring period covers the growing and harvesting period of winter season rice, wheat, and maize, and the planting of summer or "second" crops. Rainfall (RAIN, +2%) was slightly above average. Except for India (RAIN, -16%) and Laos (-9%), the nationwide rainfall was above average in most countries, mainly in Bangladesh (+76%), Thailand (+61%), Cambodia (+30%), Sri Lanka (+25%), Vietnam (+14%), and Myanmar (+5%). According to the rainfall departure clusters, the rainfall was evenly distributed over 89.4% of the region. Bangladesh and the Assam state of India received excessive rainfall in April. Rainfall was in deficit in Sri Lanka in the beginning and end of January and the whole of April.

Temperature for the MPZ (TEMP, -0.1°C) and radiation were close to the average, although temperature profiles show large fluctuations. The lowest temperature departure value (-2.5°C) occurred at the end of February and April in most countries of the MPZ, such as Myanmar, Thailand, Cambodia, Laos and

Vietnam, while the highest departure value (+4°C) was observed in the middle of February in the Himachal Pradesh state of India.

The biomass production potential indicator (BIOMSS) in most of India was more than 20% below average due to dry weather. The fraction of cropped arable land (CALF) increased 5% compared to recent five-year average, while the average VCIx was 0.81 for the MPZ. The VCIx values below 0.5 were mainly distributed in the Indian states of Andhra Pradesh, Karnataka, and Tamil Nadu and "sprinkled" over Thailand, mostly coinciding with the uncropped regions shown by the CALF map. With local exceptions, the MPZ nevertheless experienced favorable conditions.

Figure 2.4. South and Southeast Asia MPZ: Agroclimatic and agronomic indicators, January-April 2017

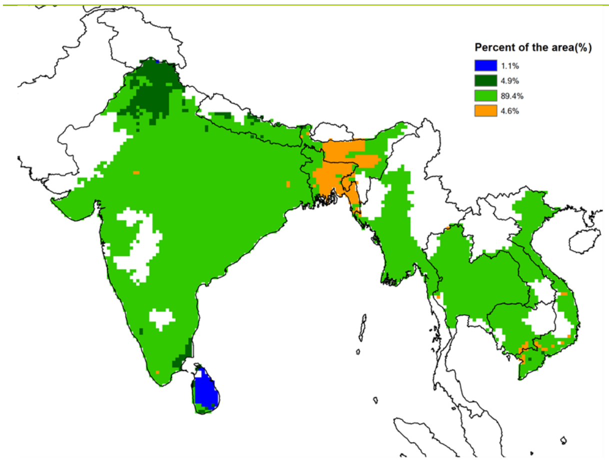

a. Spatial distribution of rainfall profiles

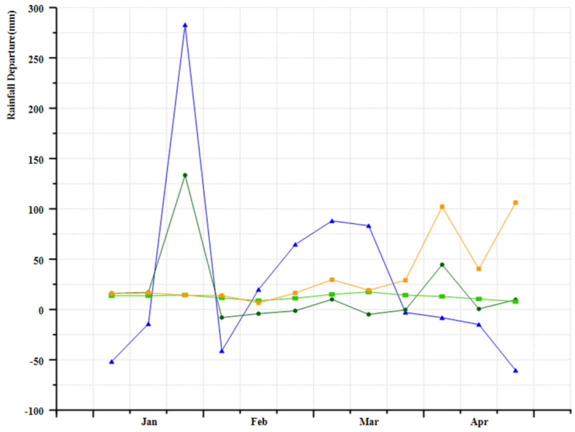

b. Profiles of rainfall departure from average (mm)

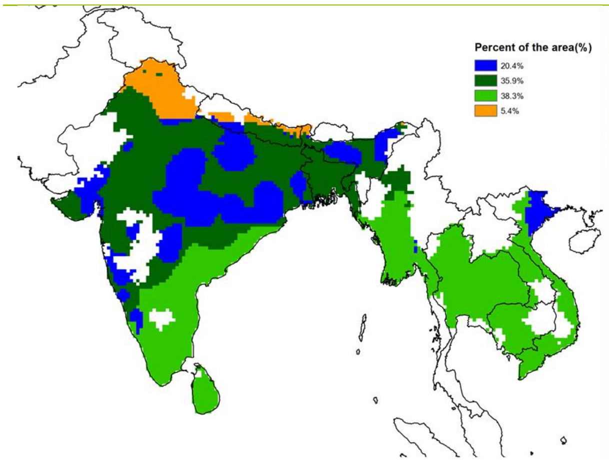

c. Spatial distribution of temperature profiles

d. Profiles of temperature departure from average (mm)

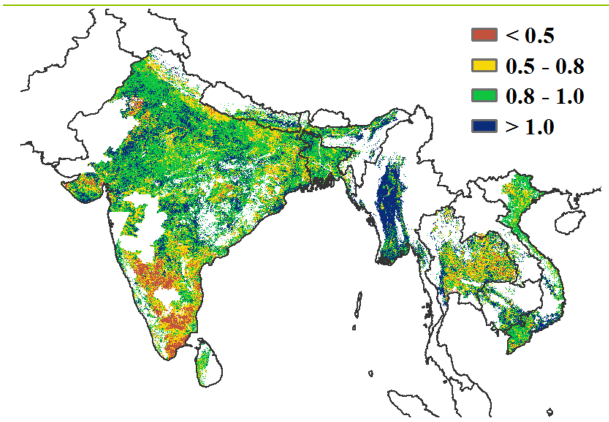

e. Maximum VCI

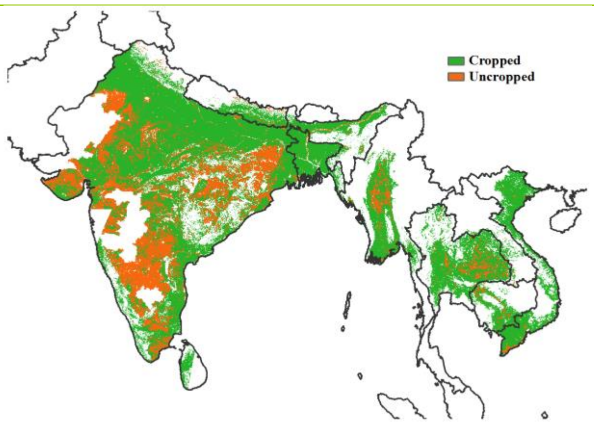

f. Cropped arable land

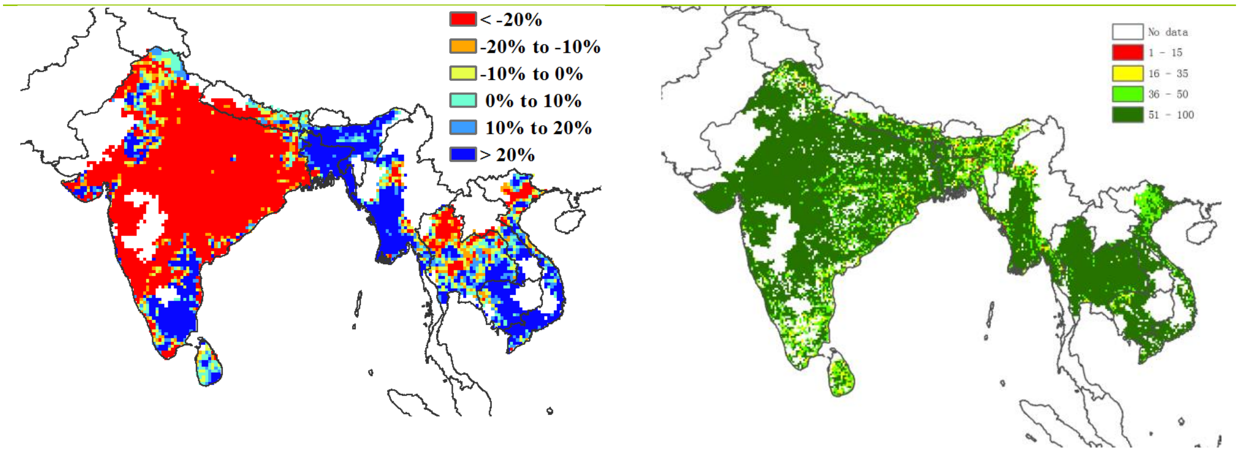

g. Biomass accumulation potential departure h. VHI minimum

Note: For more information about the indicators, see Annex C.

2.6 Western Europe

In general, crop condition was above average in many parts of the continental Western European MPZ based on the integration of agroclimatic and agronomic indicators (figure 2.5).

The agroclimatic indicators show that total rainfall was 22% below average over the region, resulting from marked negative departures in central England, southwest Germany, most of France, the north and south of Italy, eastern Austria, and southern Hungary. The most severely affected country was France with a 36% drop nationwide. Exceptional positive departures, however, were recorded over most of Germany, Denmark, the Czech Republic, northwest Austria, the south of Slovakia, northern Hungary, and east and western parts of England from late February to mid-March and also in early April, as well as in southwest France and northern Spain in a period from late January to mid-February and in late March. Abundant precipitation, with accumulated values above 120 mm, was recorded in northern Italy from mid-February to mid-March, while sparse rainfall was registered in northeastern Italy in April. More rain is needed in some Western European countries for winter crop growth and the early stages of summer crops.

Radiation for the MPZ as a whole was 2% below average, and so was temperature (-0.3°C). A cold spell persisted throughout January in central Europe with several days with minimum temperatures around -15°C. Since the first days of February, however, temperatures have exceeded their long-term-average by 1 to 4°C in most of Europe, and frost events were sparse. Drier-than-usual weather conditions were observed in southern Italy. The exceptionally mild temperature conditions in late February and late March have been favorable for winter crop growth and spring sowing activities. Low minimum temperatures that set in after early April, however, are likely to have affected flowering rapeseed in eastern France, western and southern Germany, the Czech Republic, Slovakia, Austria, Hungary, and Slovenia.

Due to the continuous rainfall deficit (especially after early March), and coupled with the impact of low temperature (in particular in France, the United Kingdom, northern Italy, northeast Austria, the south of Hungary, and the middle of Spain), the biomass accumulation potential BIOMSS was 16% below the recent five-year average. The lowest BIOMSS values (-20% and less) occurred in France, the south of the United Kingdom, Spain, Italy, and the south of Hungary. In contrast, BIOMSS was above average (sometimes exceeding a 10% departure) in parts of Germany, the Czech Republic, and Denmark.

The average maximum VCI for the MPZ reached a value of 0.84 during this reporting period, indicating favorable crop condition. More than 94% of arable lands were cropped, which is the same as the recent five-year average. Most uncropped arable land is concentrated in Spain, southeast France, and northern

Italy. Generally, crop condition in Western Europe was favorable, but more rain is needed in several important crop production areas to sustain good yields.

Figure 2.5. Western Europe MPZ: Agroclimatic and agronomic indicators, January-April 2017

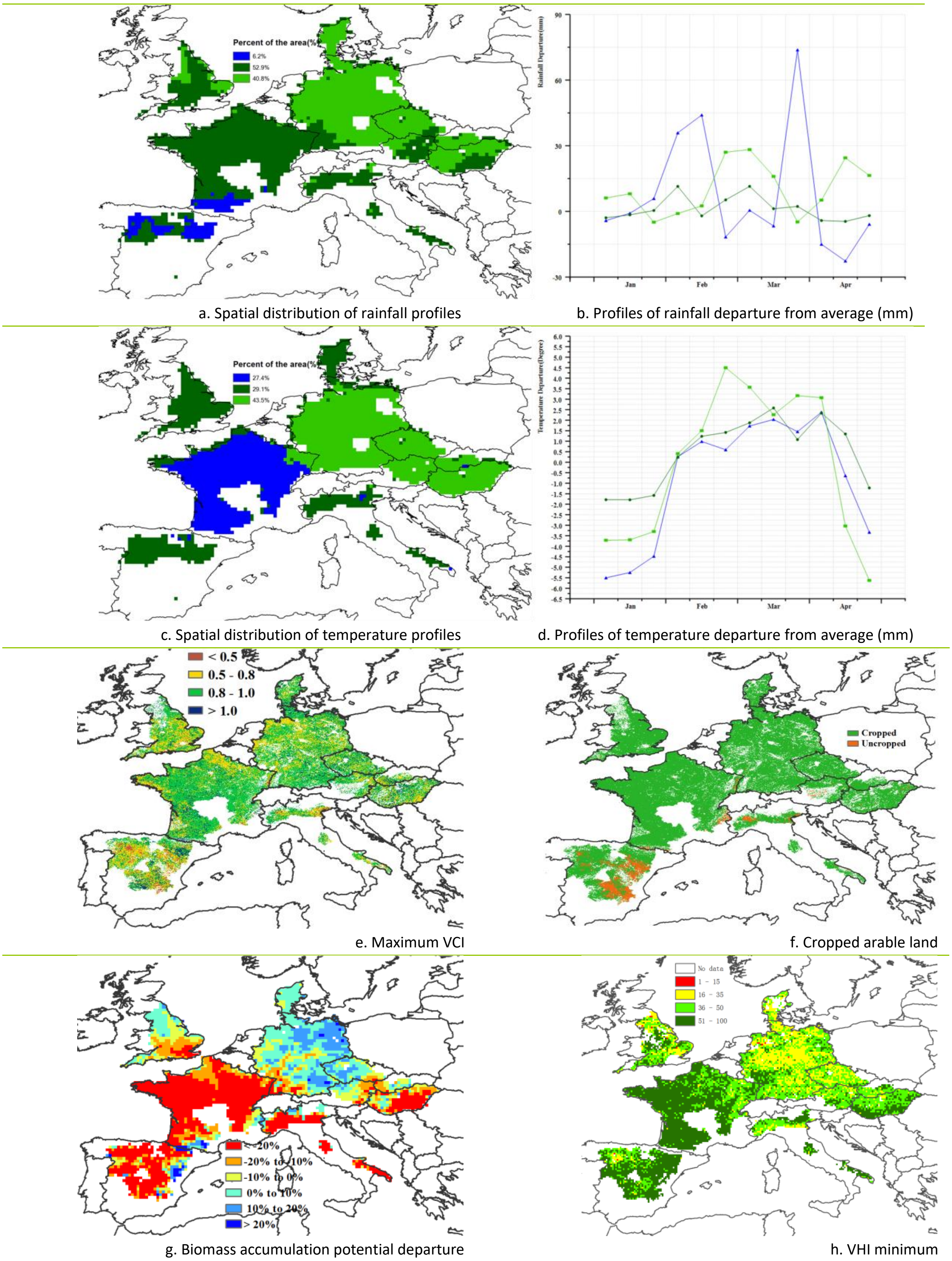

a. Spatial distribution of rainfall profiles
b. Profiles of rainfall departure from average (mm)
c. Spatial distribution of temperature profiles
d. Profiles of temperature departure from average (mm)
e. Maximum VCI
f. Cropped arable land
g. Biomass accumulation potential departure
h. VHI minimum

Note: For more information about the indicators, see Annex C.

2.7 Central Europe to Western Russia

During the current monitoring period, dormant winter crops in central Europe to western Russia were in the vegetative stage. The agroclimatic indicators showed favorable condition for crop growing, with a 16% increase of rainfall over average—which provided ample soil moisture—and a 0.5°C increase in temperature, while radiation was below average by 5% (figure 2.6).

Temperature profiles showed correlated variations from February to April for most countries in the MPZ. The whole region experienced high temperatures from late-January to March (as much as 8°C above average in the east, including most of southwestern Russia which forms almost 63% of the MPZ), which had positive effects on the development of winter crops. Temperatures in most areas started to fall starting in April, and more than 3°C below average values occurred in Belarus, Poland, and western Ukraine in late-April. As indicated by the rainfall profiles, the north of central Europe to western Russia—about two thirds of the MPZ's territory, enjoyed above average precipitation over the monitoring period, including Poland (RAIN, +23%), Belarus (RAIN, +31%), and the northern part of Ukraine and southern Russia. The maximum precipitation occurred in early-January when precipitation was 90% above average in Romania and in the south of Ukraine. Unfavorable rainfall was recorded in southern Russia (from the Kray of Krasnodar to the Kabardino balkariya republic) in late-January and early-April.

As a result of the large precipitation increase and above average temperature, the biomass accumulation potential (BIOMSS) of the MPZ was 5% above the recent five-year average. However, a decrease (more than 20%) in BIOMSS occurred in Krasnodarskiy Kray in Russia and Timis in Romania. The maximum VCI (0.65) is lower than those of other MPZs. According to the maximum VCI map of this monitoring period, most pixels were below 0.5 in southwestern Russia, where most uncropped arable land is concentrated. Across the MPZ, 72% of arable lands were cropped in the monitoring period, a decrease of 8 percentage points compared to the recent five-year average for this indicator.

Figure 2.6. Central Europe-Western Russia MPZ: Agroclimatic and agronomic indicators, January-April 2017

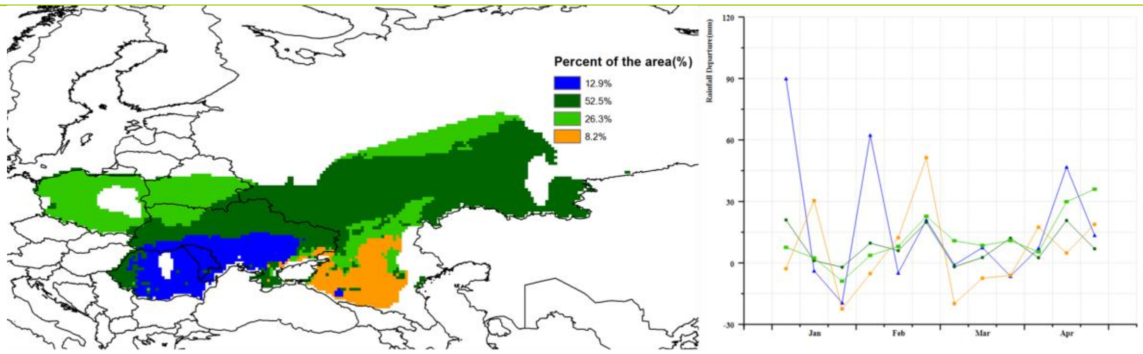

a. Spatial distribution of rainfall profiles   b. Profiles of rainfall departure from average (mm)

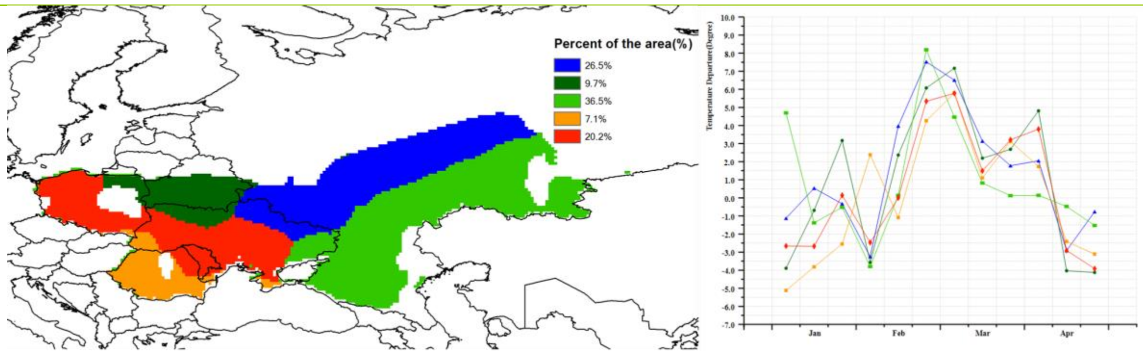

c. Spatial distribution of temperature profiles   d. Profiles of temperature departure from average (mm)

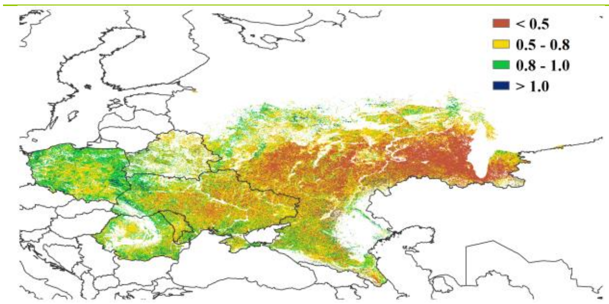

e. Maximum VCI

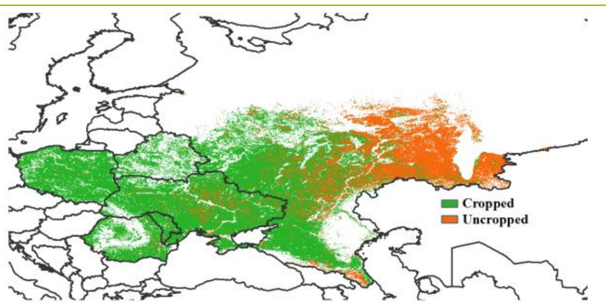

f. Cropped arable land

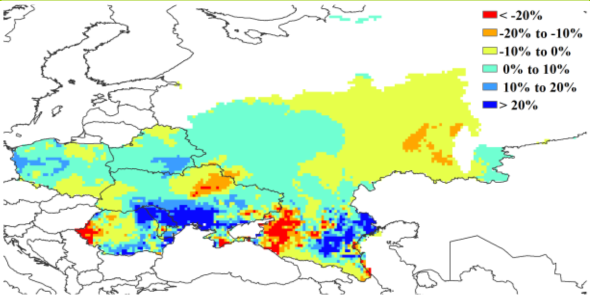

g. Biomass accumulation potential departure

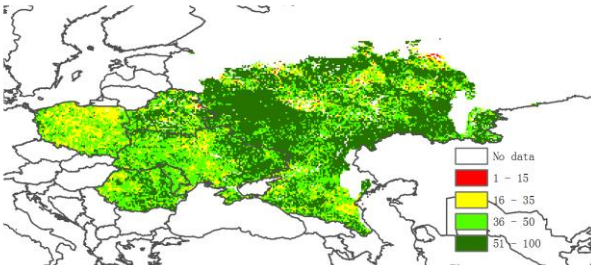

h. VHI minimum

Note: For more information about the indicators, see Annex C.

Chapter 3. Main producing and exporting countries

Building on the global patterns presented in previous chapters, this chapter assesses the situation of crops in 30 key countries that represent the global major producers and exporters or otherwise are of global or CropWatch relevance. In addition, the overview section (3.1) pays attention to all countries worldwide, to provide some spatial and thematic detail to the overall features described in section 1.1. In section 3.2, the CropWatch monitored countries are presented, and for each country maps are included illustrating NDVI-based crop condition development graphs, maximum VCI, and spatial NDVI patterns with associated NDVI profiles. Additional detail on the agroclimatic and BIOMSS indicators, in particular for some of the larger countries, is included in Annex A, tables A.2-A.11. Annex B includes 2017 production estimates for Argentina, Brazil and the United States.

3.1 Overview

The current reporting period recorded relatively few extreme conditions among the 30 countries specifically monitored by CropWatch and described in this chapter. Some, however, are part of the large anomaly patterns described in Chapter 1, and they are often surrounded by less important countries in terms of agricultural production where conditions may be more extreme.

Table 3.1 presents the agroclimatic and agronomic indicators for January-April 2017, showing their departure from the five and fifteen-year averages as applicable; the underlying CWAI indicators are presented in figures 3.1-3.4.

Rainfall

Positive rainfall departures

Rainfall departures larger than 50% above average were recorded in three Asian countries: 367 mm (RAIN, +76%) in Bangladesh, 880 mm (+69%) in the Philippines, and 302 mm (+61%) in Thailand. Some detail about Bangladesh is provided in section 5.2 about disasters. Among the listed countries, BIOMSS increased in both Bangladesh and the Philippines (+48% and +33%, respectively), while in Thailand BIOMSS was +9%, due to somewhat below average temperature (-0.7°C). A similar situation is observed in Argentina (rainfall 696 mm, +40%), with a smaller relative biomass increase due to below average temperature and the use of the two different reference periods (15 years for the agroclimatic indicators and only five for BIOMSS). In Bhutan, rainfall reached 411 mm in agricultural areas (+75%).

In other areas, Peru, Ecuador, and Colombia are also mentioned in the section on disasters due to exceptional precipitation recorded in their common border area in the north of Peru, northeast Ecuador, and southwest Colombia. Rainfall departures for the three countries are high even at the national level (+29%, +41%, and +29%, respectively), which results from the common and large scale cause for the phenomenon: a “coastal El Niño”. Other significant rainfall excesses in the same region, though probably unrelated as far as causes are concerned (except maybe for Bolivia), include Bolivia (+32%), Venezuela (+29%), and the two countries on the island of Hispaniola: Haiti (+67%) and the Dominican Republic (+72%). The countries are part of a larger ensemble that encompasses about half the South American continent.

Figure 3.1. Global map of January-April 2017 rainfall (RAIN) by country and sub-national areas, departure from 15YA (percentage)

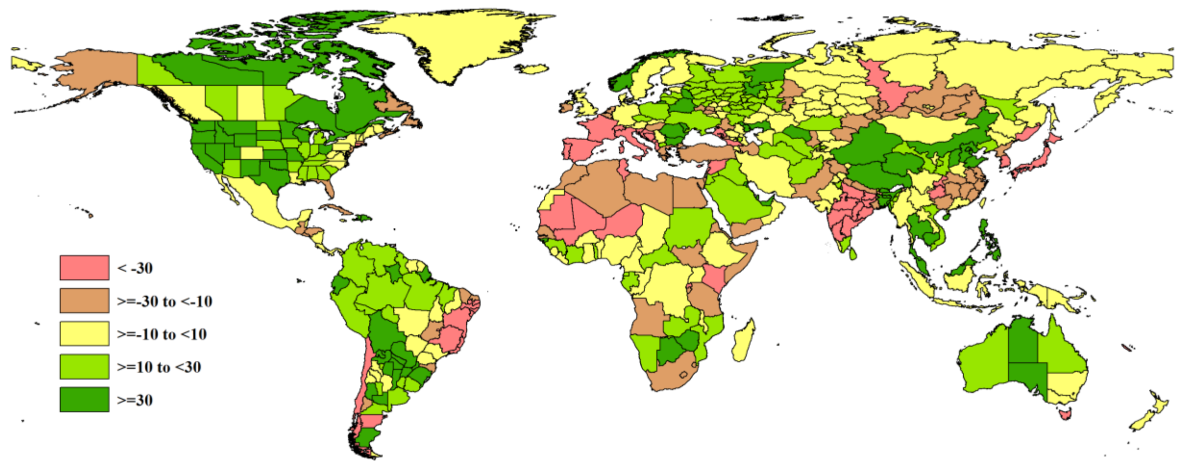

Figure 3.2. Global map of January-April 2017 biomass (BIOMSS) by country and sub-national areas, departure from 15YA (percentage)

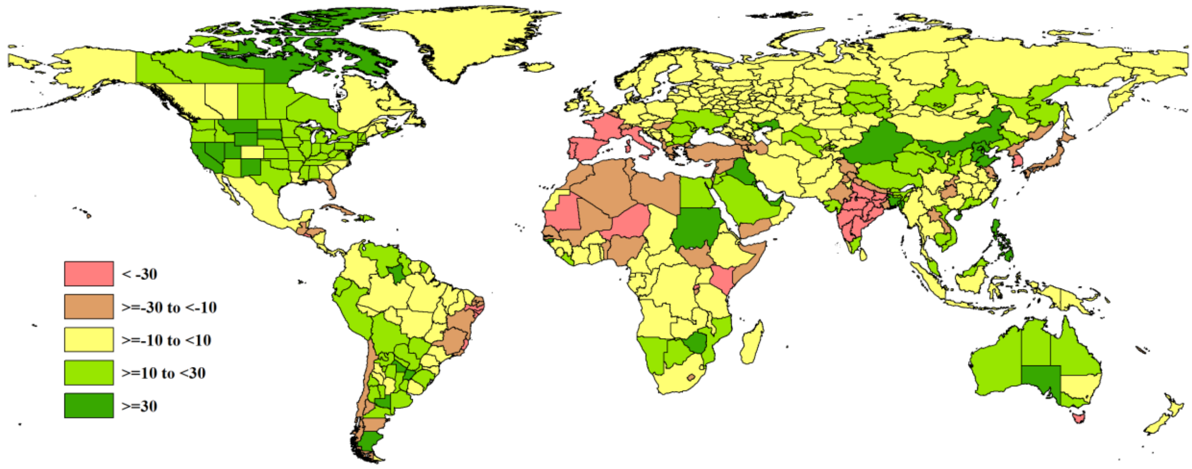

In other parts of the world, large positive rainfall departures also are reported for southern Africa (where some of them also resulted in local floods), such as in Mozambique (RAIN, +18%; see disasters section), Botswana (+39%), and Zimbabwe (+52%). For those and several neighboring countries, the abundant precipitation was much needed relief after last year's drought. Interestingly, the southern African countries are also those with the largest negative temperature anomalies, such as for example -2.2°C in Botswana, -1.9°C in Swaziland, and -1.5°C in Namibia and Zimbabwe. In contrast, South Africa, where the rainfall deficit was moderate, recorded a temperature drop of "only" -0.7°C. The same general area was also characterized by low sunshine in Botswana and Zimbabwe (RADPAR, -7%).

Still significant, but less spectacular positive rainfall departures occurred in North America, central and eastern Europe and western Russia, western West Africa, in an area of the southeastern Caspian up to northern China, and in Australia. And finally, positive departures need to be mentioned for the countries around the South China Sea (some already mentioned above), which, in addition to high rainfall and low temperature, also recorded low sunshine values, such as a RADPAR of -8% in Vietnam and -5% in the Philippines. It is likely that the large increases in cropped arable land fraction in Thailand (CALF, +12%) and Cambodia (+22%, the largest cropped arable land fraction increase among all CropWatch countries) derive directly from the favorable water supply.

Rainfall deficits

Negative rainfall departures—though usually not severe enough to qualify as “drought” because of seasonally low temperatures that reduce water consumption in winter crops—occurred in the Mediterranean and the eastern Black Sea countries, with some neighboring countries also in need of mentioning, starting in the east with Georgia (RAIN, -60%), Cyprus (-54%), Lebanon (-46%), and Syria (-35%). In Europe, the area encompasses Montenegro (RAIN, -58%), Bosnia-Herzegovina (-37%), Slovenia (-33%), and Croatia (-32%), as well as Albania (-54%). In the European Union, the most important agricultural countries in this group are France (-36%), together with Italy (-51%) and, on the Atlantic Ocean, Spain (-38%) and Portugal (-58%). France suffered a marked drop in biomass production potential (BIOMSS, -31%) due to the mentioned shortage of rainfall while temperature (-0.8°C) and RADPAR were closer to average. In the southern Mediterranean, Tunisia is the most affected country with a rainfall deficit of 37%. Meanwhile, Turkey, with a 22% rainfall deficit, also suffered a very significant drop in its cropped arable land fraction (CALF, -28%), which is further discussed in the country narrative. This is not unlike Iran (CALF down 19%), where other indicators, however, took relatively average values.

In Asia, the Republic of Korea deserves mentioning with -55% precipitation compared with average, together with Japan (-33%) and most of eastern and southwestern China (such as Chongqing -37% and Guizhou -30%).

For the Horn of Africa, the section on disasters (5.2) also mentions droughts in parts of this region, although national precipitation values are generally fair, such as in Ethiopia (-9%), resulting from a mix of areas with favorable and unfavorable rain. In Rwanda, however, which borders the Horn, rainfall dropped 46%, while Kenya recorded -42% and Somalia -26%.

Finally, in terms of precipitation deficits compared to average, Chile (-41%) is mentioned, as well as two large countries where national averages hide contrasting sub-national conditions: India (-16% nationwide but -65% in Orissa and -81% in Chhattisgarh) and Brazil (+6% nationwide but -32% in Minas Gerais). The case of India is particularly worrying as the drought follows widespread excess water in previous seasons.

Temperature and radiation

For temperature, above average values are noted for China (+0.5°C) and Russia (+1.2°C) on the Eurasian continent, as well as in North America with significant increases in the United States (+1.8°C) and Canada (+1.4°C). In both China and the United States, the positive temperature departure was accompanied by below average RADPAR (-6% in both countries), which may result from increased cloudiness.

Figure 3.3. Global map of January-April 2017 temperature (TEMP) by country and sub-national areas, departure from 15YA (degrees)

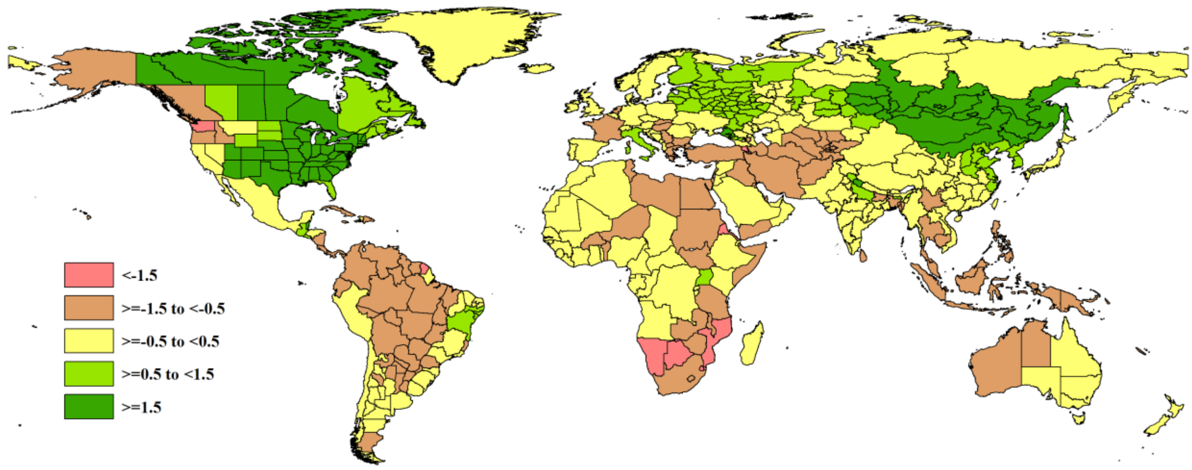

Low temperature departures (close to -1°C) occurred in several areas, notably an area stretching from Hungary to Afghanistan, thus approximately centered around Armenia (departure: -2.1°C); northern to central South America, and Southeast Asia.

Finally, the largest sunshine deficits affected Baltic countries, extending into central Europe and including Belarus (RADPAR, -15%, which is a very significant value for a national average), Lithuania and Latvia (both -13%) and Estonia (-10%). Generally smaller deficits occur south of this area in Poland (-13%) and Czech Republic (-9%), and west of it in Denmark and the United Kingdom (both at -9%), to increase again in Ireland (-14%).

Table 3.1. CropWatch agroclimatic and agronomic indicators for January-April 2017, departure from 5YA and 15YA

Country	Agroclimatic Indicators			Agronomic Indicators		
	Departure from 15YA (2002-2016)			Departure from 5YA (2012-2016)		Current
	RAIN (%)	TEMP (°C)	RADPAR (%)	BIOMSS (%)	CALF (%)	Maximum VCI
Argentina	40	-0.6	-1	19	1	0.85
Australia	14	0	-2	7	3	0.64
Bangladesh	76	-1.1	-5	48	1	0.87
Brazil	6	-0.4	1	-2	-1	0.77
Cambodia	30	-1	0	26	22	0.84
Canada	17	1.4	-6	11	-	0.76
China	-13	0.5	-6	5	-2	0.62
Egypt	-18	-0.9	-1	27	1	0.75
Ethiopia	-9	-0.4	4	-5	-	0.59
France	-36	-0.8	0	-31	0	0.87
Germany	-4	-0.2	-5	2	0	0.85
India	-16	0.2	1	-28	4	0.80
Indonesia	7	-0.7	-4	2	0	0.73
Iran	-9	-0.6	-2	-7	-19	0.50
Kazakhstan	-2	0.4	-1	2	-	0.57
Mexico	-9	0.4	3	-3	3	0.72
Myanmar	5	-0.2	-3	5	13	0.92
Nigeria	-1	-0.4	0	-10	-24	0.69
Pakistan	-15	-0.1	-1	-8	6	0.68
Philippines	69	-0.9	-5	33	0	0.69
Poland	23	-0.2	-13	6	0	0.82
Romania	33	-0.4	1	12	-1	0.77
Russia	6	1.2	-3	5	-	0.58
S. Africa	-11	-0.7	-2	-7	8	0.74
Thailand	61	-0.7	-1	9	12	0.77
Turkey	-22	-0.5	3	-11	-28	0.57
Ukraine	20	0.3	-3	10	-17	0.68
United Kingdom	-1	-0.2	-9	-1	1	0.82
United States	25	1.8	-6	17	7	0.85
Uzbekistan	21	-1.2	0	11	-	0.70
Vietnam	14	-0.1	-8	17	2	0.83

Note: No sign means a positive (+) departure.

Figure 3.4. Global map of January-April 2017 PAR (RADPAR) by country and sub-national areas, departure from 15YA (percentage)

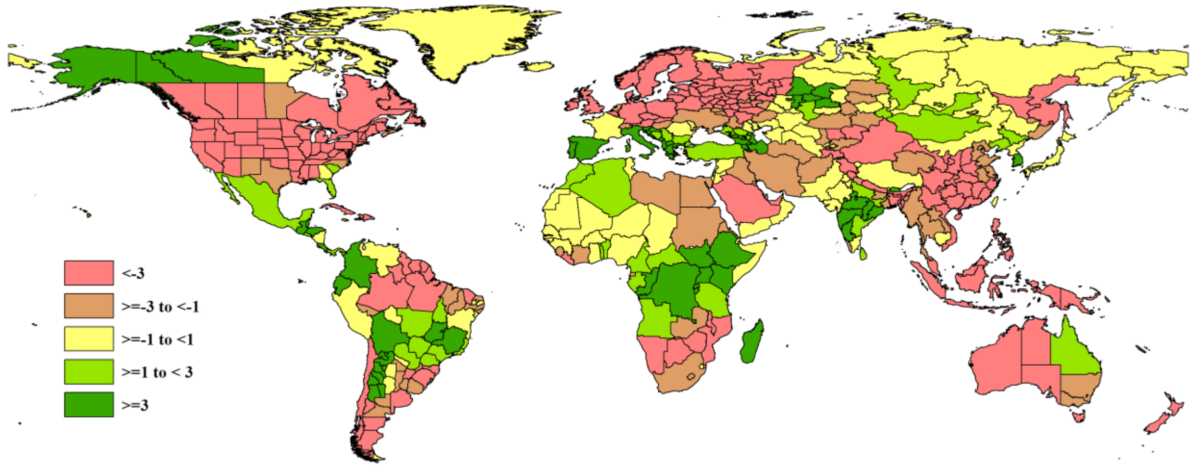

3.2 Country analysis

This section presents CropWatch results for each of thirty key countries (China is addressed in Chapter 4). The maps refer to crop growing areas only and include (a) Crop condition development graph based on NDVI average over crop areas, comparing the January-April 2017 period to the previous season and the five-year average (5YA) and maximum; (b) Maximum VCI (over arable land mask) for January-April 2017 by pixel; (c) Spatial NDVI patterns up to April 2017 according to local cropping patterns and compared to the 5YA; and (d) NDVI profiles associated with the spatial pattern under (c). See also Annex A, tables A.1-A.11, and Annex B, tables B.1-B.3, for additional information about indicator values and production estimates by country. Country agricultural profiles are posted on www.cropwatch.com.cn.

Figures 3.5-3.34. Crop condition for individual countries ([ARG] Argentina- [ZAF] South Africa) January-April 2017

ARG AUS BGD BRA CAN DEU EGY ETH FRA GBR IDN IND IRN KAZ KHM MEX MMR NGA PAK PHL POL ROU RUS THA TUR UKR USA UZB VNM ZAF

[ARG] Argentina

Argentina experienced generally favorable conditions during the monitoring period. Wheat harvest ended in early January, while harvesting of summer crops (soybean and maize) are still ongoing. TEMP (-0.6°) and RADPAR (-1%) were slightly below average, while RAIN was 40% above, resulting in a 19% above average BIOMSS for the reporting period compared to average. The abundant rainfall in Chaco (+70%), Corrientes (+81%), and La Pampa (+73%) account for respectively +34%, +33%, and +35% BIOMSS increases in those provinces. The cropped arable land fraction (CALF) in Argentina increased 1 percentage point over average, indicating more land is cropped. According to the NDVI based development profile, the NDVI values from January to April were overall lower than those in 2016, with the exception of the second half of April. The spatial NDVI patterns and corresponding profiles demonstrate that 42.5% of arable land had above average conditions during the summer crop season, while the VCIx map shows that VCIx values in most parts of the major maize and soybean producing areas (including Cordoba, Santa Fe, and northwestern Buenos Aires) were above 0.8. Moreover, VCIx values in the middle part of Chaco were overall above 1.0, which shows an unusually good crop growth situation. Altogether, indicators show a promising summer season output for Argentina. CropWatch puts maize production at 29.9 million tons (a 16% increase over 2016) and soybean production at 51.1 million tons, a level similar to that of last year. Production figures by provinces are provided in table B.1 in Annex B.

Figure 3.5. Argentina crop condition, January-April 2017

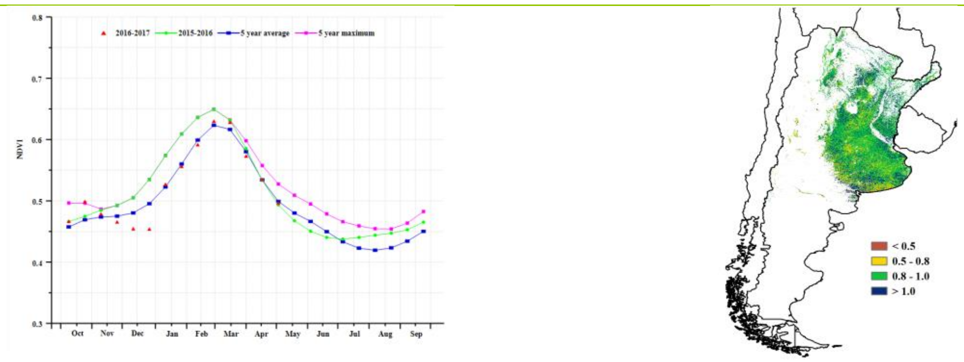

(a) Crop condition development graph based on NDVI (b) Maximum VCI

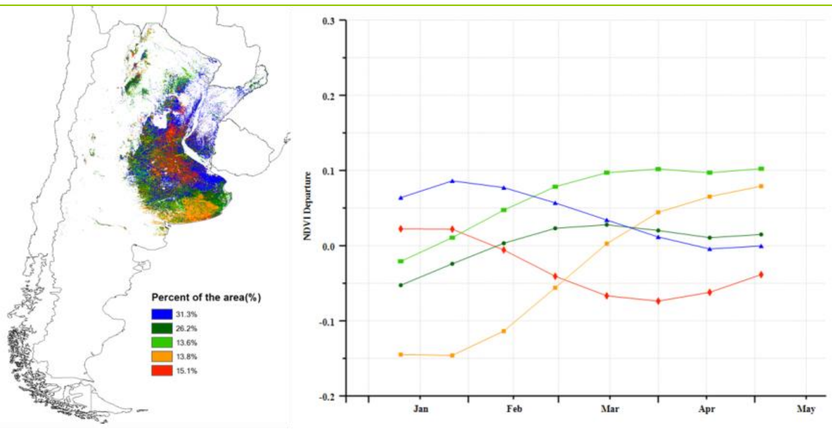

(c) Spatial NDVI patterns compared to 5YA (d) NDVI profiles

[AUS] Australia

Indicators in Australia show generally average condition for the January to April period, which is out of season for wheat and barley. The maximum VCI is 0.64 throughout the region, with a 3 percentage point increase in CALF compared with the recent five-year average. Compared to the same average, the spatial NDVI patterns and corresponding time profiles show below average conditions in central and northern New South Wales, with agroclimatic and biomass indicator departures for this state as follows: RAIN, -6%; TEMP average; RADPAR, -1%; and BIOMSS, -5%. Nationwide, agroclimatic indicators display average conditions (RAIN +14%, TEMP +0°C, and RADPAR -2%), resulting in a slightly positive biomass accumulation potential (BIOMSS +7%) compared with recent years. Positive departures of rain were recorded in South and Western Australia (+47% and +29%, respectively), contributing to favorable soil moisture conditions for the planting of wheat and barley in the coming month.

Figure 3.6. Australia crop condition, January-April 2017

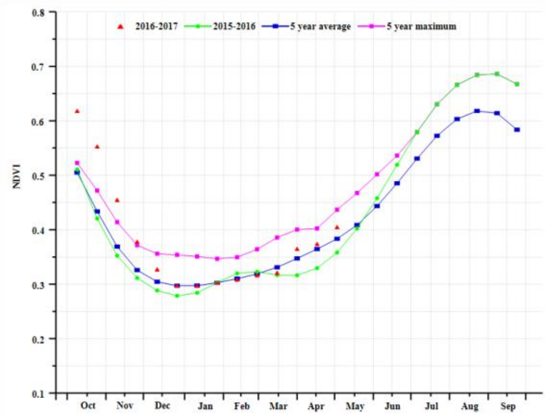

(a) Crop condition development graph based on NDVI

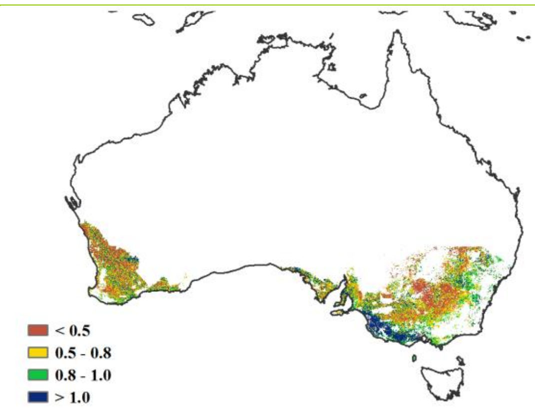

(b) Maximum VCI

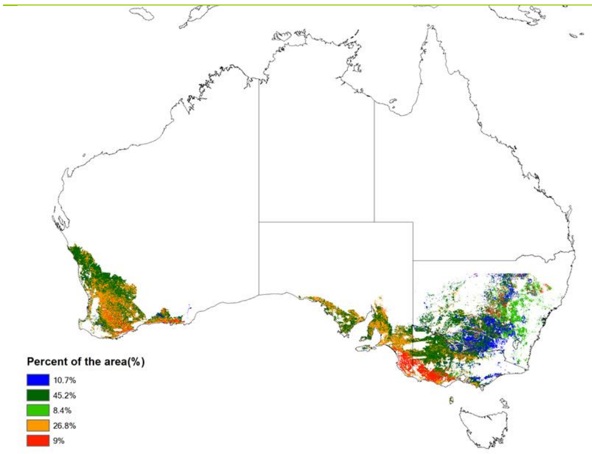

(c) Spatial NDVI patterns compared to 5YA

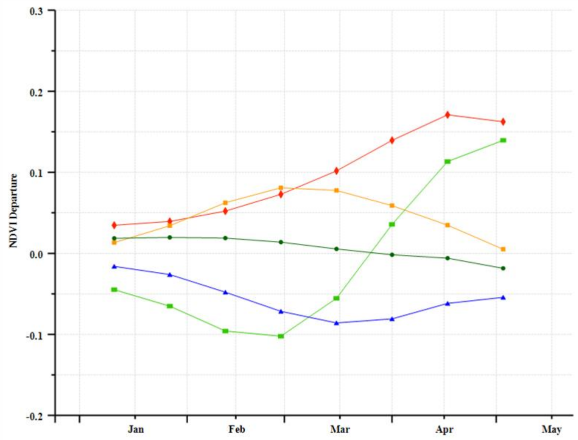

(d) NDVI profiles

[BGD] Bangladesh

CropWatch indicators show average crop condition for Bangladesh during the reporting period, which is the country's growing and harvesting season of irrigated boro rice. Crop condition was generally above average, even if it went through periods with depressed condition from late March to late April. The national average VCIx was 0.87, while the fraction of arable land (CALF) increased by 1 percentage point compared to the five-year average. Among the CropWatch agroclimatic indicators, RAIN was above average (+76%), while TEMP and RADPAR were below by -1.1°C and -5% respectively. The combination of factors resulted in high BIOMSS (+48%) compared to the five-year average. As shown by the crop condition development graph, average NDVI was below average from late January to April. Spatial NDVI patterns and profiles show that crop condition in 23.1% of the agriculture areas was below average, while for the other 76.9% it was above. Favorable weather conditions benefited boro paddy development this season. Although excess precipitation caused flooding in the northeast of the country in late March and early April (clearly visible in the NDVI profiles map), overall output of boro is expected to be favorable.

Figure 3.7. Bangladesh crop condition, January-April 2017

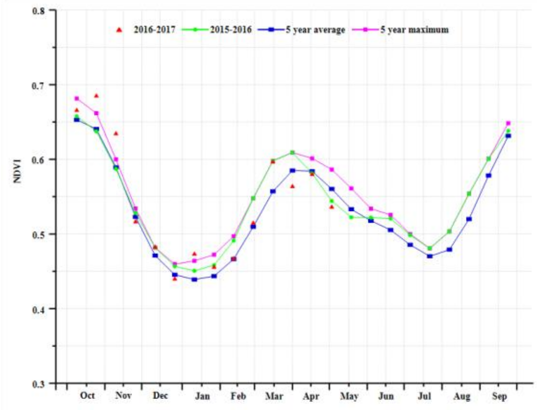

(a) Crop condition development graph based on NDVI

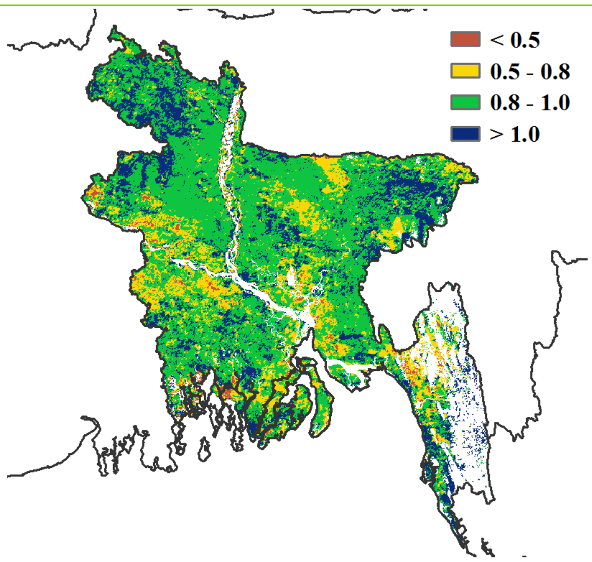

(b) Maximum VCI

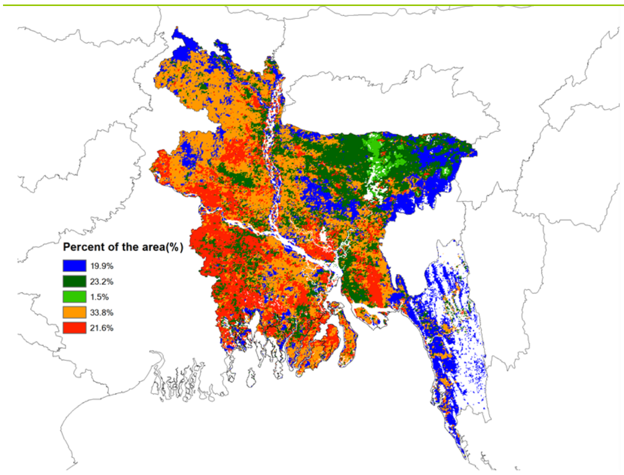

(c) Spatial NDVI patterns compared to 5YA

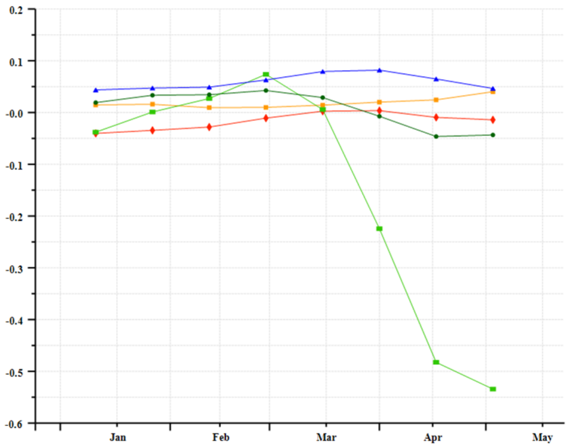

(d) NDVI profiles

[BRA] Brazil

Generally, crop condition in Brazil was slightly above the average of the previous five years during the monitoring period. Winter wheat was out of season. The harvest of maize (main season), rice, and soybean just started in early April and will last several months. Favorable agroclimatic conditions were observed at the national level, with RAIN at 6% above average, TEMP at -0.4°C, and RADPAR -2%, resulting in a 2% below average BIOMSS. Agroclimatic conditions, however, vary a lot among the major agricultural production states. Rio Grande do Sul for example received sufficient rainfall (RAIN, +57%), while Minas Gerais suffered from drought with a 32% rainfall shortage compared with average. Rainfall in Santa Catarina, Ceará, and Goias was recorded at -13%, -15%, and -18% compared to the fifteen-year average for RAIN. Temperature and RADPAR were close to “normal” except in Mato Grosso do Sul where TEMP was 1.3°C below average. Altogether, BIOMSS at the state level was below average in Minas Gerais, Santa Catarina, Ceará, and Goias, while 12% and 19% above average in Mato Grosso do Sul and Rio Grande do Sul, dominated by rainfall departure.

Unevenly distributed climatic conditions lead to differences in agronomic indicators. The maximum VCI map presents overall favorable condition, and VCIx in part of Mato Grosso do Sul and Rio Grande do Sul was above 1.0, indicating a crop condition above the situation over the past five-years. Spatial NDVI patterns and corresponding NDVI departure profiles also confirm that continuously above average NDVI mainly occurred in Mato Grosso do Sul, Rio Grande do Sul, and Pará. Below average NDVI mostly occurred in coastal areas of Bahia, Sergipe, and Alagoas. According to the NDVI-based crop condition development graph, national NDVI was below average due to the cloudy and rainy weather, but recovered to an average level and above that of the previous year by the end of April. Altogether, CropWatch projects the maize, rice, and soybean productions for Brazil above the previous harvest season (see Annex B). Even in Santa Catarina, which experienced a rainfall shortage, an increased planted area will result in crop production at a level similar to 2016.

Figure 3.8. Brazil crop condition, January-April 2017

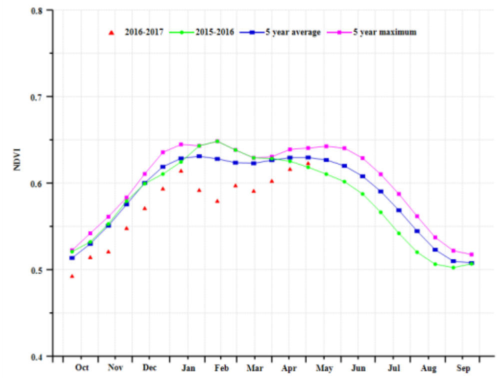

(a) Crop condition development graph based on NDVI

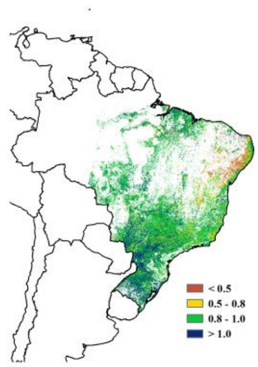

(b) Maximum VCI

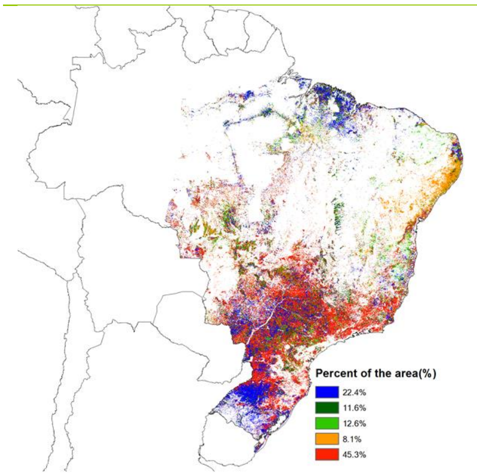

(c) Spatial NDVI patterns compared to 5YA

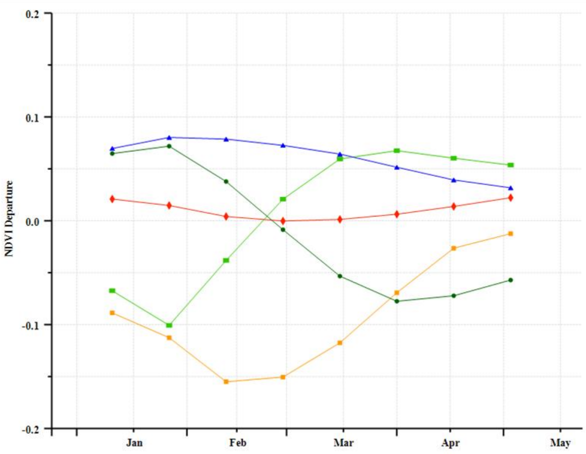

(d) NDVI profiles

[CAN] Canada

The current monitoring period is the growth and wintering season of winter crops in Canada. Overall, CropWatch agroclimatic and agronomic indicators indicate above average crop condition in the country. While RAIN and TEMP were above average (+17% and +1.4°C, respectively), RADPAR was significantly below (-6%) due to rainy weather. Above average rainfall fell in major crop production provinces, and the accumulated rainfall (RAIN) for Alberta, Manitoba, and Saskatchewan was +13%, +10%, and +3% respectively, according to this CropWatch agroclimatic indicator. Over the reporting period, temperatures (TEMP) in the same three provinces were +1°C, +2°C, and +2°C, respectively. Warm and humid weather is good for the growth of winter crops, and most parts of Alberta, Manitoba, and Saskatchewan showed positive NDVI departures. Altogether, crop condition is assessed as favorable.

Figure 3.9. Canada crop condition, January-April 2017

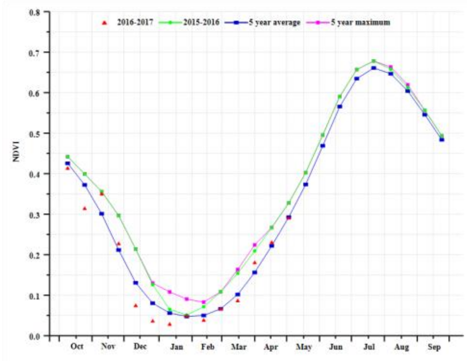

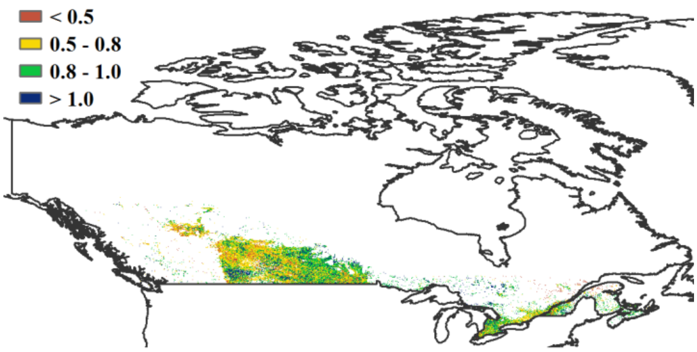

(a) Crop condition development graph based on NDVI (b) Maximum VCI

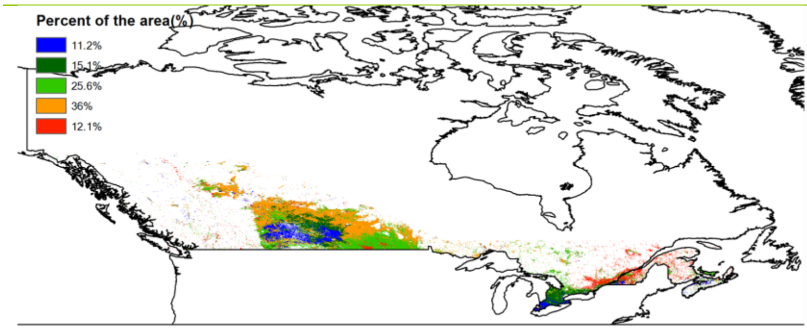

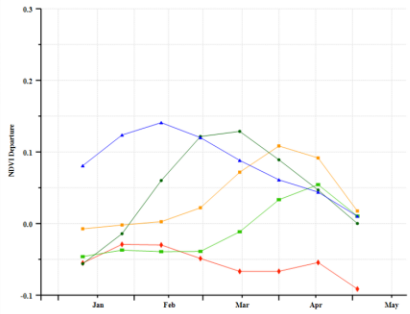

(c) Spatial NDVI patterns compared to 5YA (d) NDVI profiles

ARG AUS BGD BRA CAN **DEU** EGY ETH FRA GBR IDN IND IRN KAZ KHM MEX MMR NGA PAK PHL POL ROU RUS THA TUR UKR USA UZB VNM ZAF

[DEU] Germany

Crop condition in Germany shows spatially contrasted patterns. Winter wheat and winter barley are currently in the vegetative stages, and maize is being planted. The CropWatch agroclimatic indicators show below average rainfall (RAIN, -4%), below average temperature (TEMP, -0.2°C, except in the northern wheat zone where TEMP was +0.2°C), and RADPAR at the national level at 5% below average. Above average rainfall occurred throughout the middle-north of Germany, including in the northern wheat zone (RAIN, +13%), a northwest mixed wheat and sugar beets area (+3%), and an eastern area with sparse crops (+15%, also the largest positive departure). With close to average and generally favorable rainfall conditions in the crop planting areas, BIOMSS is expected to increase by 2% nationwide compared to the five-year average, and even more in some areas such as in the eastern sparse crop area and the northern wheat zone, two areas where the projected BIOMSS departure reaches +12% over average.

As shown by the crop condition development graph, national NDVI values were below average from January to early March due to low temperature, and then above average from early March to early April as a result of favorable rainfall and suitable temperature. After early April, values were again below average due to sparse rainfall and low minimum temperature. This observation is confirmed by the NDVI profiles and the country's spatial NDVI patterns, which are also reflected by the maximum VCI in the different areas, with a VCIx of 0.85 for Germany overall. Generally, the values of the indicators mentioned above point at average condition for most winter crop areas in Germany.

Figure 3.10. Germany crop condition, January-April 2017

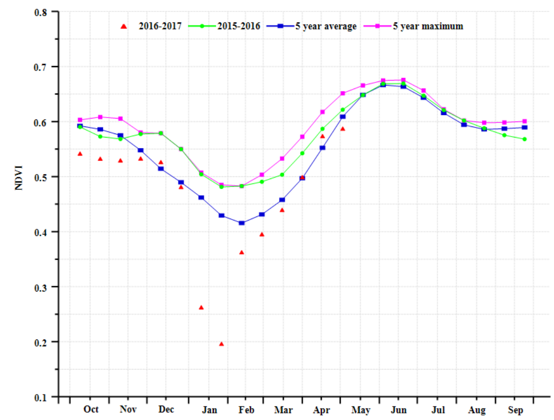

(a) Crop condition development graph based on NDVI

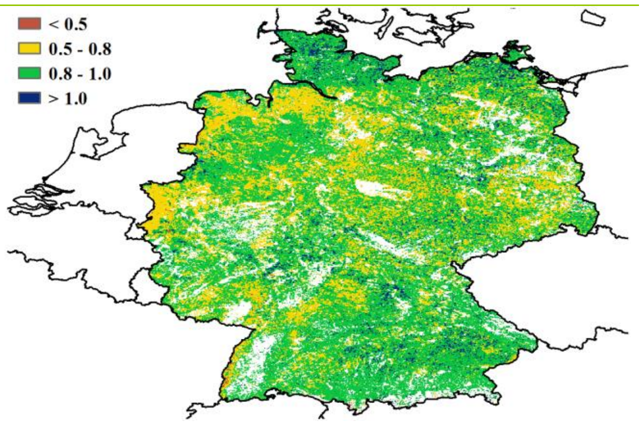

(b) Maximum VCI

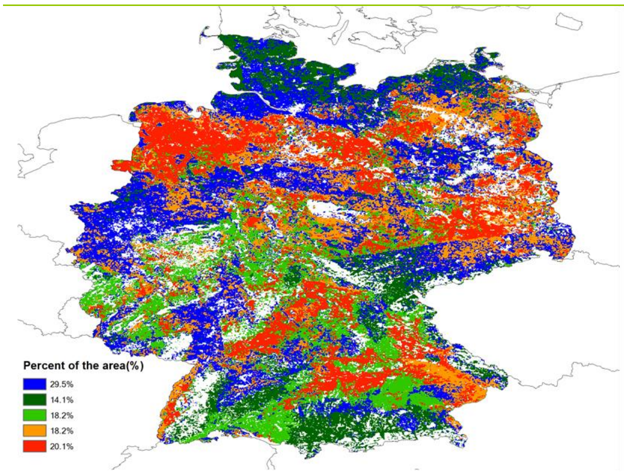

(c) Spatial NDVI patterns compared to 5YA

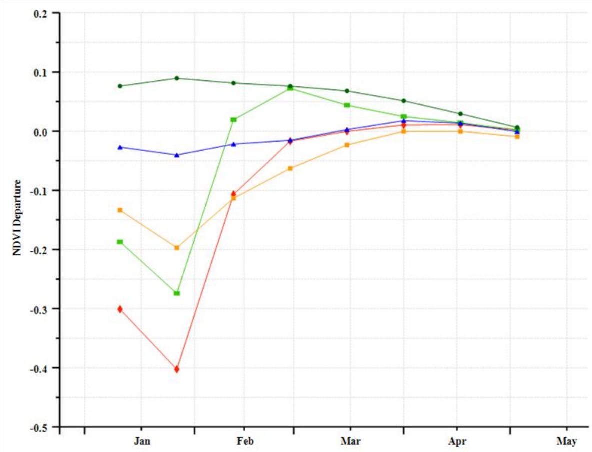

(d) NDVI profiles

[EGY] Egypt

In Egypt, where the most common crops are clover, wheat, sugar beet, and vegetables, the recent monitoring period covers the winter season. The period was characterized by agroclimatic conditions that were below average, with values for RAIN of -18%, TEMP -0.9°C, and RADPAR -1%. Nevertheless, the biomass production potential (BIOMSS) increased over the five-year average by 27%. Because of the country's prevailing desert conditions, more than 95% of cultivated land is irrigated, and rainfall plays a minor part.

The national crop condition development graph based on NDVI shows that crops were below the average condition of the last five years and almost at the same level as those of the same monitoring period for the 2015-2016 season. The spatial NDVI profile shows relatively good crop condition in the Nile valley and delta. The fraction of cropped arable land (CALF) increased by 1 percentage point, compared to average values, and VCIx reached 0.75. In general, for this monitoring period, winter crops in Egypt are assessed as slightly below average.

Figure 3.11. Egypt crop condition, January-April 2017

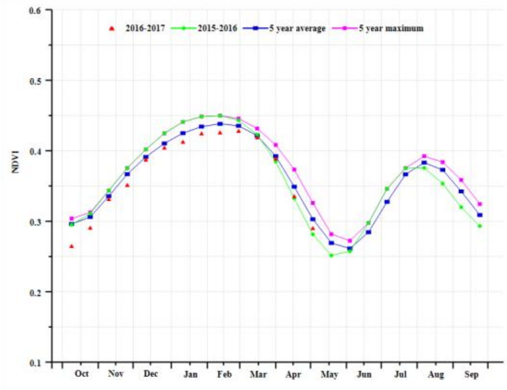

(a) Crop condition development graph based on NDVI

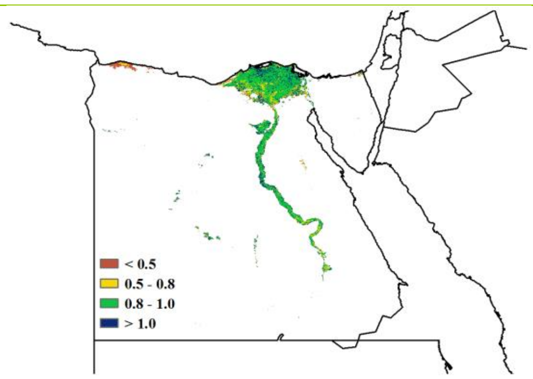

(b) Maximum VCI

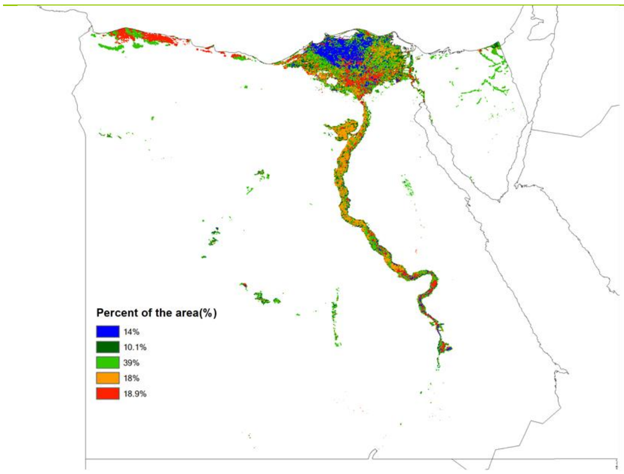

(c) Spatial NDVI patterns compared to 5YA

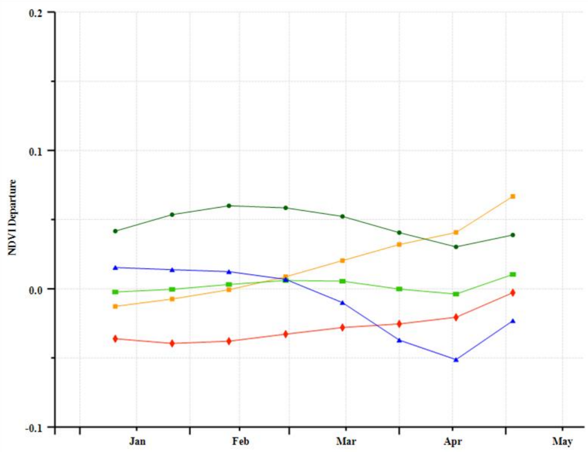

(d) NDVI profiles

ARG AUS BGD BRA CAN DEU EGY **ETH** FRA GBR IDN IND IRN KAZ KHM MEX MMR NGA PAK PHL POL ROU RUS THA TUR UKR USA UZB VNM ZAF

[ETH] Ethiopia

The monitoring period from January to April coincides with the early Belg cropping season; rainfall in this period is generally less reliable than during the main Meher season that corresponds to all crops harvested from August. With the exception of radiation (RADPAR, +4%), agroclimatic indicators show a general reduction in observed values compared to average: temperature (TEMP) -0.4°C and rainfall (RAIN) -9%, corresponding to an amount of 171 mm. However, the northwestern lowlands of Tigray, Amhara, and Benishangul-Gumuz, which are prominent cereal-producing areas, recorded a significant rise in rainfall of about 53%, which subsequently resulted in an increased biomass production potential (BIOMSS) of 44% above the five-year average for the period. Similarly, a large surplus of rainfall of about +136% was received in the western parts of Addis Ababa and Benishangul-Gumuz. BIOMSS in this area was 104% above average, which was very beneficial for the development of rangelands. In contrast, dry conditions prevailed in the eastern parts of the country, including the southeast highlands (Somali area), which recorded a rainfall deficit of 34%. BIOMSS departure in the southeastern mixed maize zone was -28%, which was the worst of all negative departures.

The spatial NDVI profiles show areas with negative values amidst positive ones, corresponding with the rainfall variations across the different areas. In addition, maximum VCI was about 0.59, indicating just fair crop condition; VCIx was highest (above 1) in some patches of Amhara and southwest Tigray, consistent with the increased biomass recorded in these areas. The western mixed-maize areas of SNNP, due to normal RAIN and increased RADPAR (+4.3%), experienced a BIOMSS increase of about 7.6% compared to average. Overall, crop condition seems to be favorable, but because most production occurs during the Meher season the final outcome of the situation is still very open.

Figure 3.12. Ethiopia crop condition, January-April 2017

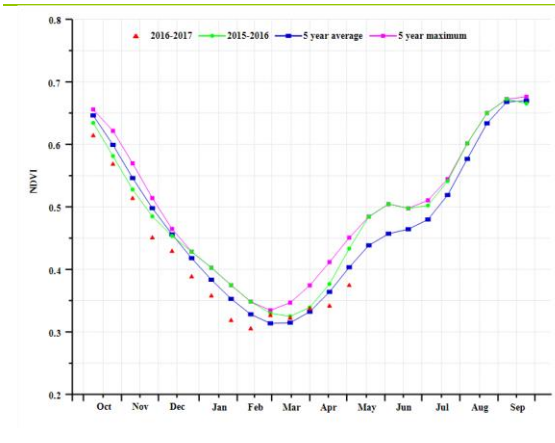

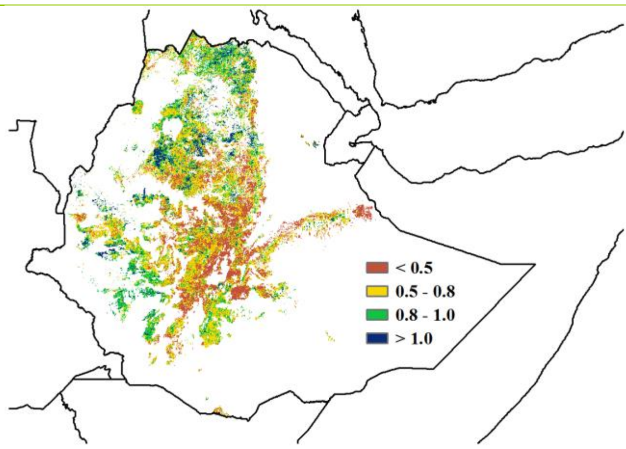

(a) Crop condition development graph based on NDVI (b) Maximum VCI

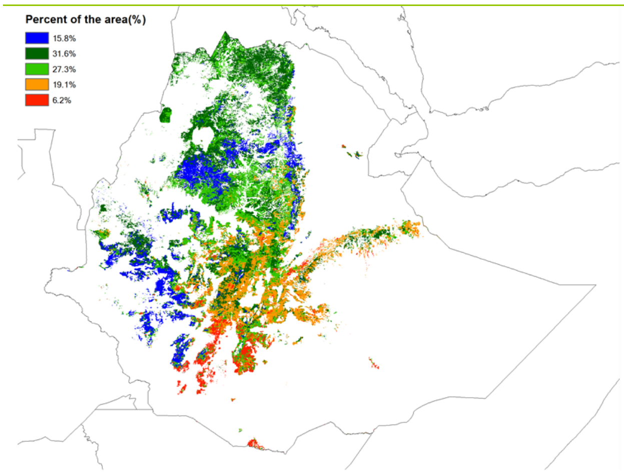

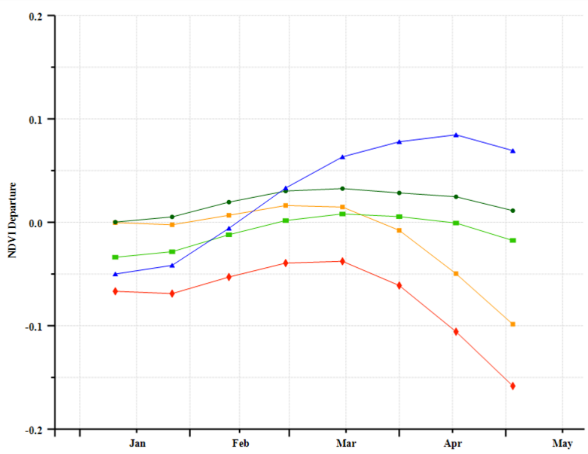

(c) Spatial NDVI patterns compared to 5YA (d) NDVI profiles

[FRA] France

According to the overall NDVI-based season development graph and spatial NDVI patterns, the condition of crops in France was spatially contrasted over the January-April monitoring period. Currently, winter wheat, winter barley, and spring barley are in the vegetative stages. At the national level, compared with the average for the same period, CropWatch agroclimatic indicators show a 36% decrease in RAIN, a 0.8°C decrease in TEMP, and close to average RADPAR. Subsequently, BIOMSS presents a 31% decrease over average due to the continuous rainfall deficit, especially after mid-March, coupled with the impact of low temperature. As shown by crop condition development graph based on NDVI, however, national NDVI values were well above average and close to the five-year maximum from early March to early April, consistent with a VCIx of 0.87 for France.

The spatial NDVI patterns for France show that NDVI values in many areas were below the five-year average from early January to the end of February. This, however, does not apply to 4.1 percent of agricultural areas, including the east of Franche-Comte, Rhone-Alpes, Provence Alpes Cote d'Azur, and the Mediterranean region of southern and southwestern France, where favorable conditions occurred throughout the reporting period. In the areas with below average values at the beginning of the monitoring period, NDVI values went up and above average again from early March to early April as a result of favorable temperature, while again dropping below average after early April due to the distinctly drier-than-usual weather conditions and low minimum temperature, which also affected flowering rapeseed in eastern France. Observations are consistent with the crop condition development graph based on NDVI.

Generally, the agronomic indicators mentioned above point at average condition for most winter crop areas of France for the time being, but more rain is needed in several important crop production areas to sustain good yields.

Figure 3.13. France crop condition, January-April 2017

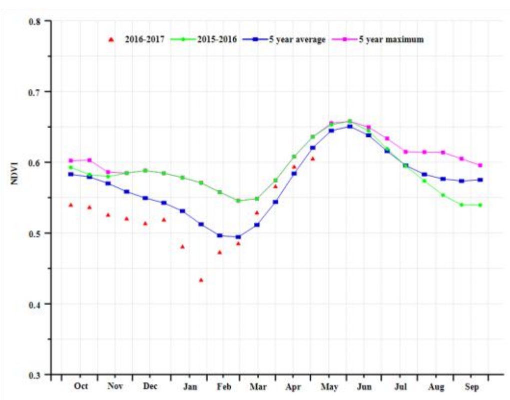

(a) Crop condition development graph based on NDVI

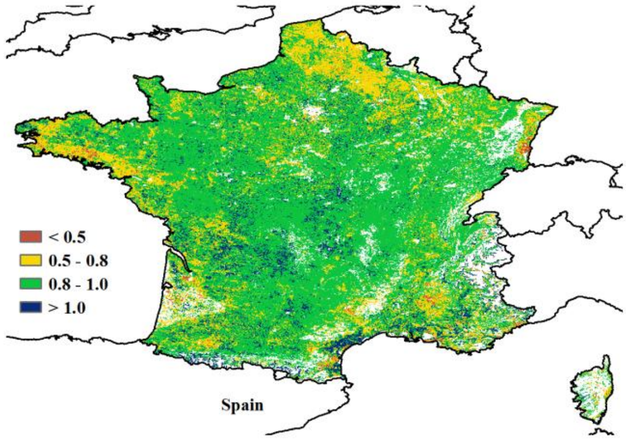

(b) Maximum VCI

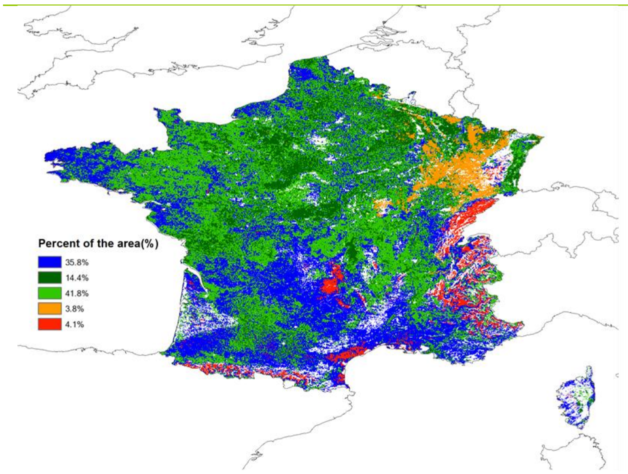

(c) Spatial NDVI patterns compared to 5YA

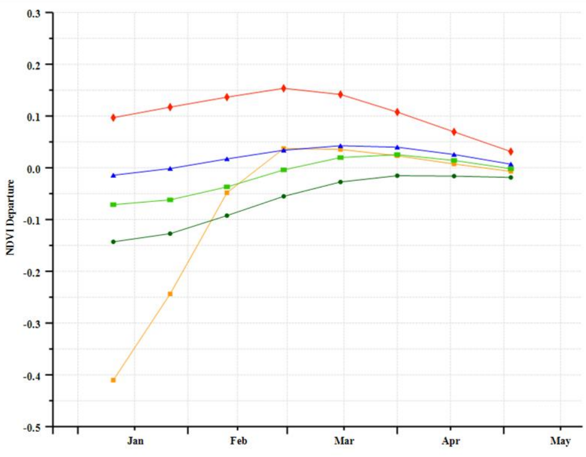

(d) NDVI profiles

[GBR] United Kingdom

Currently, wheat, winter barley, spring barley, and rapeseed are in the vegetative stages. Crop condition in the United Kingdom showed generally favorable condition over the reporting period, resulting from mostly average weather at the national scale, with only radiation (RADPAR) showing a marked decrease of 9%. The biomass production potential BIOMSS is expected to be average as well. As shown by the crop condition development graph and the national NDVI values, crop condition is average at the time of reporting, after recovering from low values from late January to late February in the south, especially the southeast in an area extending roughly from Norfolk shire to Dorset shire and south of it. This spatial pattern is also reflected by the maximum VCI in the different areas, with a VCIx of 0.82 for the country overall. The area of cropped arable land (CALF) increased by 1 percentage point compared to the five-year average.

Figure 3.14. United Kingdom crop condition, January-April 2017

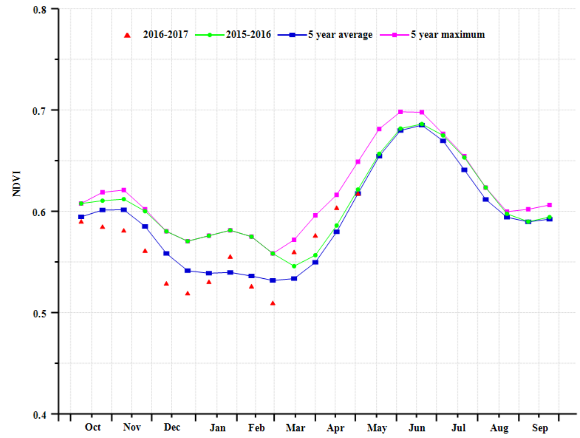

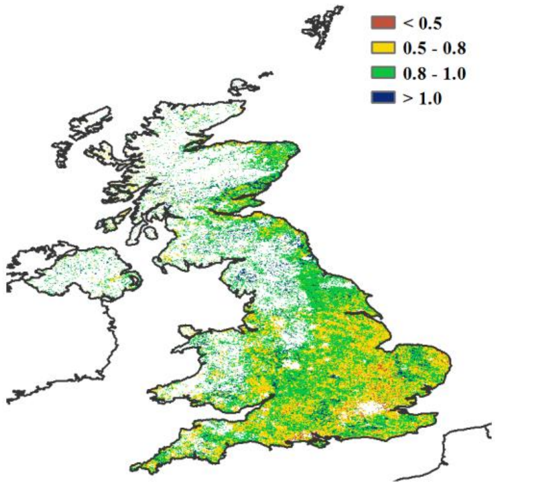

(a) Crop condition development graph based on NDVI

(b) Maximum VCI

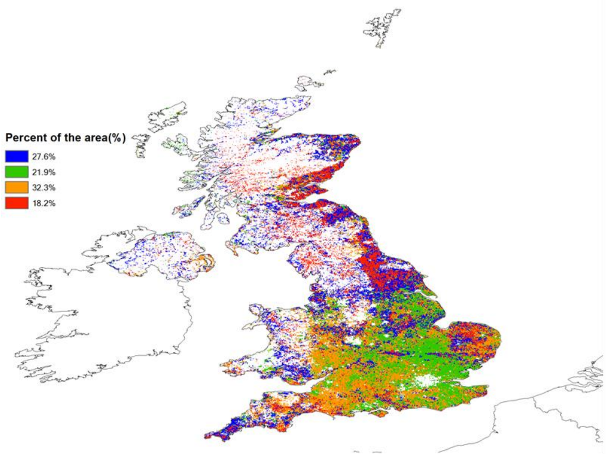

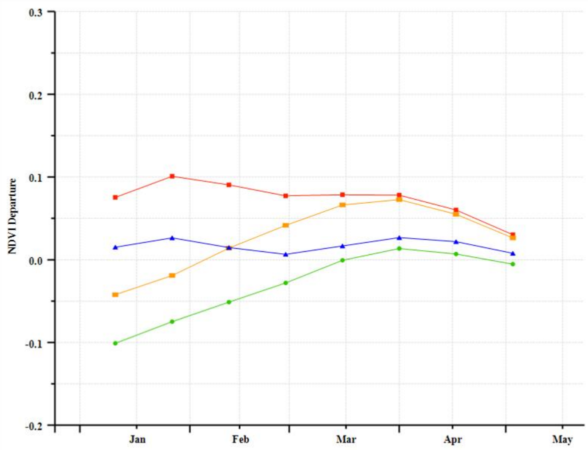

(c) Spatial NDVI patterns compared to 5YA

(d) NDVI profiles

ARG AUS BGD BRA CAN DEU EGY ETH FRA GBR **IDN** IND IRN KAZ KHM MEX MMR NGA PAK PHL POL ROU RUS THA TUR UKR USA UZB VNM ZAF

[IDN] Indonesia

Indonesia presented average crop condition over the January-April monitoring period, with a national VCIx value of 0.73. The monitoring period covers the growing and harvesting stages of the rainy season maize and rice. The area of cropped arable land (CALF) in the country is comparable with the five-year average. Compared with the recent fifteen-year average for the same period, precipitation (RAIN) was above average by 7%, while temperature was below (TEMP, -0.7°C), and sunshine (RADPAR) showed a decrease of 4%. The biomass production potential BIOMSS was up 2% compared to its recent five-year average.

According to the NDVI patterns and profiles, the condition of crops was above average throughout the reporting period in Jambi, Sumatera Selatan, and Riau, while it has been below average since February in Sindang Regency in West Kalimantan province. Nationwide, the NDVI based crop condition development graph was below both the five-year average and last year’s values from January to late February.

Overall, the abundant rainfall during the reporting period provided favorable soil moisture condition for the secondary crops, and overall prospects for the country are favorable.

Figure 3.15. Indonesia crop condition, January-April 2017

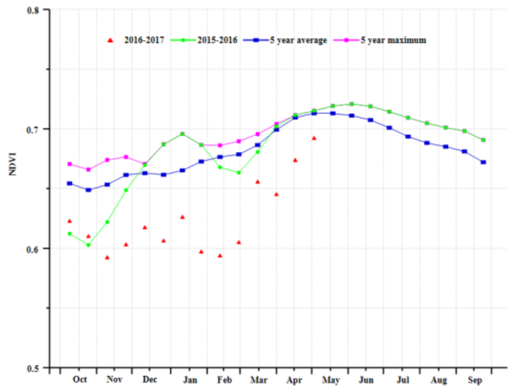

(a) Crop condition development graph based on NDVI

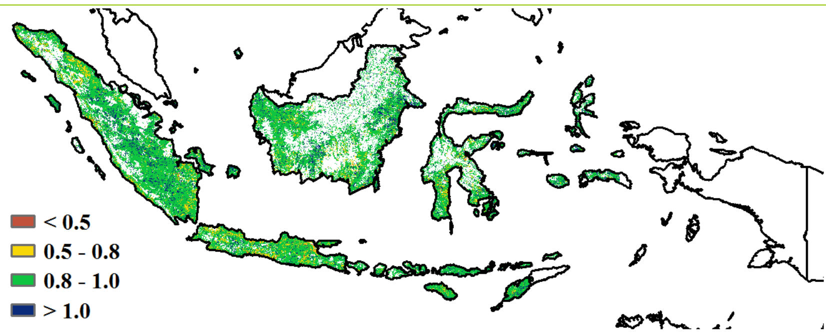

(b) Maximum VCI

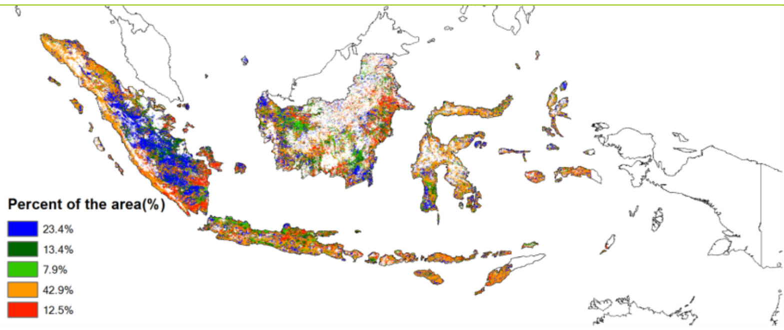

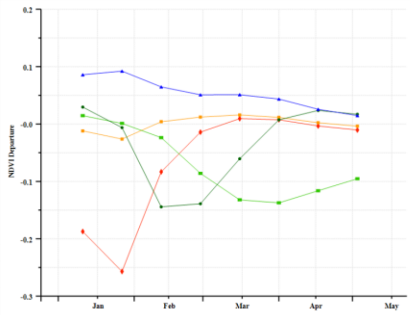

(c) Spatial NDVI patterns compared to 5YA

d) NDVI profiles

[IND] India

The monitoring period coincides with the growing and harvesting seasons of rabi (winter) crops, such as wheat, maize, sorghum, groundnuts, rapeseed, and rice. Temperature and radiation for the country overall were about average (TEMP, +0.2°C and RADPAR, +1%), but rainfall (RAIN) showed a 16% drop, and the biomass production potential (BIOMSS) is down 28% compared to its five-year average. Marked rainfall deficits occurred in Uttar Pradesh (RAIN, -52%), Bihar (-47%), Andhra Pradesh (-41%), and Karnataka (-39%), among others. National crop condition development was comparable to 2015-2016 and below the average of the previous five years. The maximum VCI index was low (VCIx<0.5) in the southern areas of Mysore and Madras. The NDVI profile values remained favorable for the entire country, exception for some areas in the southern part of the country (8.5% of croplands) and north (18.7%). With a favorable maximum vegetation condition index (0.83) and an increase in the fraction of cropped arable land (CALF) by 4 percentage points over average, crop prospects for the country remain average.

Figure 3.16. India crop condition, January-April 2017

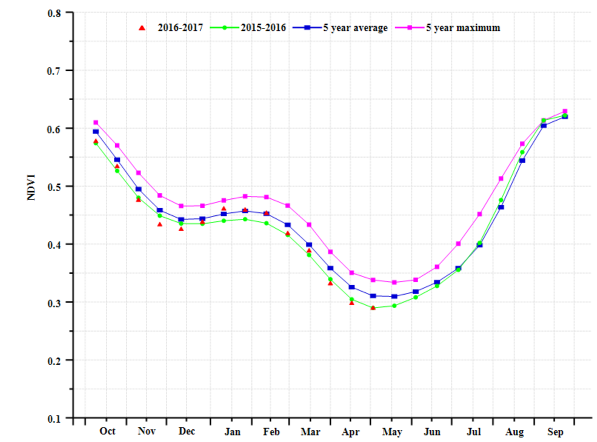

(a) Crop condition development graph based on NDVI

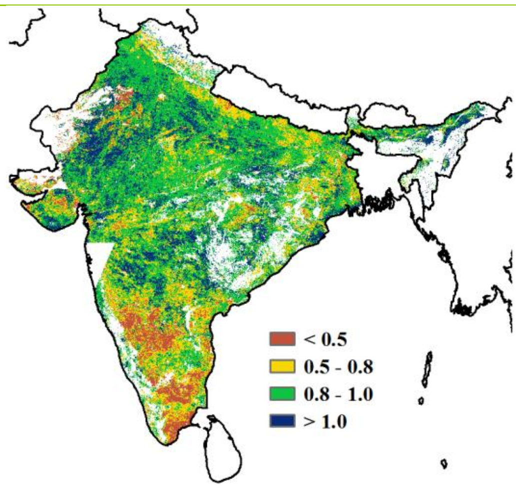

(b) Maximum VCI

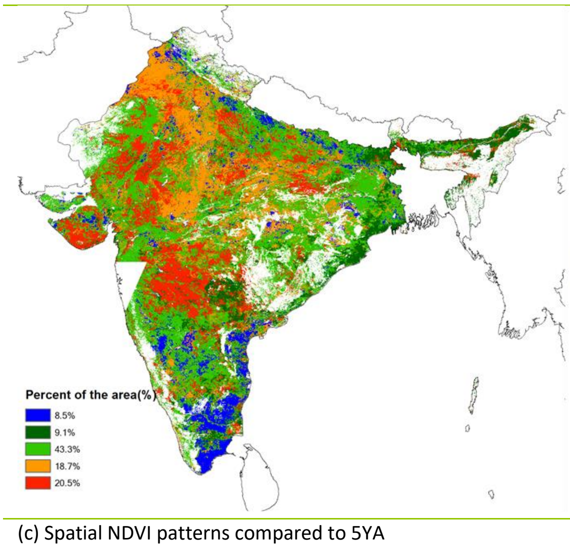

(c) Spatial NDVI patterns compared to 5YA

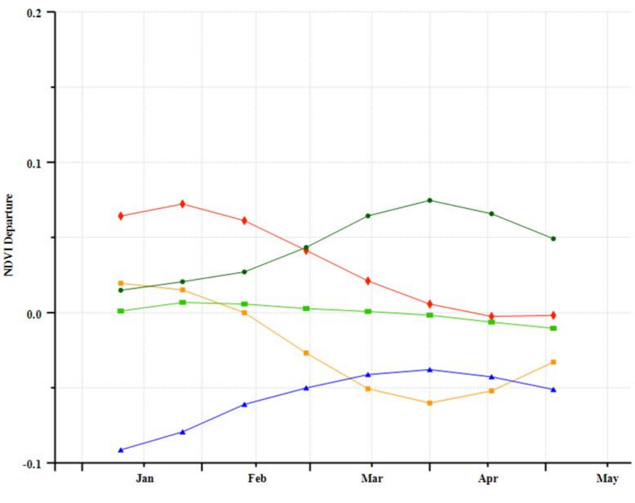

(d) NDVI profiles

ARG AUS BGD BRA CAN DEU EGY ETH FRA GBR IDN IND **IRN** KAZ KHM MEX MMR NGA PAK PHL POL ROU RUS THA TUR UKR USA UZB VNM ZAF

[IRN] Iran

Crop condition in Iran was generally below average over the reporting period. During this time, winter wheat was still growing, and barley was harvested. Accumulated rainfall (RAIN, -9%), temperature (TEMP, -0.6°C), and radiation (RADPAR, -1%) were below average, leading to a decrease in the BIOMSS index by 7% compared to previous years. The national average of the maximum VCI index was 0.5, while the cropped arable land fraction (CALF) significantly decreased by 19 percentage points compared to the five-year average. The available information implies that crop phenology for winter wheat is likely delayed due to the unfavorable weather conditions.

From February to April, crop condition was below average almost across the country, in an area accounting for 89.7% of total arable land. Areas with above average condition are mainly distributed in Hormozgan province and surrounding regions. In West Azerbaijan, Kermanshah, and Golestan provinces, condition of crops was even below the five-year average over the entire period. In the East Azerbaijan, Ilam, Luristan, and Bushehr provinces, crop condition was below average from January to March, but recovered to average in April.

Overall, winter crop condition in Iran has not been favorable over the monitoring period. Due to the crop phenology change, the final outcome of winter wheat in Iran depends on weather and crop conditions in the next few months.

Figure 3.17. Iran crop condition, January-April 2017

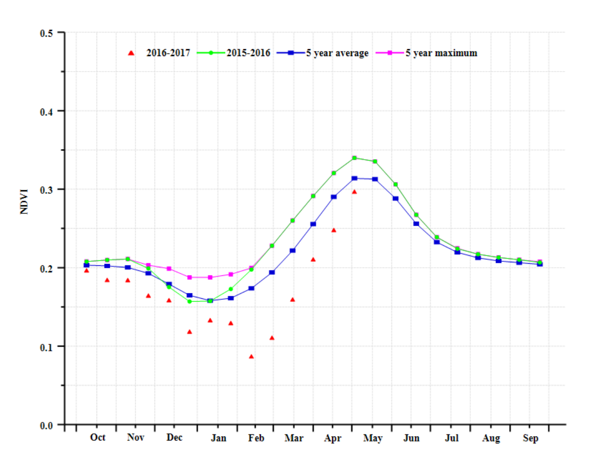

(a) Crop condition development graph based on NDVI

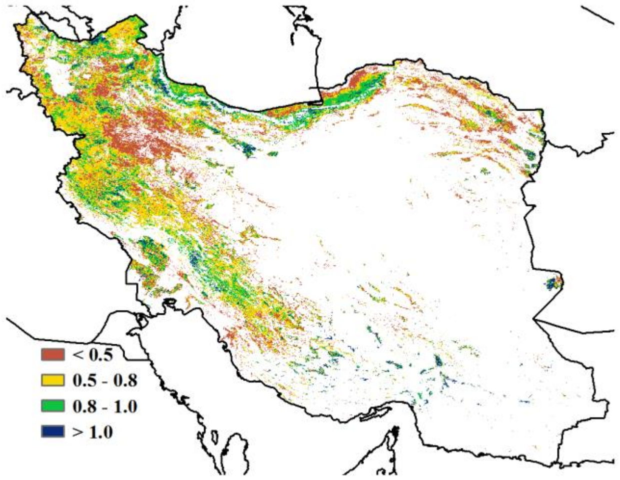

(b) Maximum VCI

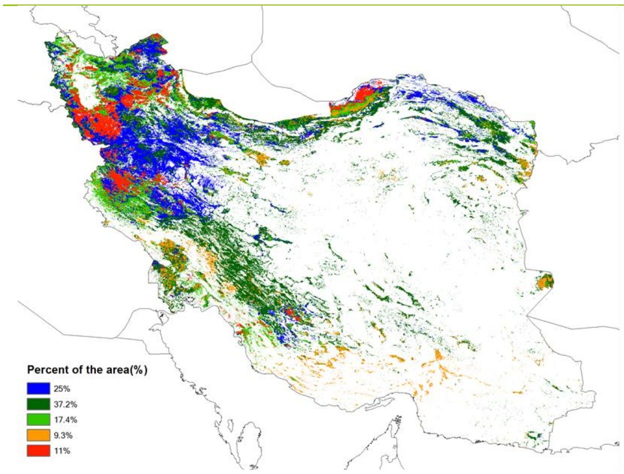

(c) Spatial NDVI patterns compared to 5YA

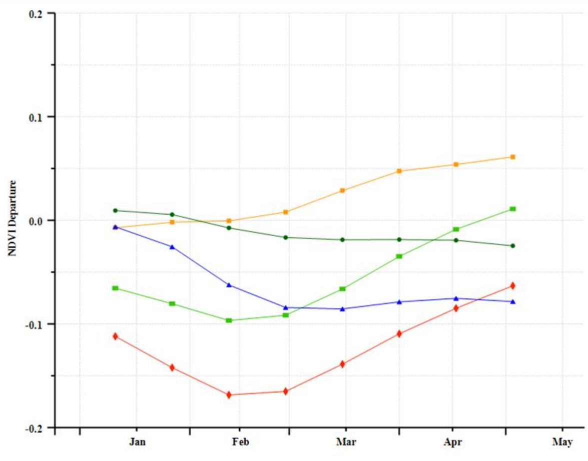

(d) NDVI profiles

[KAZ] Kazakhstan

As shown by the national NDVI development graph, no winter crops are normally cultivated in Kazakhstan, while spring crops are currently at the sowing and vegetative stages. During the monitoring and reporting period, rainfall (RAIN) was below average by 2%, while temperature (TEMP) was above by 0.4°C, and PAR accumulation (RADPAR) again below average by 2%, leading to a small biomass potential (BIOMSS) increase of 2% over the recent five-year average. In the main agricultural regions, rainfall was down 11% in northeastern Zapadno-Kazakhstanskaya, 3% in the north of Severo Kazakhstanskaya, and 6% in the Akmolinskaya oblast. However, spatial NDVI patterns compared to the recent five years and NDVI profiles indicate that the south and north had favorable vegetation development, an important observation in a country where livestock plays a major role. Poor vegetation that occurs in about 10.6% of areas is concentrated along the Chinese border. Current NDVI profiles and values of maximum VCI are about average, with more favorable areas in the south.

Altogether, crop prospects for the country are currently average, with the exception of limited patches along the Chinese border.

Figure 3.18. Kazakhstan crop condition, January-April 2017

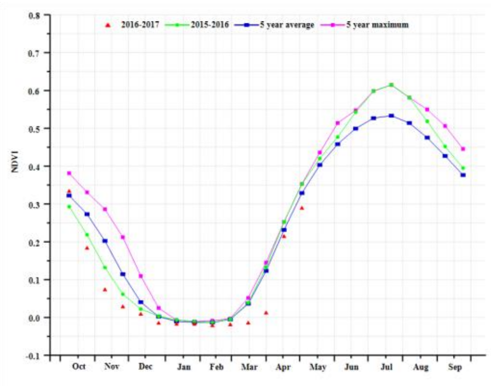

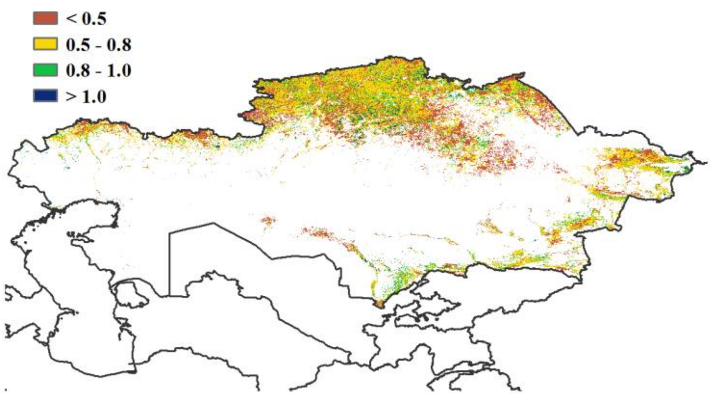

(a) Crop condition development graph based on NDVI (b) Maximum VCI

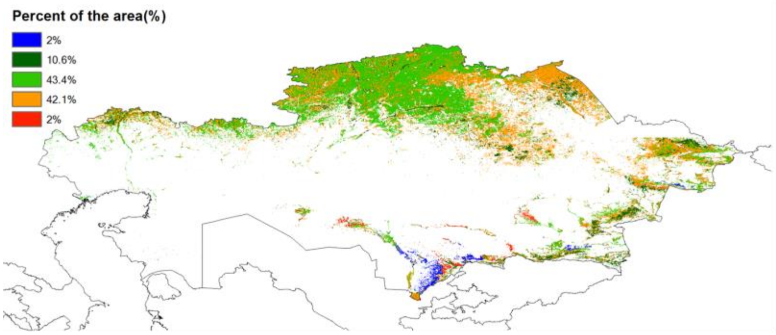

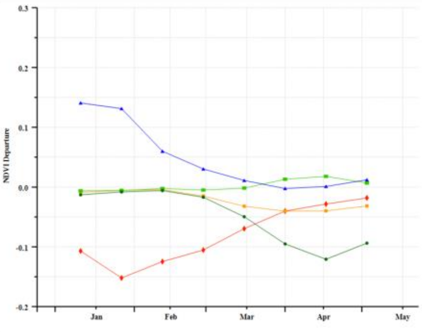

(c) Spatial NDVI patterns compared to 5YA (d) NDVI profiles

[KHM] Cambodia

The January to April monitoring period covers the growing stage of the second (dry season) rice in Cambodia. Compared to average, the CropWatch agroclimatic indicators show markedly over average rainfall (RAIN, +30%), but a decrease in temperature (TEMP, -1.0°C) and normal sunshine. Average and even better than maximum NDVI profiles all point at very favorable conditions at the end of the reporting period. Moreover, vegetation condition indices (VCIx) are above 0.8 in large expanses of the country, which points at unusually good conditions. Considering, in addition, that the fraction of cropped arable land (CALF) was 22 percentage points above the five-year average, crop prospects in Cambodia are very favorable.

Figure 3.19. Cambodia crop condition, January-April 2017

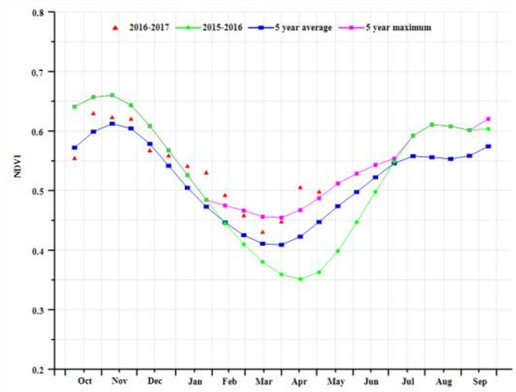

(a) Crop condition development graph based on NDVI

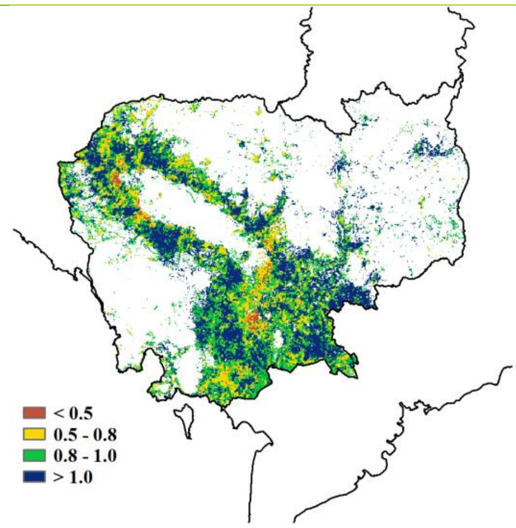

(b) Maximum VCI

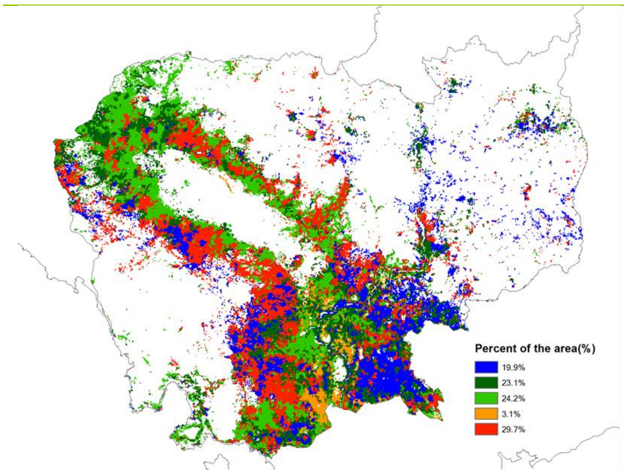

(c) Spatial NDVI patterns compared to 5YA

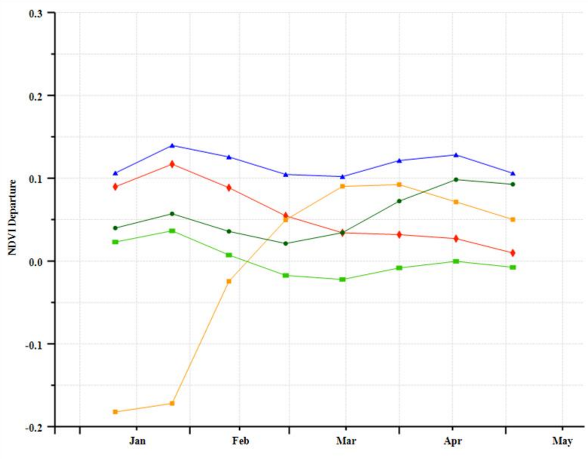

(d) NDVI profiles

[MEX] Mexico

In Mexico, maize, sorghum, and rice for the spring to summer season have been harvested during late January and early February this year, while winter crops—maize, sorghum, and wheat—have been growing since February. During the current monitoring period, according to the crop condition development graph based on NDVI, crop condition was generally below average with increasing departures over time.

The CropWatch agroclimatic indicators show that rainfall (RAIN) dropped 9% below average, while temperature (TEMP) and radiation (RADPAR) increased by 0.4°C and 3%, respectively. The resulting biomass production potential (BIOMSS) was 3% below average. The maximum VCI at the national level was 0.72, with lower values located in central and southern Mexico, such as in the states of Zacatecas, Aquascalientes, Jalisco, Michoacan, Mexico, Tiaxcala, Morelos, Puebla, and Guerrero. In contrast, high values of maximum VCI occur in eastern Mexico, including Veracruz, Tobasco, and Oaxaca states. As shown by the map of spatial NDVI patterns and corresponding profiles, 51.4% of planted areas in the country experienced generally below average condition at the end of the reporting period, with these areas mainly located in Zacatecas, Aquascalientes, Jalisco, Michoacan, Guerrero, Campeche, and Yucatan, which agrees well with the pattern of lower VCIx values. Favorable crop condition occurred in Coahuila, Nuevo Leon, Tamaulipas, Sonora, Chihuahua, and Tobasco.

Based on the above analysis and the fact that the fraction of cropped arable land (CALF) is 3 percentage points over average, crops yields for Mexico's current season are estimated to be slightly below average.

Figure 3.20. Mexico crop condition, January-April 2017

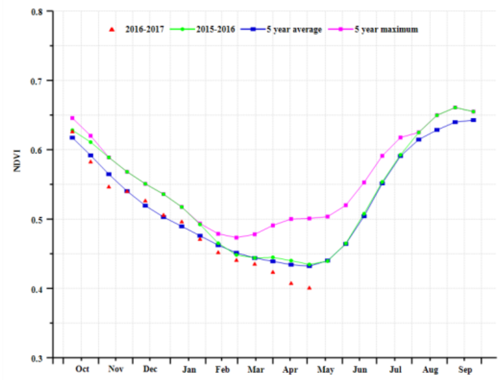

(a) Crop condition development graph based on NDVI

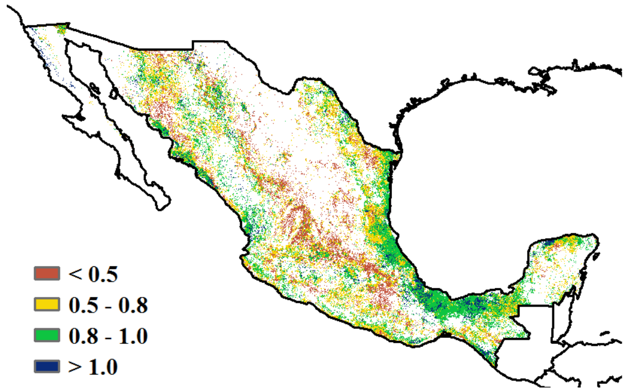

(b) Maximum VCI

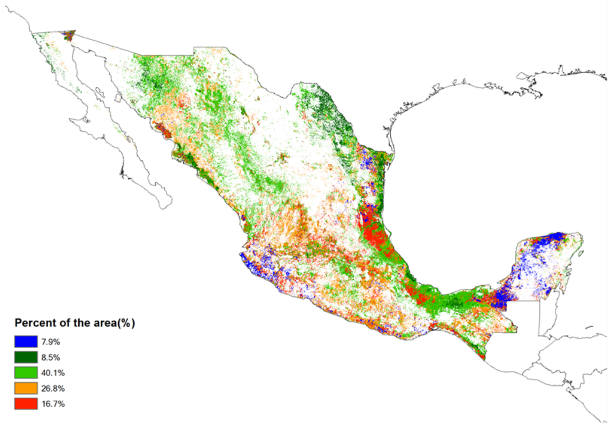

(c) Spatial NDVI patterns compared to 5YA

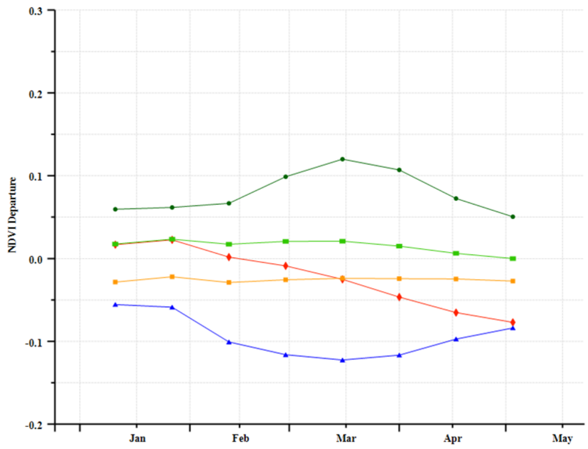

(d) NDVI profiles

ARG AUS BGD BRA CAN DEU EGY ETH FRA GBR IDN IND IRN KAZ KHM MEX **MMR** NGA PAK PHL POL ROU RUS THA TUR UKR USA UZB VNM ZAF

[MMR] Myanmar

The reporting period from January to April covers the growing and harvesting season of winter rice; all maize was harvested by mid-April. According to the CropWatch indicators, crop condition was average during the monitoring period. Rainfall (RAIN) was 5% above average, temperature was close to average (TEMP, -0.2°C), and radiation (RADPAR, -3%) was only slightly below average. Across the country, the fraction of cropped arable land (CALF) increased by 13 percentage points over the five-year average for the January-April period, and the biomass accumulation potential (BIOMSS) was 5% above average. As a result, national crop condition development profiles were also mostly above average and even exceeded the five-year maximum in February and mid-April. Spatial NDVI profiles are also mostly positive (above average) throughout the country and across the reporting period, especially in southern Myanmar, including Kayah, Bago, Yangon, Ayeyarwaddy, and some scattered locations in the center. It is worth mentioning that VCIx performed well all over the country, especially in Magwe, Mandaly, Shan and northern Bago, which had not only high VCIx values (>1), suggesting a better condition than ever before, but also high NDVI values. Overall, crop condition for Myanmar is assessed as above average.

Figure 3.21. Myanmar crop condition, January-April 2017

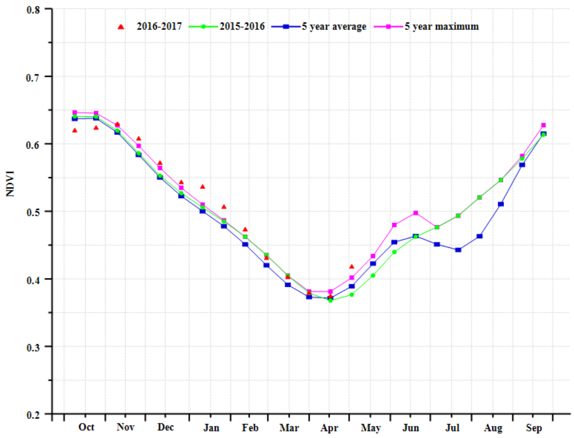

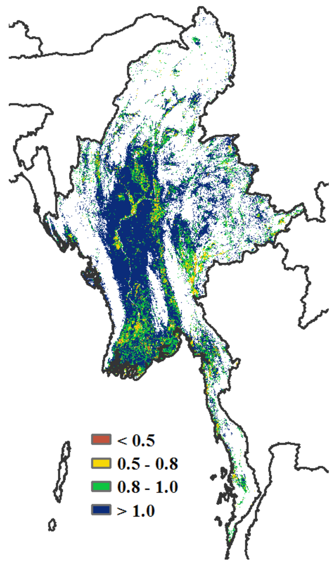

(a) Crop condition development graph based on NDVI

(b) Maximum VCI

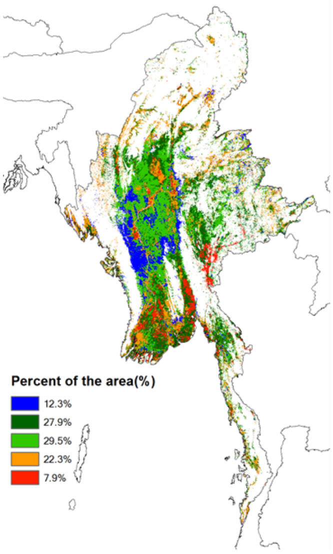

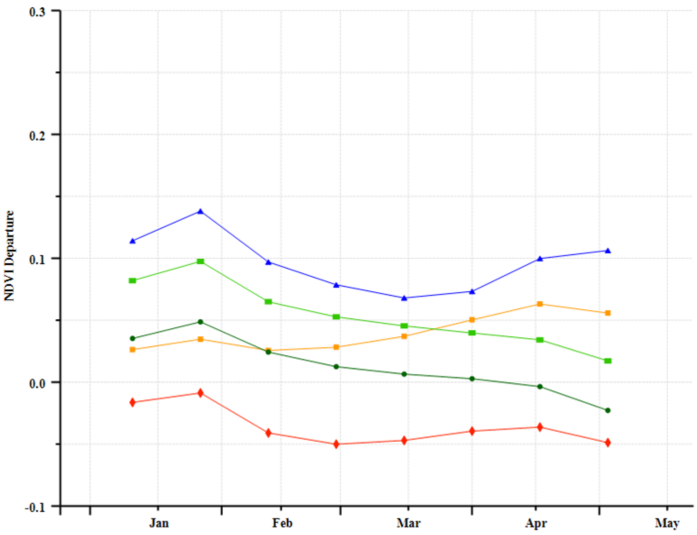

(c) Spatial NDVI patterns compared to 5YA

(d) NDVI profiles

ARG AUS BGD BRA CAN DEU EGY ETH FRA GBR IDN IND IRN KAZ KHM MEX MMR **NGA** PAK PHL POL ROU RUS THA TUR UKR USA UZB VNM ZAF

[NGA] Nigeria

The monitoring period covers the harvesting season of the second rice crop for the southern region of the country, as well as harvests of cotton, second maize, and sweet potato. In addition, the period included sowing seasons for cassava (south region), maize (main, south), and yams. Rainfall (RAIN) and radiation (RADPAR) were about average, while temperature (TEMP) was well below (-4°C). The period experienced a poor vegetation condition index (VCIx: 0.69), as well as a reduction in both the biomass production potential (BIOMSS, -10%) and the fraction of cropped arable land fraction (CALF, -24 percentage points) compared to the five-year averages for the same period for these indicators.

Nationwide, crop development based on NDVI was always below both the average of the previous five years and last year's values. Favorable crop condition development, compared to average, was observed for Borno, Gygawa, and Sokoto in the northern region of the country, and in some areas of south Kogi in the south. Unfavorable crop condition occurred in the central region of the country, corresponding to Massarawa, Niger, and Kaduna.

Figure 3.22. Nigeria crop condition, January-April 2017

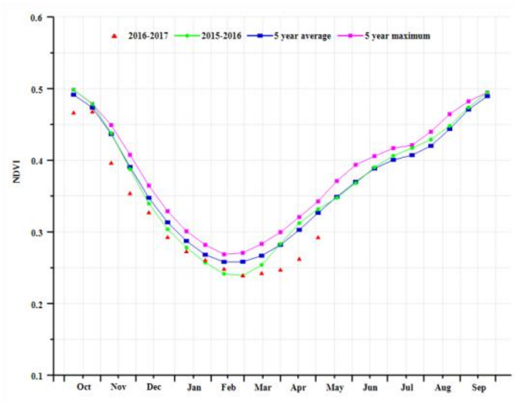

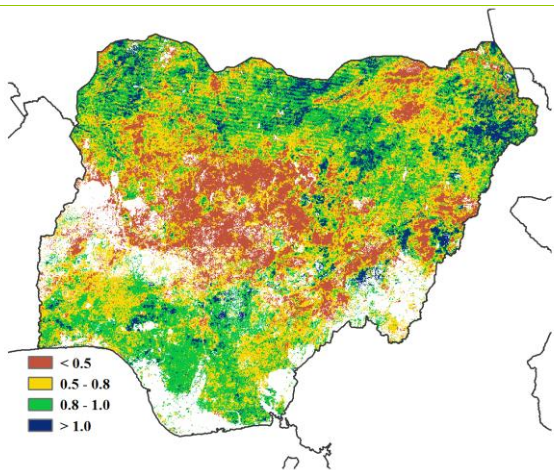

(a) Crop condition development graph based on NDVI (b) Maximum VCI

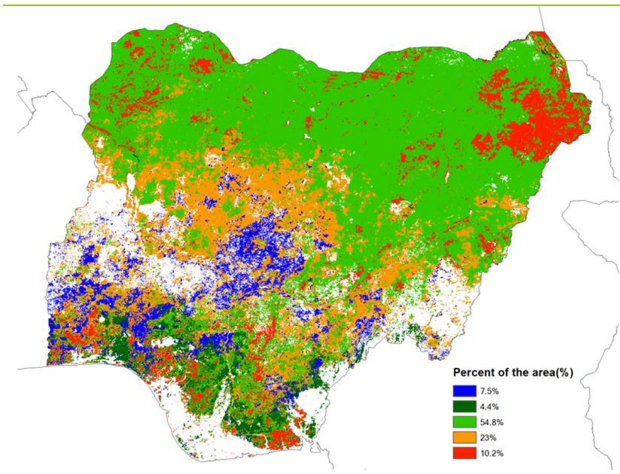

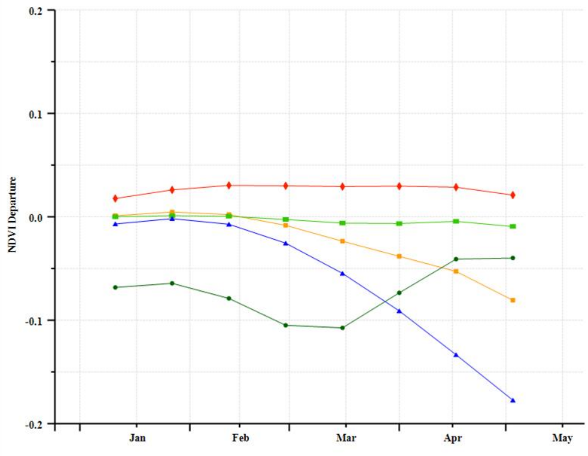

(c) Spatial NDVI patterns compared to 5YA (d) NDVI profiles

ARG AUS BGD BRA CAN DEU EGY ETH FRA GBR IDN IND IRN KAZ KHM MEX MMR NGA **PAK** PHL POL ROU RUS THA TUR UKR USA UZB VNM ZAF

[PAK] Pakistan

The harvesting of winter wheat and barley was completed during the recent monitoring period. Crop condition was generally unfavorable, as indicated by the national NDVI development graph. Compared with average, rainfall (RAIN) suffered a significant decrease of 15%, while temperature (TEMP, -0.1°C) and radiation (RADPAR, -1%) were close to average. As a result, the biomass production potential (BIOMSS) was 8% below the average of the recent five years.

In about 56.7% of the country's arable land, mostly distributed in the north and northeast, crop condition was slightly below average. In areas mainly in the south and southeast, crops did better than average in February and March, but condition deteriorated again later on. Crop condition was unfavorable in the north and northeast of the country, with VCIx values below 0.5. Overall, the anticipation for 2017 crops is a below but close to average output, considering also an increase in the fraction of cropped arable land (CALF) of 6 percentage points over the average for this indicator for the January-April period.

Figure 3.23. Pakistan crop condition, January-April 2017

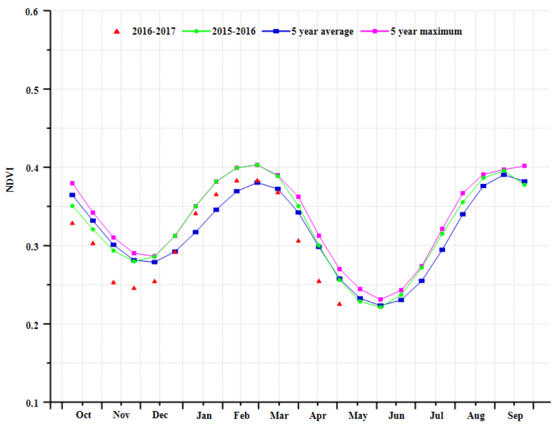

(a) Crop condition development graph based on NDVI

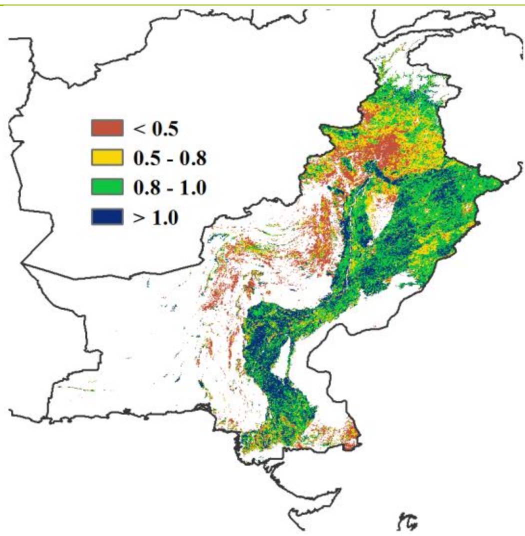

(b) Maximum VCI

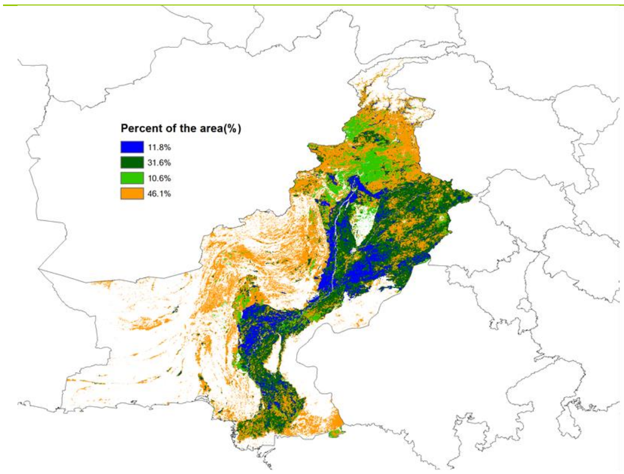

(c) Spatial NDVI patterns compared to 5YA

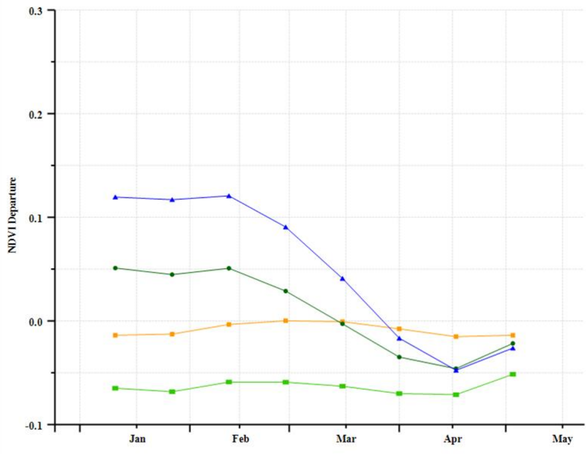

(d) NDVI profiles

[PHL] The Philippines

The monitoring period covers the harvesting stage of secondary rice and maize, as well as the sowing stage of main rice and maize for the country. Crop condition was favorable from January to April, with a VCIx of 0.69 for the country overall. The cropped arable land fraction (CALF) was average.

Over the reporting period, the Philippines enjoyed a large increase of rainfall over average (RAIN, +69%), while temperature and PAR were below average (TEMP, -0.9°C and RADPAR, -5%). Benefiting from the abundant rainfall, the biomass accumulation potential (BIOMSS) was 33% above the recent five-year average, a finding confirmed by the national NDVI development curve exceeding the recent five-year average and last year's values in April. According to the maximum VCI distribution map, many pixels' VCIx values exceed 1 in the regions of Ilocos and Mimaropa, indicating very favorable crop condition. Altogether, the output of the main season crops in the Philippines is expected to be above average.

Figure 3.24. Philippines crop condition, January-April 2017

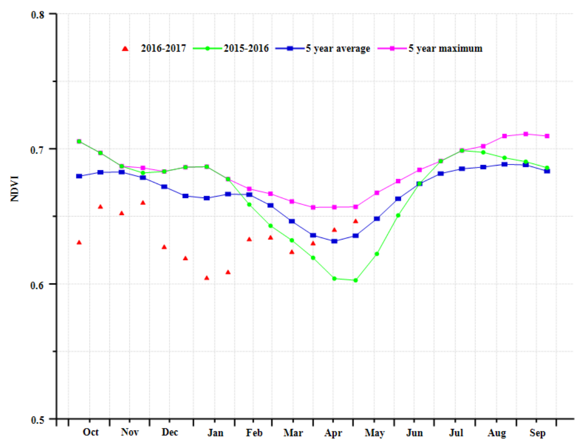

(a) Crop condition development graph based on NDVI

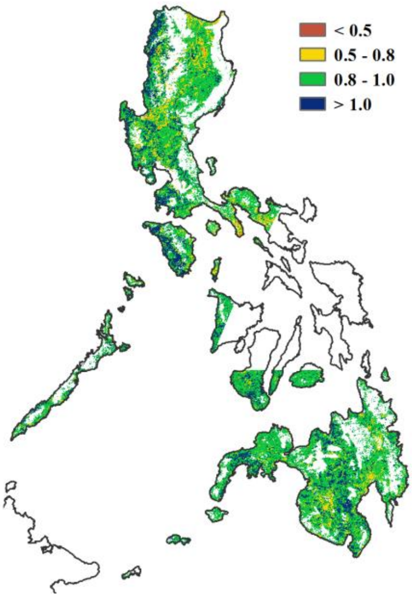

(b) Maximum VCI

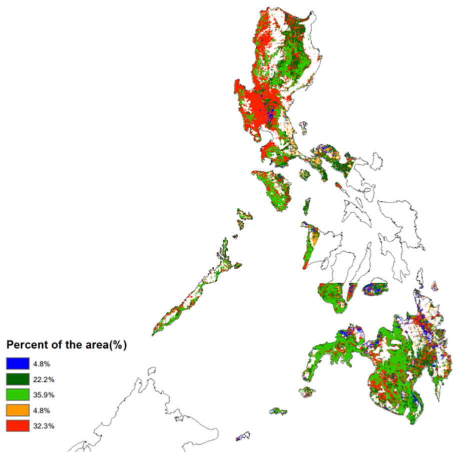

(c) Spatial NDVI patterns compared to 5YA

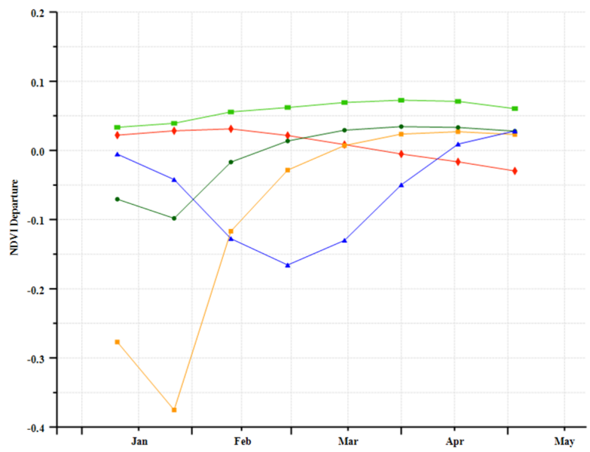

(d) NDVI profiles

ARG AUS BGD BRA CAN DEU EGY ETH FRA GBR IDN IND IRN KAZ KHM MEX MMR NGA PAK PHL **POL** ROU RUS THA TUR UKR USA UZB VNM ZAF

[POL] Poland

Poland enjoyed favorable crop condition during this monitoring period (VCIx=0.82), which corresponds with the wintering stage of winter wheat, while maize seeding started in the beginning of April. The cropped arable land fraction (CALF) for the country is the same as the average of the last five years. Weather during January to April was much wetter and somewhat colder than average, with rainfall (RAIN) up 23% and temperature (TEMP) down 0.2°C. Radiation (as indicated by the RADPAR indicator) dropped 13% below average, while the potential biomass production potential (BIOMSS) was up 6% due to the combination of abundant precipitation and slightly colder weather.

As shown in the national crop condition development graph and NDVI profiles, NDVI values were significantly below average from the start of the monitoring period to the middle of March, but then quickly reverted to average. The reason for this is the snow that had been covering almost the entire country from last October on forward, with NDVI starting to drop already in October last year. Only in 13% of croplands, mainly concentrated on Malopolake and Slaskie, was NDVI above average during the monitoring period.

The national VCIx in Poland during this monitoring period was 0.82. The snow has probably protected crops from cold weather, and the sufficient rainfall will provide enough soil moisture. The overall outlook of winter crops for the country is mixed to average.

Figure 3.25. Poland crop condition, January-April 2017

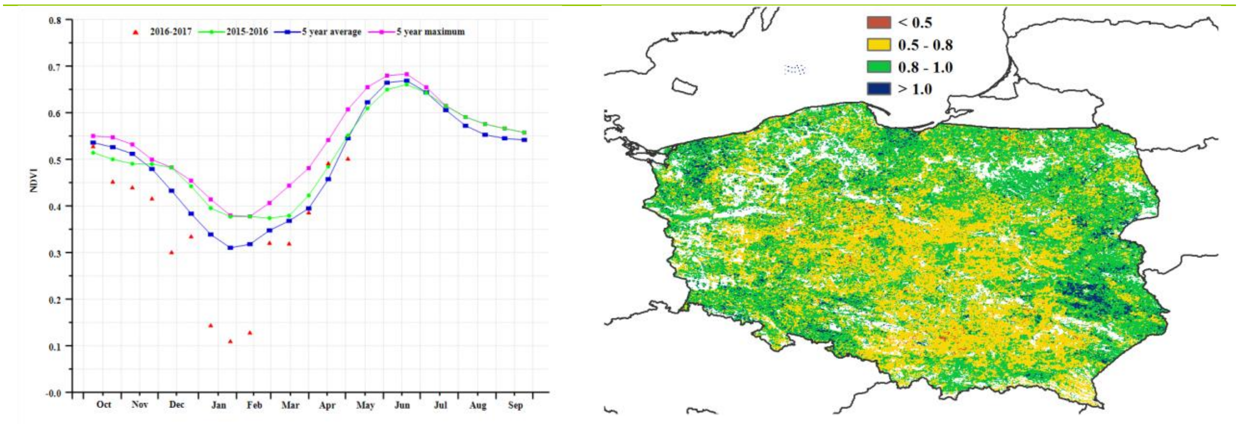

(a) Crop condition development graph based on NDVI (b) Maximum VCI

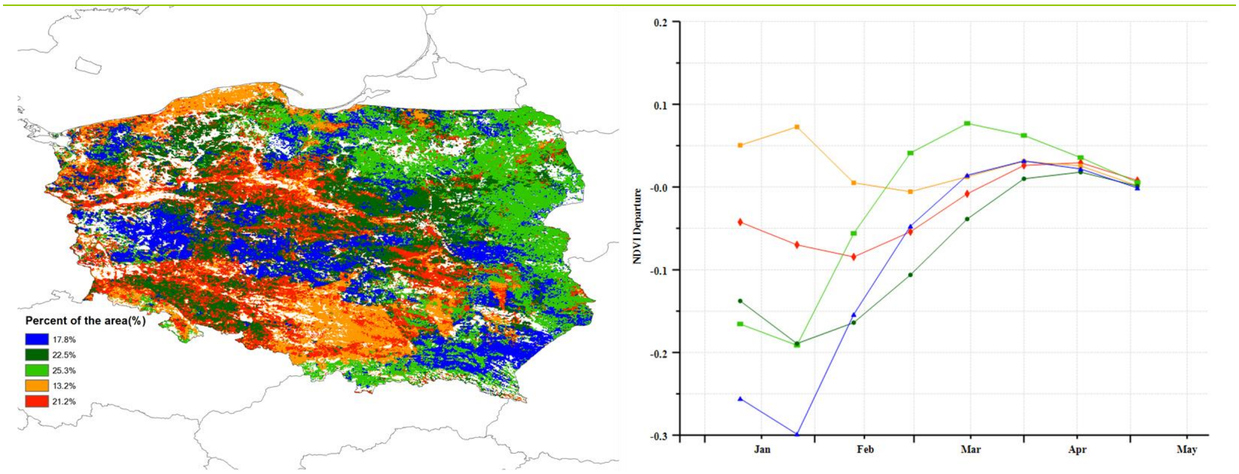

(c) Spatial NDVI patterns compared to 5YA (d) NDVI profiles

ARG AUS BGD BRA CAN DEU EGY ETH FRA GBR IDN IND IRN KAZ KHM MEX MMR NGA PAK PHL POL **ROU** RUS THA TUR UKR USA UZB VNM ZAF

[ROU] Romania

Romania presented average crop condition over the reporting period, with an overall maximum VCI index of 0.77. NDVI showed a sharp drop in mid-January during the dormancy period of winter wheat, also resulting in a drop in the fraction of cropped arable land (CALF) of 1 percentage points. Overall, temperature (TEMP) was slightly below average (-0.4°C), while the rainfall (RAIN) anomaly was +33% and radiation about average (RADPAR, +1%). The biomass production potential was above average (BIOMSS, +12%).

As shown in the nationwide crop condition development graph, NDVI was below the five-year average before March, with the lowest NDVI (below 0.05) happening in January, after which values again became rather close to average. In most parts of middle Romania near Targu Mures, crop condition was average (VCIx values of 0.5-0.8), while in the northeast (for example in Lasi) above average crop conditions were experienced (VCIx values near or above 0.8). In contrast, southern regions around Bucharest had below average VCIx values, with values close to or below 0.5.

As for crop condition development during the monitoring period, the NDVI profiles linked to the NDVI spatial patterns show that crop condition went down in northeastern Romania (including Suceava), while it partly went up in the southeast border area. Most parts of the west and middle of the country only experienced slight changes in condition, while in some southern regions (Craiova, Ciurgiu, and Olenita) an improvement in crop condition was recorded after mid-February.

Overall, crop condition is favorable in Romania for both past winter crops and summer crops as a result of abundant soil moisture.

Figure 3.26. Romania crop condition, January-April 2017

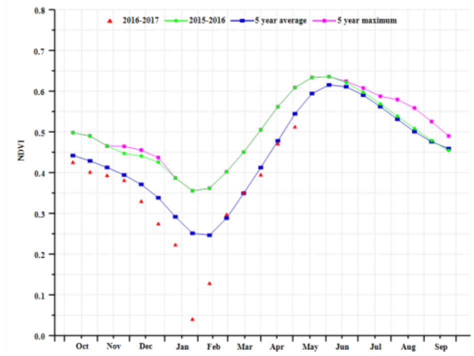

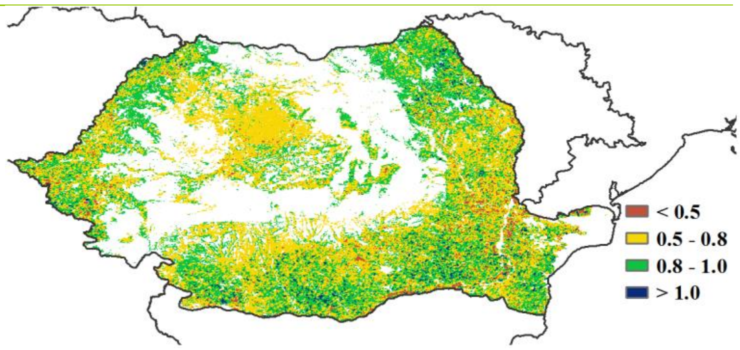

(a) Crop condition development graph based on NDVI

(b) Maximum VCI

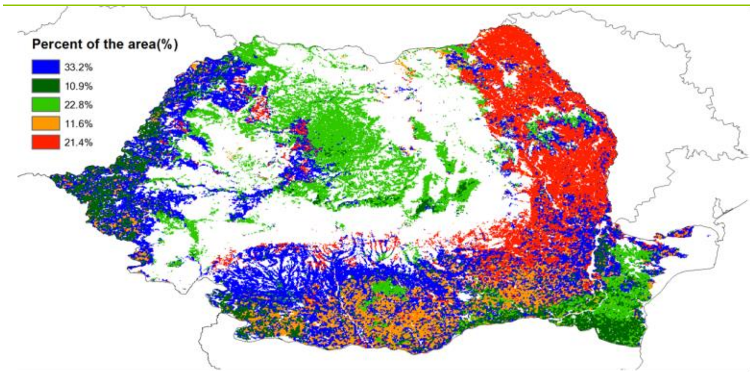

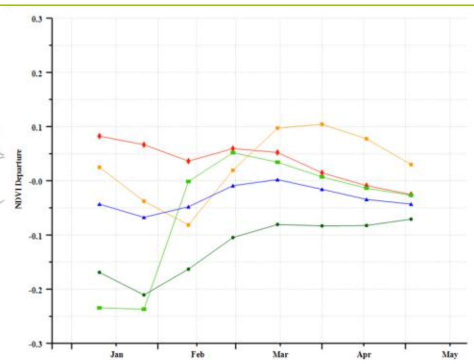

(c) Spatial NDVI patterns compared to 5YA

(d) NDVI profiles

[RUS] Russia

On average, Russia experienced unfavorable crop condition from January to April (VCIx=0.58), which coincides with the wintering stage of winter wheat and early planting of spring wheat. The fraction of cropped arable land (CALF) was not monitored because of the serious snow cover during the monitoring period. Overall Russia experienced suitable climate conditions in these four months, with sufficient rainfall and warm temperatures (RAIN, +6%, and TEMP, +1.2°C). Due to the joint effect of rainfall and temperature, the BIOMSS indicator rose 5% above the five-year average.

As the crop condition development graph based on NDVI illustrates, NDVI was significantly lower than usual from the middle of October last year on forward, a situation due to the abundant snow cover on most croplands in Russia. With spring wheat being sowed, NDVI reverted to close to average. NDVI in Kaliningrad, Volga, and Northwestern Federal District (mainly concentrated in Kirovskaya Oblast, Gorodovikovsk, Samarskaya Oblast, Udmurtiya Republic, Ulyanovskaya Oblast and Volgogradskaya Oblast) consistently exceeded the average of the last five years, especially in February, resulting mostly from the abundant rainfall in these places (RAIN, +40%, +18%, and +29%, respectively). In most parts of croplands in the southern Urals (including Penzenskaya Oblast and Bashkortostan and Udmurtiya Republics), NDVI was close to average until the middle of February, after which it decreased.

Based mostly on the low VCIx values for the country (0.58), the outlook for Russia's wheat production is considered mixed.

Figure 3.27. Russia crop condition, January-April 2017

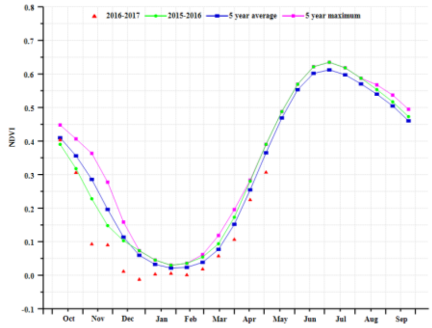

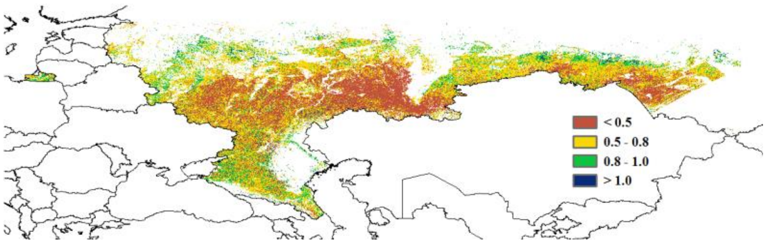

(a) Crop condition development graph based on NDVI (b) Maximum VCI

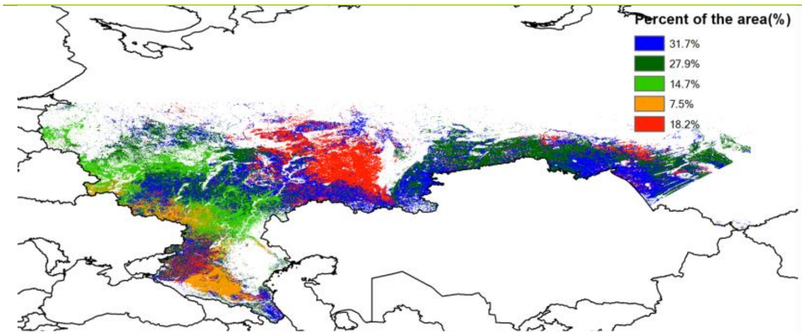

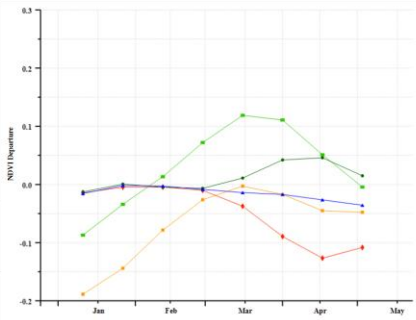

(c) Spatial NDVI patterns compared to 5YA (d) NDVI profiles

ARG AUS BGD BRA CAN DEU EGY ETH FRA GBR IDN IND IRN KAZ KHM MEX MMR NGA PAK PHL POL ROU RUS **THA** TUR UKR USA UZB VNM ZAF

[THA] Thailand

Thailand’s main rice crop was harvested in January, while its second season rice matured and was ready for harvesting in April. Rainfall was abundant over the reporting period (RAIN, +61%), while temperature (TEMP, -0.1°C) and radiation (RADPAR, -1%) were slightly below average. The biomass production potential (BIOMSS) is up 9%, and the fraction of cropped arable land (CALF) also increased by 12 percentage points over its average for the period.

Crop condition based on NDVI was below average in mid-February and March, but improved later. Considering the spatial NDVI patterns and corresponding profiles, crop condition in most regions was slightly above but close to average, while for about 19.5% of cropped land, located in the center (Pichit, Petchabun, Uthai Thani, Chai Nat, and Lop Buri) and northeast (Nong Khai, Kalasin, Roi Et, Khon Kaen, Surin, and Ubon Ratchathani), slightly below average conditions were observed with VCIx values below 0.5.

Overall, crop production prospects for the country remain close to average or above.

Figure 3.28. Thailand crop condition, January-April 2017

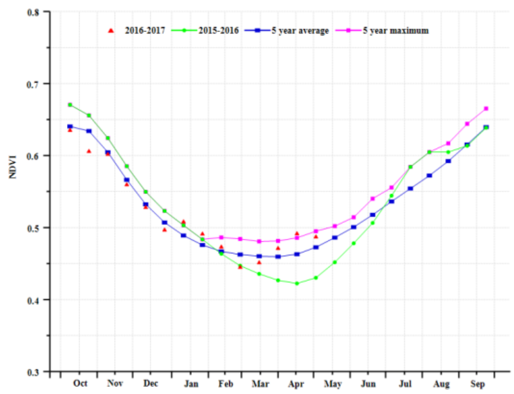

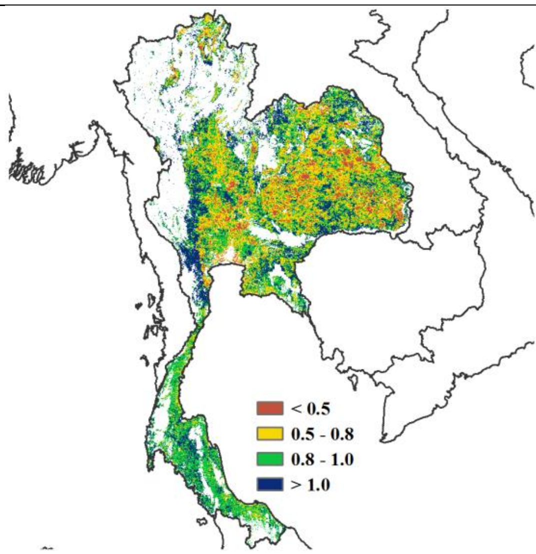

(a) Crop condition development graph based on NDVI (b) Maximum VCI

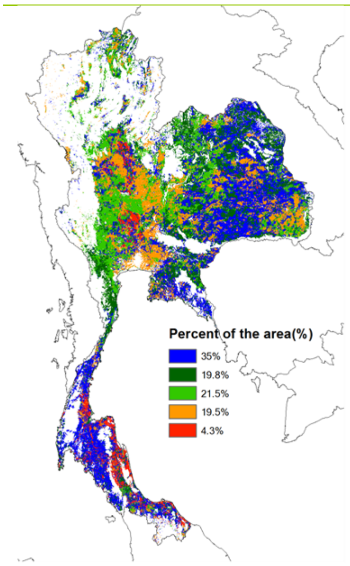

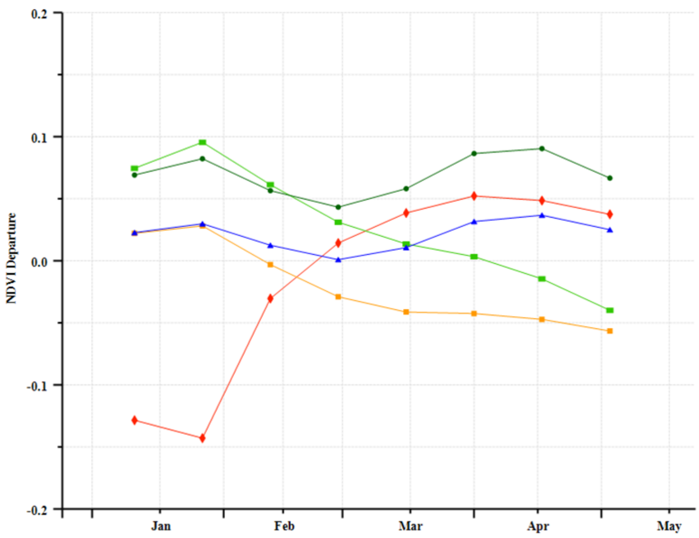

(c) Spatial NDVI patterns compared to 5YA (d) NDVI profiles

ARG AUS BGD BRA CAN DEU EGY ETH FRA GBR IDN IND IRN KAZ KHM MEX MMR NGA PAK PHL POL ROU RUS THA **TUR** UKR USA UZB VNM ZAF

[TUR] Turkey

The crop condition from January to April 2017 was generally well below average in Turkey. Winter crops are grown during this period, and planting of summer crops started in April. Accumulated rainfall (RAIN, -22%) and temperature (TEMP, -0.5°C) were below average. Radiation (RADPAR, +3%) was above average. The unfavorable agroclimatic conditions resulted in a negative departure of BIOMSS of 11%. The VCIx (0.57) was poor and the cropped arable land fraction CALF decreased by as much as 28 percentage points compared to the recent five-year average.

Except in the eastern half of the country, where NDVI increases from the center to the east, the country as a whole experienced poor NDVI values. Most severely affected are several central areas in and around the provinces of Afyon, Ankara, Eskisehir, and Konya. The map of maximum VCI presents a pattern consistent with the NDVI cluster map. Combined with the very marked drop in cropped arable land, the situation can only be assessed as rather poor.

Figure 3.29. Turkey crop condition, January-April 2017

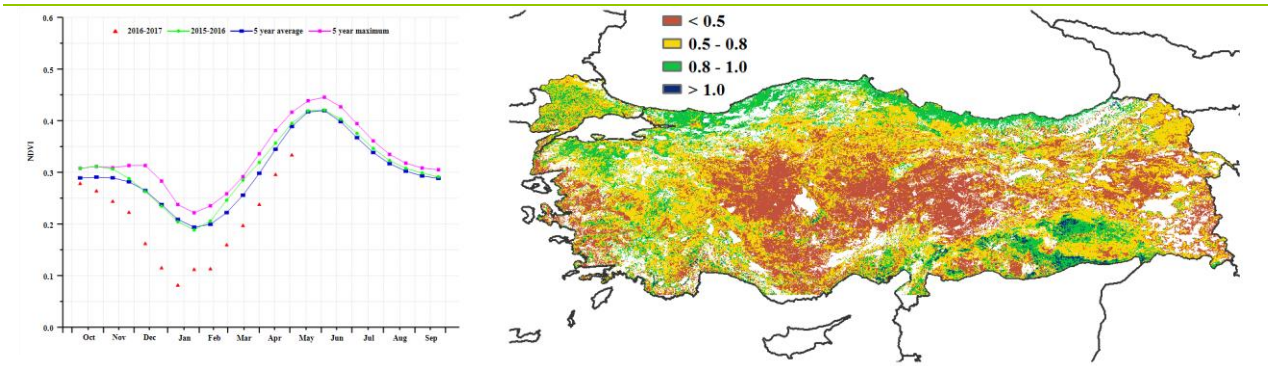

(a) Crop condition development graph based on NDVI (b) Maximum VCI

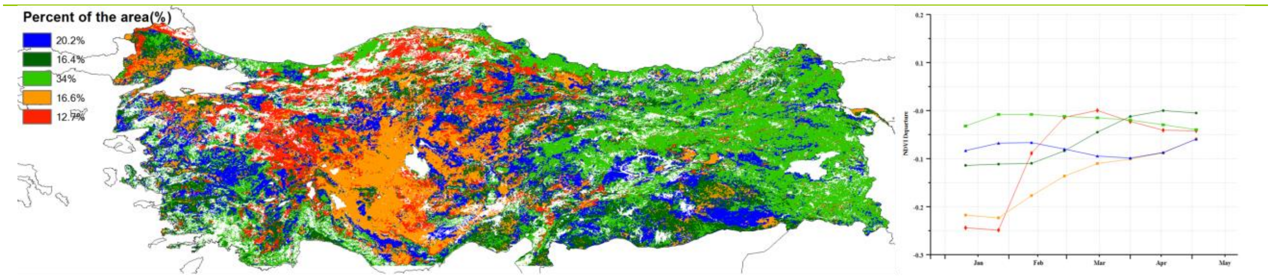

(c) Spatial NDVI patterns compared to 5YA (d) NDVI profiles

ARG AUS BGD BRA CAN DEU EGY ETH FRA GBR IDN IND IRN KAZ KHM MEX MMR NGA PAK PHL POL ROU RUS THA TUR **UKR** USA UZB VNM ZAF

[UKR] Ukraine

The main crops in the field during the reporting period were winter wheat and cereals, while spring crops (maize, barley, and other cereals) were being sowed. Agroclimatic conditions for the country were above average over the reporting period: rainfall (RAIN) increased by 20%, temperature (TEMP) was slightly above average, while radiation (RADPAR) decreased by 3%. As a result, the biomass production potential (BIOMSS) also performed well. Crop condition in the country was far below the five-year average before mid-February, but gradually returned to average afterwards. The VCIx index was also poor (0.68). According to the spatial NDVI patterns, which compare to the five-year average situation, almost the entire country underwent unfavorable conditions, with the exception of some small parts in the south. Unfavorable conditions at the time winter crops (mainly wheat) were planted resulted in a drop of the cultivated area (CALF, -17 percentage points), which is likely to lead to a reduction in winter crop production.

Figure 3.30. Ukraine crop condition, January-April 2017

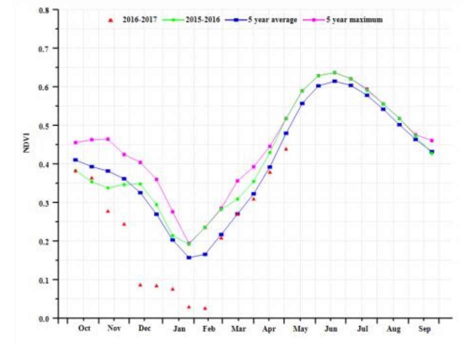

(a) Crop condition development graph based on NDVI

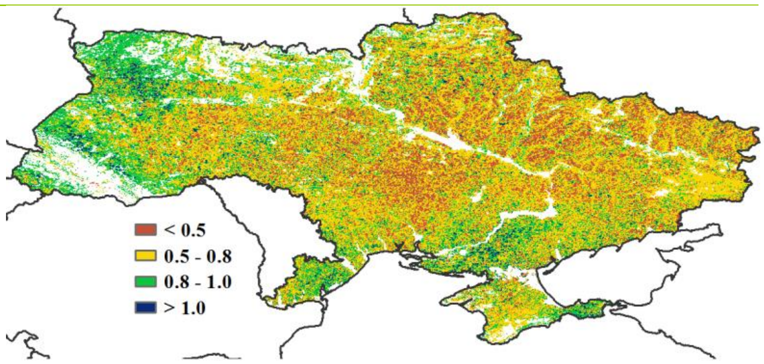

(b) Maximum VCI

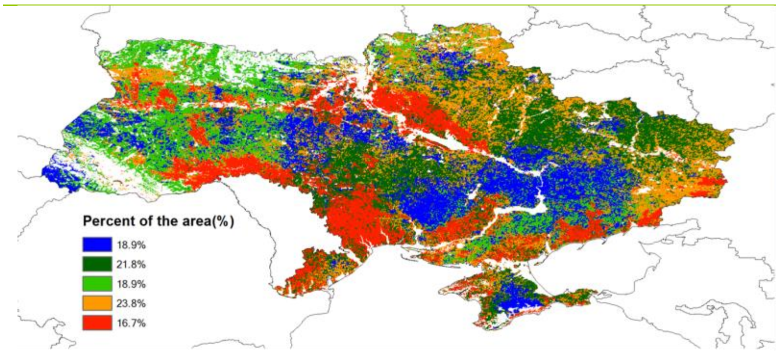

(c) Spatial NDVI patterns compared to 5YA

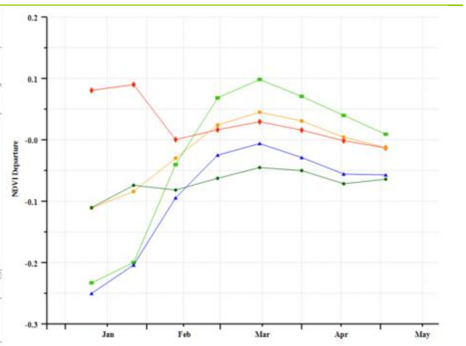

(d) NDVI profiles

[USA] United States

The current monitoring period includes wintering time of winter crops and the planting season of spring crops, with CropWatch agroclimatic and agronomic indicators for the period pointing at above average crop condition.

Rainfall (RAIN) was 25% above average, while temperature (TEMP) was 1.8°C above and radiation (RADPAR) a significant 6% below average due to the rainy weather. Abundant rainfall fell in major winter crop production states, with above average precipitation in Kansa (RAIN, +67%), Oklahoma (+48%), Texas (+35%), Nebraska (+28%), California (+76%), and Washington (+43%). Excessive precipitation locally resulted in floods, especially in California and Texas. Rainfall in Iowa (RAIN, +23%), Illinois (+21%), and Wisconsin (+48%) provided sufficient soil moisture for planting and growth of maize and soybeans.

Warm and humid weather is good for the growth of winter crops, and positive NDVI departures were observed in California, Washington, Kansas, and Nebraska. Slightly below average NDVI was observed in scattered regions of northern Texas and Oklahoma, which may have been caused by floods. The above average crop condition compared to the last five years is confirmed by the maximum vegetation condition index (VCIx=0.85) and the fraction of cropped arable land (CALF), which was significantly (7%) above average.

Altogether, all CropWatch indicators point at average or above crop production for the United States. Crop production estimates by state are presented in Annex B.

Figure 3.31. United States crop condition, January-April 2017

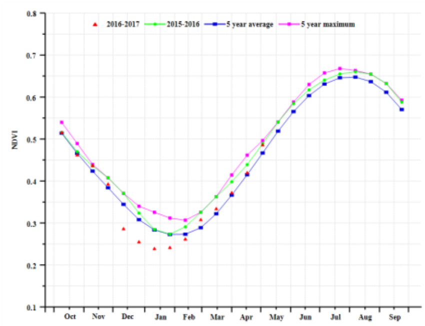

(a) Crop condition development graph based on NDVI

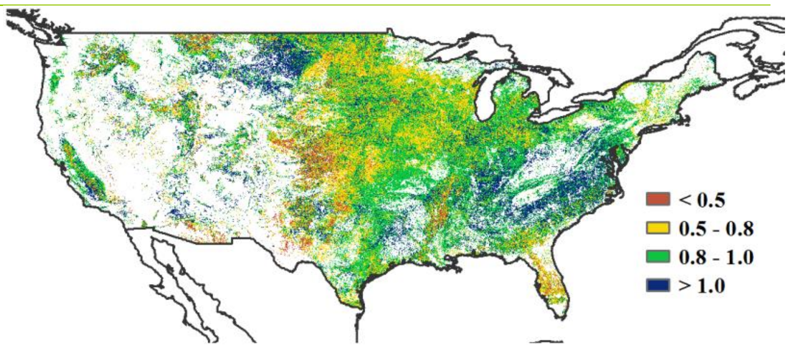

(b) Maximum VCI

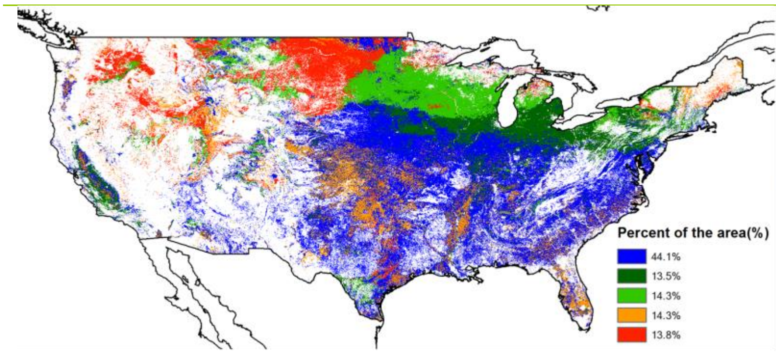

(c) Spatial NDVI patterns compared to 5YA

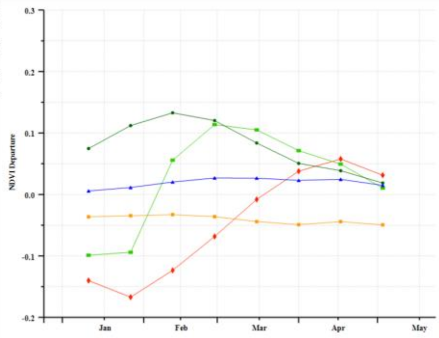

(d) NDVI profiles

[UZB] Uzbekistan

The reporting period covers the growing stage of winter cereals and the sowing stage of coarse grains, including maize. Crop condition was generally favorable. The national average VCIx was 0.70. Among the CropWatch agroclimatic indicators, RAIN was above average (+21%), TEMP was below average by -1.2°C, and RADPAR was normal. The combination of factors resulted in a high BIOMSS (+11%) compared to the five-year average. As shown by the crop condition development graph, NDVI was below average from late January to April, and conditions were generally more favorable in the east than in the west (the cotton area). NDVI was below average in 20% of croplands, mainly in parts of Qunghirot, Chimbay, and Nuhus provinces and part of Bukhoro, Kagan, and Nawoiy provinces. NDVI was also below average in parts of three wheat growing provinces in the east: Quqon, Andijon, and Namangan, but normal or above in other regions. Altogether, winter wheat condition in the country was fair.

Figure 3.32. Uzbekistan crop condition, January-April 2017

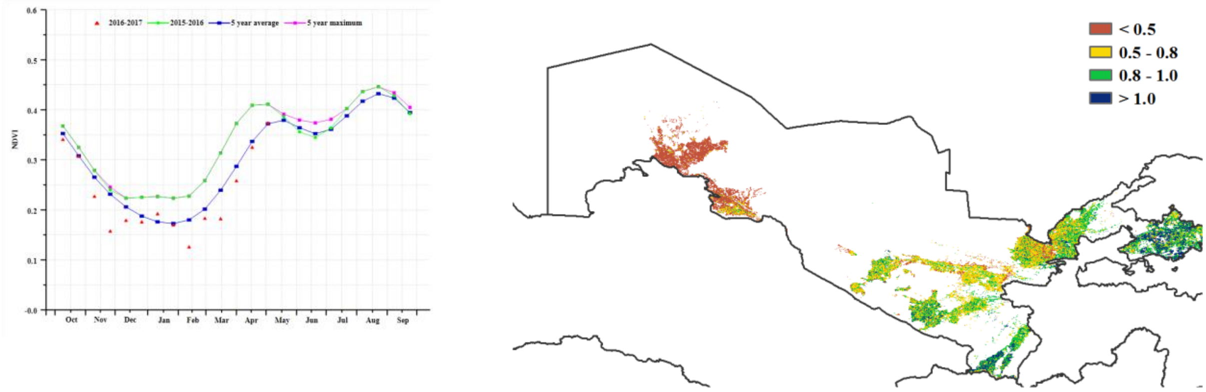

(a) Crop condition development graph based on NDVI (b) Maximum VCI

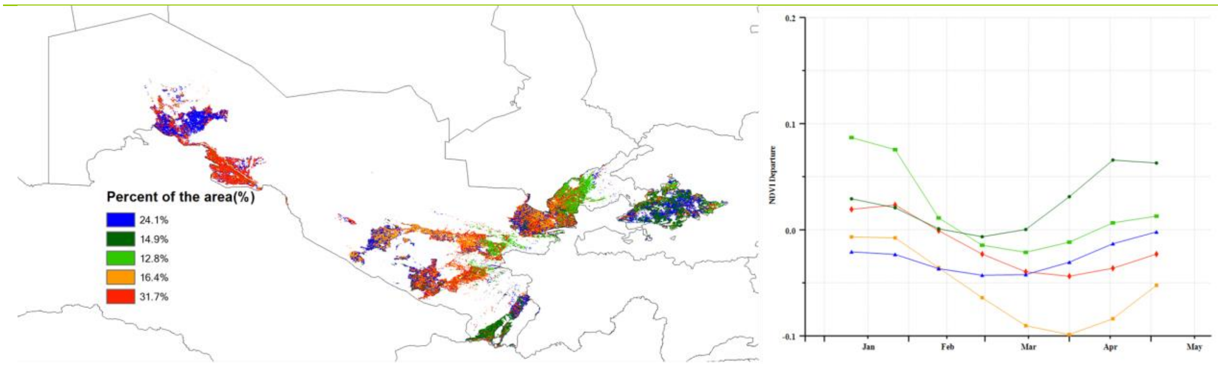

(c) Spatial NDVI patterns compared to 5YA (d) NDVI profiles

[VNM] Vietnam

The period from January to April covers the sowing and growing periods of spring rice in both the north and south of the country, with differences due to altitude. Most of the rice cultivation regions are distributed in the northern Red River delta and in the Mekong delta in the south. The fraction of cropped arable land (CALF) increased 2.1 percentage points compared with the average of the previous five years. The national maximum vegetation condition index was also favorable (0.83).

CropWatch agroclimatic indicators show above average rainfall (RAIN, +14%), a marked decrease in radiation (RADPAR, -8%), and average temperature (TEMP, -0.1°C), leading to an increase in the biomass production potential (BIOMSS, +17%). According to the NDVI profiles linked to spatial patterns, only 6% of croplands in the country suffered from poor condition, while condition for 27% of crop lands was consistently above average, with those areas mainly distributed around the Red River delta (including BacGiang and HaiDuong) in the north and Qui Nhon in the south. Considering the favorable agroclimatic conditions, the prospects of the crops in the country are good.

Figure 3.33. Vietnam crop condition, January-April 2017

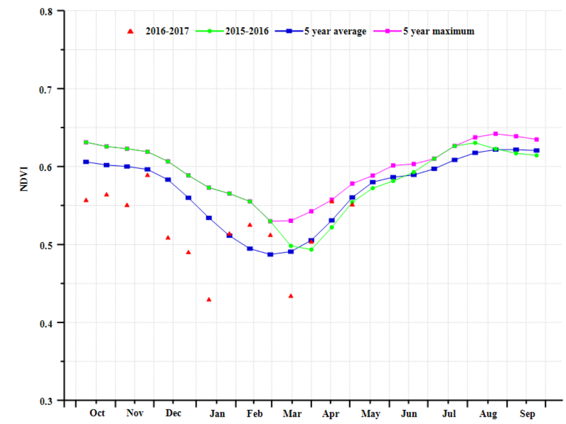

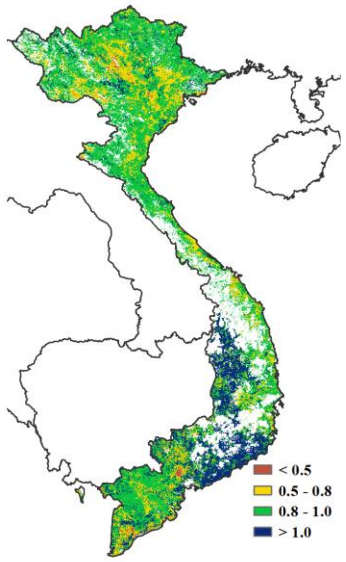

(a) Crop condition development graph based on NDVI

(b) Maximum VCI

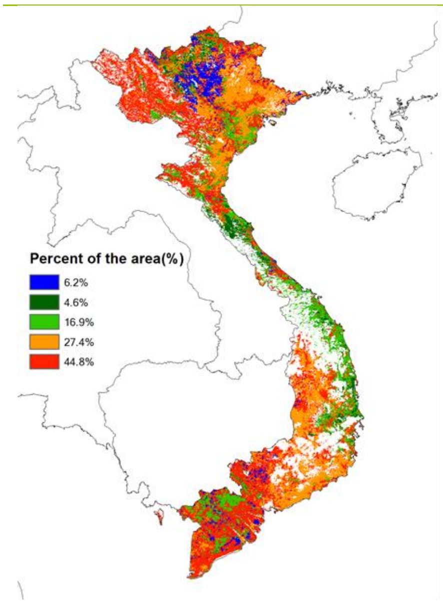

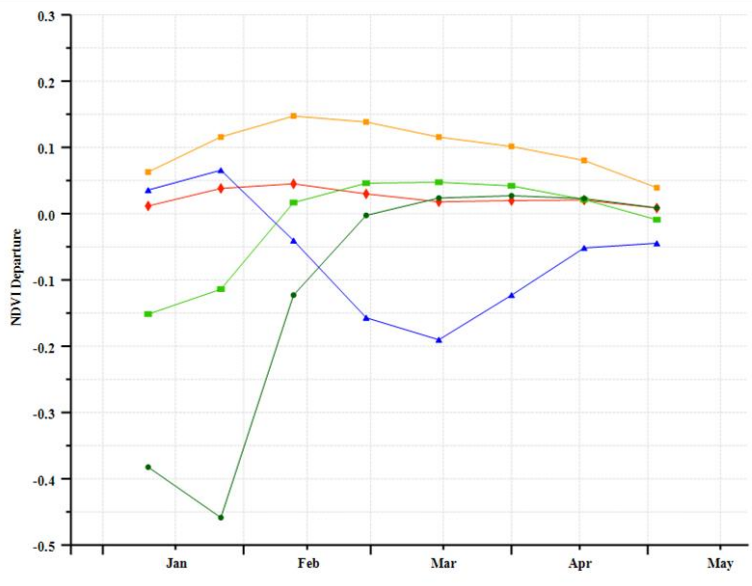

(c) Spatial NDVI patterns compared to 5YA

(d) NDVI profiles

ARG AUS BGD BRA CAN DEU EGY ETH FRA GBR IDN IND IRN KAZ KHM MEX MMR NGA PAK PHL POL ROU RUS THA TUR UKR USA UZB VNM **ZAF**

[ZAF] South Africa

Rainfall was slightly below average in South Africa as a whole (RAIN, -11%), with close to average radiation (RADPAR) and temperature (TEMP). NDVI was below average between April and May. The maximum VCI was 0.74 for the country as a whole, but in most parts of Limpopo, Mpumalanga, North-West, Free State, Gauteng, and Kwa-Zulu Natal, good crop conditions prevailed. The Western Cape, a major citrus producer, experienced a severe dry spell (RAIN, -34%), which resulted in a 21.9% reduction in BIOMSS for that area. The sub-humid tropical areas of Kwa-Zulu Natal and Eastern Cape experienced departures in RAIN (-12.8%) and RADPAR (-1.9%), as well as a 7.8% reduction in BIOMSS. The semi-arid Steppes showed a similar trend, with RAIN, -10.7%; TEMP, -0.9%; and RADPAR, -2.6%; and a BIOMSS of 7.4% below the average for the period.

The country's overall fraction of cropped arable land (CALF) increased by 8 percentage points. Despite this increment, overall BIOMSS was 7% below average, which could be attributed to the variations in the mentioned agronomic indicators. The spatial NDVI patterns showed poor conditions in about 13.3% of cropped areas, including most parts of Kwa-Zulu Natal and Eastern Cape; maize and wheat are the major crops grown here. In contrast, about 86.7% of cropped areas showed positive NDVI departures after February. Overall, crop condition was good in the major producing parts of the country and, with increasing areas cultivated, prospects for the country are at least average.

Figure 3.34. South Africa crop condition, January-April 2017

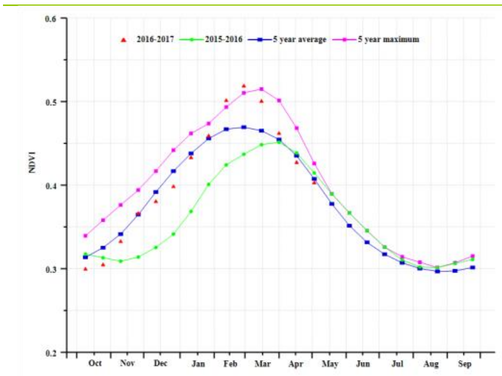

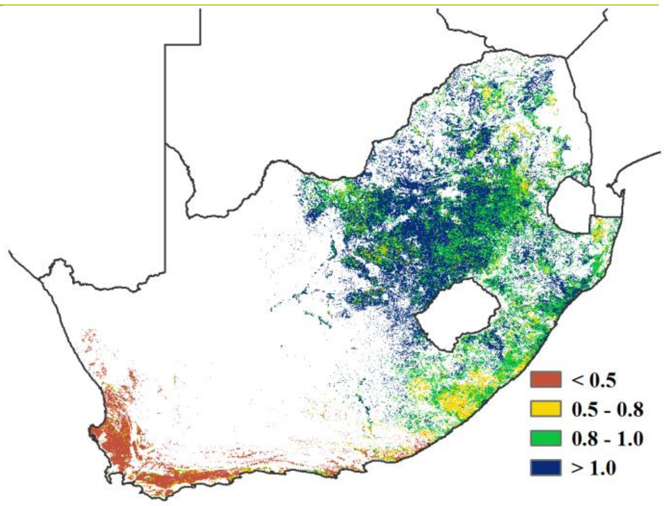

(a) Crop condition development graph based on NDVI (b) Maximum VCI

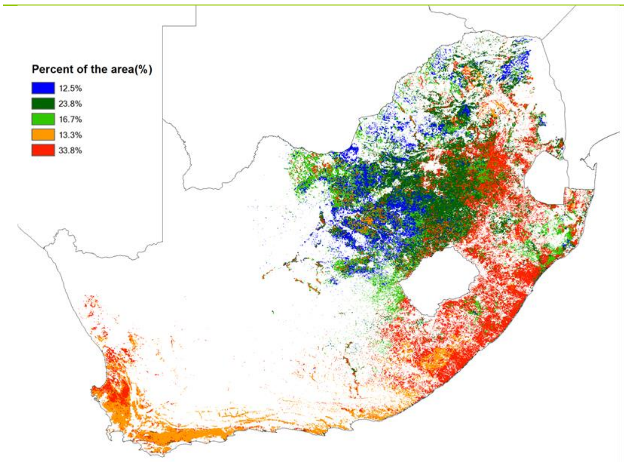

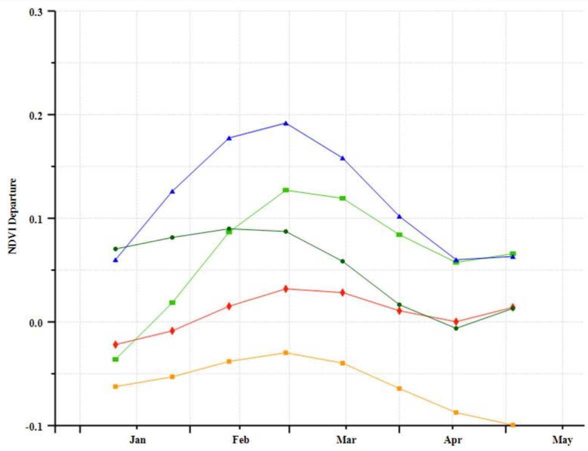

(c) Spatial NDVI patterns compared to 5YA (d) NDVI profiles

Chapter 4. China

Chapter 4 presents a detailed analysis for China, focusing on the seven most productive agro-ecological regions of the east and south. The chapter begins with a brief overview of the agroclimatic and agronomic conditions over the monitoring period (section 4.1), after which sections 4.2 and 4.3 present China winter crop production (4.2) as well as pests and diseases that have affected agricultural production over the reporting period (4.3). Next, section 4.4 presents an import and export outlook for China, and the chapter finishes with the CropWatch analysis for each of the seven individual regions (4.5). Additional information on the agroclimatic indicators for agriculturally important Chinese provinces is listed in table A.11 in Annex A.

4.1 Overview

In China, winter crops including winter wheat and rapeseed were growing during the current monitoring period. Overall, crop condition was favorable, according to above-average BIOMSS (+5%) on the national scale. CropWatch agroclimatic indicators show that rainfall and radiation for the whole country decreased by respectively 13% and 6% compared to average, while temperature increased 0.5°C (see table 3.1). At the regional level, as shown in table 4.1, rainfall was significantly above average in Inner Mongolia (RAIN, +60%), Loess region (+23%), and Huanghuaihai (+15%). In contrast, below-average precipitation occurred in the Lower Yangtze (RAIN, -21%), Southwest China (-17%), and Southern China (-7%). Rainfall for Northeast China was close to average (-1%). Compared to average, temperature increased in most regions of China except for Southwest China (-0.1°C) and Southern China (average). Radiation was significantly below average in Southwest China, with a very significant decrease of 13%. Less severe, but nevertheless significant RADPAR departures occurred in Southern China (-8%), Lower Yangtze (-7%), Loess region (-5%), and Huanghuaihai (-3%). The spatial distribution for the anomalies of agroclimatic indicators and their fluctuations over time are shown in figures 4.1 and 4.2.

According to figure 4.3, cropped areas were located in Huanghuaihai, Lower Yangtze, the southern part of the Loess region, and southern and southwestern China, while uncropped areas were in Northeast China, Inner Mongolia, and the northern part of the Loess region. Compared with the recent five-year average, the cropped arable land fraction (CALF) decreased in Huanghuaihai (CALF, -2 percentage points), Lower Yangtze (-2 percentage points), southern Loess region (-7 percentage points), and marginally in southwestern China (-1 percentage point); see also table 4.1. CALF for Southern China was average.

Table 4.1. CropWatch agroclimatic and agronomic indicators for China, January-April 2017, departure from 5YA and 15YA

Region	Agroclimatic indicators			Agronomic indicators		
	Departure from 15YA (2002-2016)			Departure from 5YA (2012-2016)		Current
	RAIN (%)	TEMP (°C)	RADPAR (%)	BIOMSS (%)	CALF (%)	Maximum VCI
Huanghuaihai	15	0.9	-3	19	-2	0.79
Inner Mongolia	60	1.5	0	48	-	0.41
Loess region	23	0.4	-5	16	-7	0.51
Lower Yangtze	-21	0.4	-7	-6	-2	0.60
Northeast China	-1	1.9	1	9	-	0.70
Southern China	-7	0.0	-8	7	0	0.56
Southwest China	-17	-0.1	-13	-6	-1	0.69

The maximum VCI (VCIx) on the national level was only moderate, with the average value at 0.62. Among the regions, high VCIx (larger than 0.5) occurred in Huanghuaihai, Lower Yangtze, and China's southwestern and southern regions, while lower values occurred in the Loess region and Inner Mongolia (figure 4.4 and table 4.1). As shown in figure 4.5, high values for minimum Vegetation Health Index (VHIn) were mainly distributed in Huanghuaihai and Southwest China, with lower values occurring in Lower Yangtze and Southern China.

Figure 4.1. China spatial distribution of rainfall profiles, January-April 2017

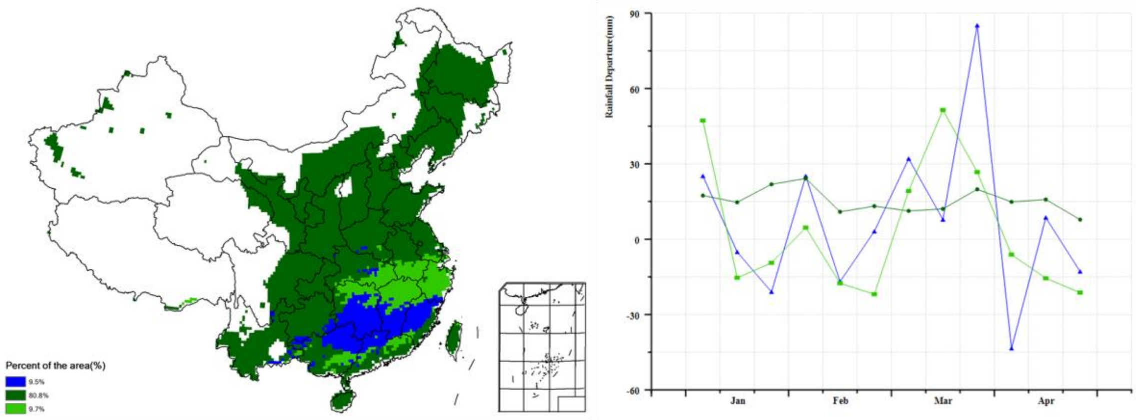

Figure 4.2. China spatial distribution of temperature profiles, January-April 2017

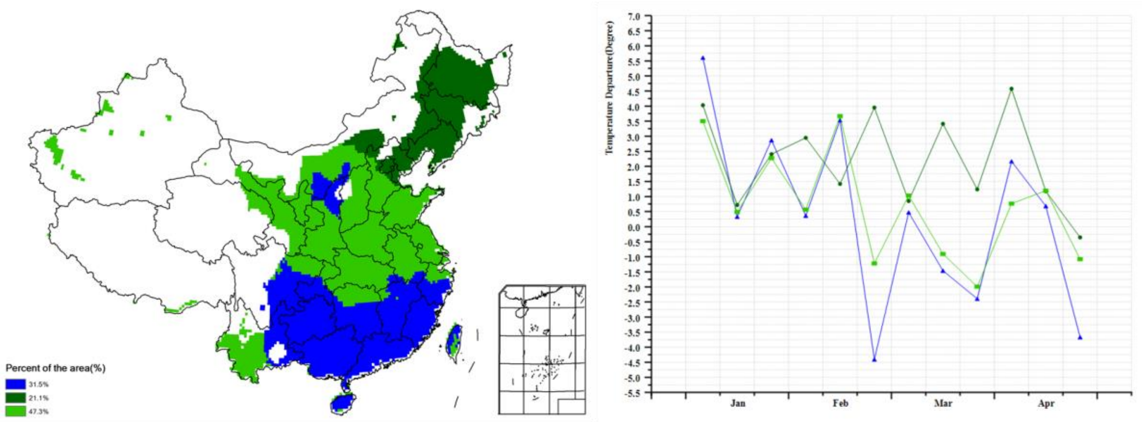

Figure 4.3. China cropped and uncropped arable land, by pixel, January-April 2017

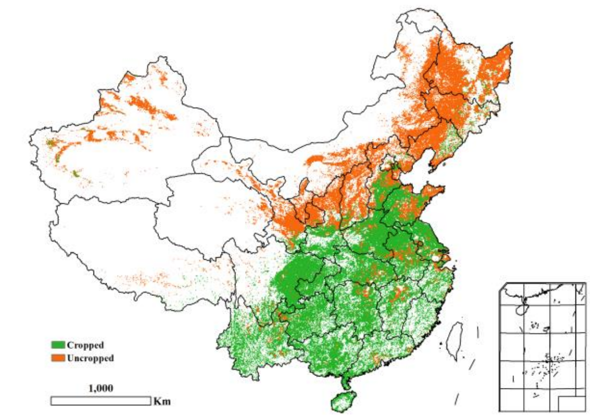

Figure 4.4. China maximum Vegetation Condition Index (VCIx), by pixel, January-April 2017

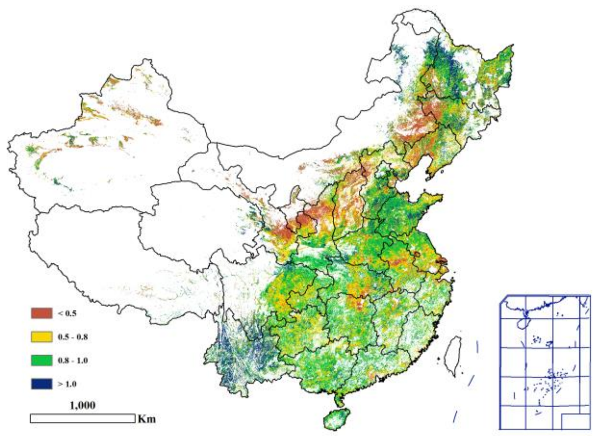

Figure 4.5. China minimum Vegetation Health Index (VHIn), by pixel, January-April 2017

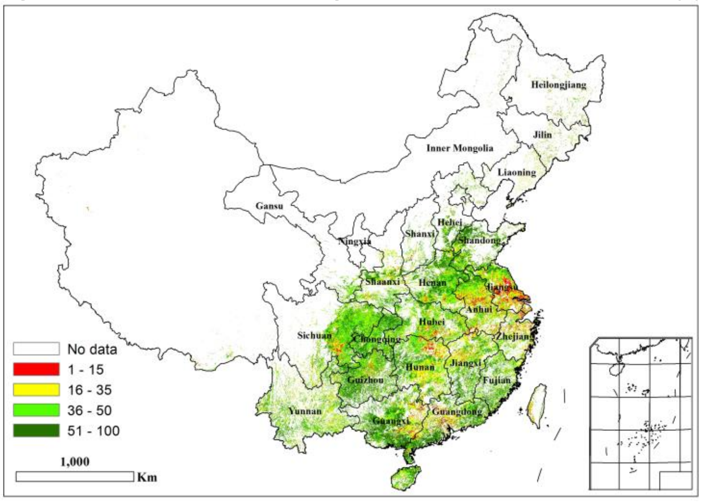

4.2 Winter crop production

Overall favorable agroclimatic conditions benefited winter crops, resulting in a 2.2% increase of winter wheat yield at the national level. Winter wheat production is forecast at 116 million tons, an increase of 1.9 million tons or 1.7% up from the 2016 output (table 4.2). The total planted area is 23,548 thousand hectares, 2% down from 2016. GaoFen-1 (GF-1) satellite data show that the planted area decreased by 7.8% in Anhui (mostly in the center-east of the province) and 4.6% in Jiangsu (mostly in the center-west), which is equivalent to 299 thousand hectares in two major wheat producing areas (figure 4.6). Arable land that is uncropped in early 2017 compared with early 2016 is shown in figure 4.7.

According to information from China Meteorological Administration, the large decrease resulted from unsuitable weather during the planting window in October to November 2016 for Anhui and Jiangsu provinces. Even if the winter wheat yield increased in Anhui and Jiangsu, wheat production still decreased by 5.2% and 1.9% compared with 2016. Other provinces with large production decreases include Hubei (-1.1%, due to both decreased planted area and yield), Chongqing (-1.9% because of decreased yield), and Shaanxi (-4.2%, due to both decreased planted area and yield). Yield increased in Hebei (+4.0%), Shanxi (+5.7%), Shandong (+3.3%), and Henan (+3.9%)

Table 4.2. China, 2017 winter wheat area, yield, and production and percentage difference with 2017, by province

	Area (kha)			Yield (kg/ha)			Production (thousand ton)		
	2016	2017	Δ(%)	2016	2017	Δ(%)	2016	2017	Δ(%)
Hebei	2048	2048	0.0%	5671	5898	4.0%	11615	12080	4.0%
Shanxi	520	517	-0.5%	4038	4289	6.2%	2099	2219	5.7%
Jiangsu	2057	1962	-4.6%	4730	4863	2.8%	9729	9540	-1.9%
Anhui	2624	2420	-7.8%	4322	4441	2.7%	11340	10747	-5.2%
Shandong	4076	4113	0.9%	5824	5963	2.4%	23741	24527	3.3%
Henan	4991	5115	2.5%	5041	5111	1.4%	25160	26142	3.9%
Hubei	1047	1040	-0.7%	4137	4117	-0.5%	4330	4281	-1.1%
Chongqing	357	350	-2.1%	3294	3299	0.2%	1177	1155	-1.9%
Sichuan	1299	1290	-0.7%	3577	3627	1.4%	4646	4677	0.7%
Shaanxi	1056	1027	-2.8%	3798	3740	-1.5%	4011	3841	-4.2%
Gansu	387	388	0.4%	3879	3858	-0.5%	1500	1499	-0.1%
Sub total	20462	20270	-0.9%	-	-	-	99349	100709	1.4%
Other provinces	3210	3278	2.1%	-	-	-	14690	15273	4.0%
National total*	**23672**	**23548**	**-0.5%**	**4817**	**4925**	**2.2%**	**114039**	**115981**	**1.7%**

*Note: * National total production does not include Taiwan province.*

Figure 4.6. Winter crops planted area changes in border areas between Anhui and Jiangsu as shown from 16m GF-1 imagery in 2016(a) and 2017(b)

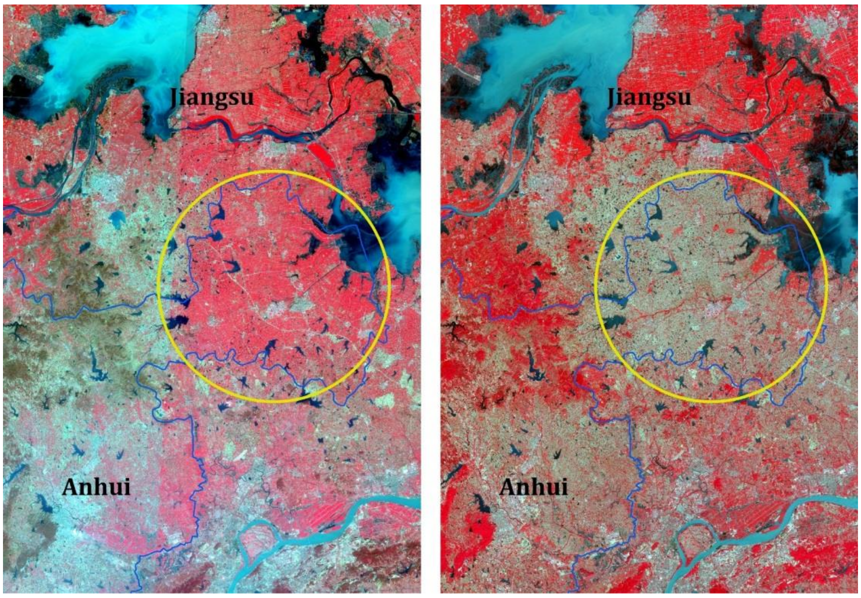

(a) (b)

Winter wheat represents almost 91% of the total output for winter crops in China. For 2017, CropWatch puts the total winter crop production at 126 million tons, a 1.3% increase from 2016's low production (table 4.3). Due to the low income from for rapeseed cultivation and unfavorable climatic conditions during the planting window, the total planted area dropped by 0.8% compared to 2016. The most significant decrease of planted area occurred in Shanxi (-3.1%), Jiangsu (-6%), Anhui (-5.1%), and Shaanxi (-3.3%). Yield nevertheless increased by 2.1% at the national level as a result of favorable climatic conditions. Total winter crop output is estimated to increase from last year's low output in most provinces, except for Hubei (-0.2%), Shaanxi (-1.5%), and Gansu (-0.5%).

Considering the relatively severe impacts from pest and diseases (see section 4.3), however, production of winter wheat and total winter crops could be lower at final estimates. CropWatch will continue to monitor the crop condition and provide updates in future bulletins.

Table 4.3. China, 2017 winter crops production (thousand tons) and percentage difference with 2016, by province

	2015 (thousand ton)	**2016**			
		Area change (%)	Yield change (%)	Production change (%)	Production (thousand ton)
Hebei	11615	0.0	4.0	4.0	12077
Shanxi	2218	-3.1	4.7	1.5	2251
Jiangsu	9971	-6.0	2.3	-3.9	9585
Anhui	12044	-5.1	2.0	-3.2	11662
Shandong	24100	0.9	2.4	3.3	24898
Henan	25305	2.5	1.4	3.9	26293
Hubei	5875	-1.8	-0.2	-2.0	5756
Chongqing	2316	-1.5	0.4	-1.1	2289
Sichuan	5541	-1.7	1.2	-0.5	5513
Shaanxi	4085	-3.3	-1.5	-4.8	3889
Gansu	3002	0.4	-0.5	-0.1	2999
Sub total	106072	-	-	1.1	107211
Other provinces	18613	-	-	2.4	19064
National total*	**124685**	**-0.8**	**2.1**	**1.3**	**126275**

Note: * National total production does not include Taiwan province.

Figure 4.7. Winter crops planted area in 2017 and changes from 2016 based on 16m GF-1 imagery

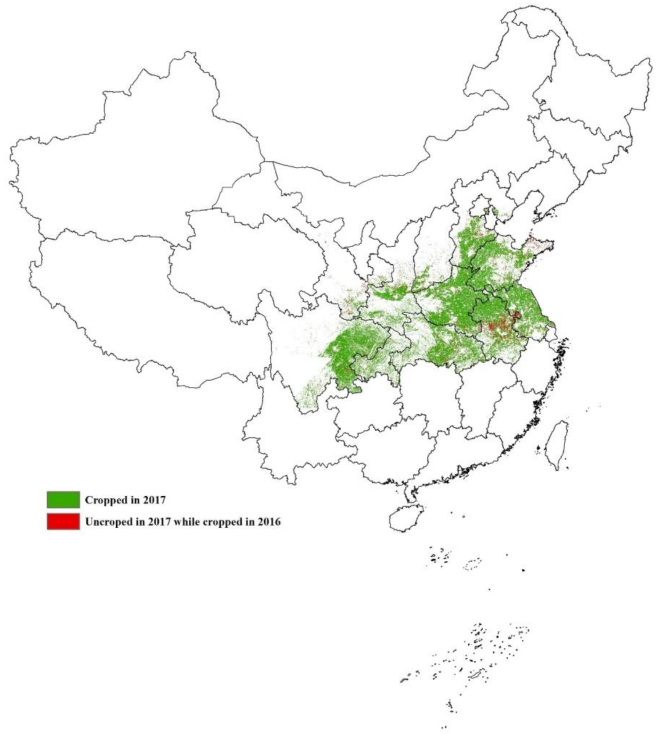

4.3 Pest and diseases monitoring

The impact of pests and diseases[2] was relatively severe in mid-May 2017 in the main wheat regions, at a time when the crop was mainly in the mid and late stages of grain filling in the Huanghuaihai and Lower Yangtze regions. According to the rainfall and irrigation data for southern Huanghuaihai and Southwest China, conditions were conducive to wheat yellow rust and sheath blight dispersal. In northern Huanghuaihai, high temperature and low precipitation provided conditions conducive for wheat aphid reproduction.

Wheat yellow rust

The mid-May distribution of wheat yellow rust is shown in figure 4.8 and table 4.4. The total area affected by the disease reached 3.7 million hectares, severely affecting central Ningxia, most of Henan, central Anhui, and central Shandong, but only moderately impacting eastern Gansu, eastern Anhui, and southern Jiangsu.

Figure 4.8. Distribution of wheat yellow rust in China (mid-May 2017)

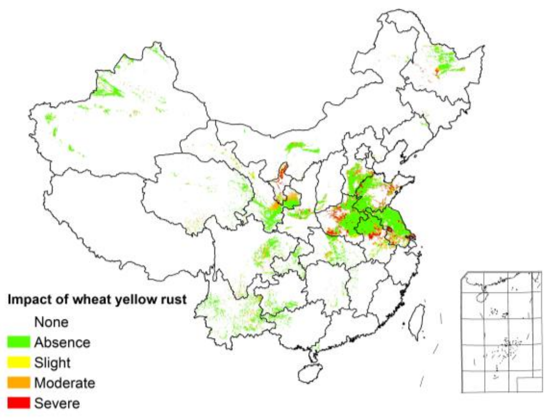

[2] Please see Annex C on more information about the classification of pests and diseases.

Table 4.4. Statistics of wheat yellow rust in China (mid-May 2017)

Region	Occurrence ratio (%)			
	Absence	Slight	Moderate	Severe
Huanghuaihai	84	5	4	7
Inner Mongolia	88	4	4	4
Loess region	85	4	5	6
Lower Yangtze	86	4	4	6
Northeast China	90	4	4	2
Southern China	100	0	0	0
Southwest China	88	4	3	5

Wheat sheath blight

Wheat sheath blight—with distributions shown in figure 4.9 and table 4.5—damaged around 8.7 million hectares. The disease was found in most of Ningxia, most of Henan, and in central Anhui where impact was severe. In most of Shandong, eastern Gansu, southern Jiangsu, and eastern Sichuan, damage remained moderate.

Figure 4.9. Distribution of wheat sheath blight in China (mid-May 2017)

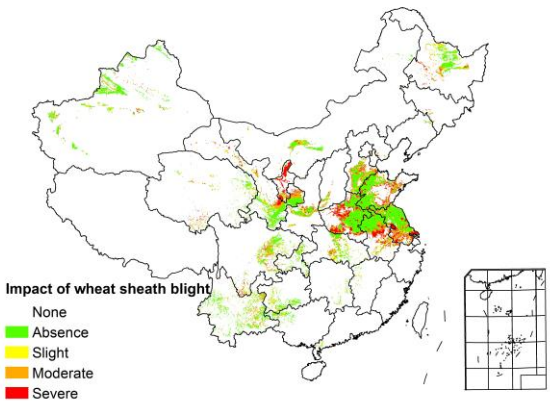

Table 4.5. Statistics of wheat sheath blight in China (mid-May 2017)

Region	Occurrence ratio (%)			
	Absence	Slight	Moderate	Severe
Huanghuaihai	61	7	14	18
Inner Mongolia	67	8	14	11
Loess region	65	5	13	17
Lower Yangtze	65	5	14	16
Northeast China	73	8	11	8
Southern China	86	5	7	2
Southwest China	73	6	13	8

Wheat aphid

Finally, wheat aphid (figure 4.10 and table 4.6) damaged around 12.7 million hectares, with the pest occurring in most of Henan, northern Shandong, and most of Heilongjiang with a severe impact. In northern Anhui, eastern Gansu, most of Yunnan, and eastern Sichuan, the impact was only moderate.

Figure 4.10. Distribution of wheat aphid in China (mid-May 2017)

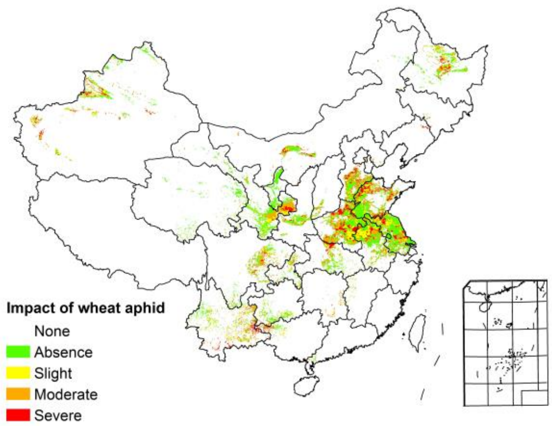

Table 4.6. Statistics of wheat aphid in China (mid-May 2017)

Region	Occurrence ratio (%)			
	Absence	Slight	Moderate	Severe
Huanghuaihai	47	16	19	18
Inner Mongolia	49	14	18	19
Loess region	50	16	19	15
Lower Yangtze	47	16	20	17
Northeast China	49	13	17	21
Southern China	46	14	19	21
Southwest China	52	14	17	17

4.4 China food imports and exports outlook for 2017

Analysis of food import and export in the first quarter of 2017

Wheat

Wheat imports for China in the first quarter of 2017 reached 1.08 million tons, an increase of 91.7% over the same period the previous year. Main sources of imported wheat were Australia (57.9% of total imports), the United States (26.7%), Kazakhstan (8.1%), and Canada (6.8%); the total value of the wheat imports amounted to US$ 227 million. Exports (21,100 tons) went mainly to Hong Kong and the Democratic People's Republic of Korea, which received respectively 79.7% and 12.6% of the total, the value of which amounted to US$ 11 million.

Rice

In the first quarter, 0.871 million tons of rice were imported, which was 3.0% less than the year before. The main sources of imported rice were Vietnam, Thailand, and Pakistan (accounting for 48.3%, 30.3%, and 11.0% of China's total rice imports, respectively), for a total value of US$ 412 million. Rice exports (0.2044 million tons worth US$ 119 million) went mainly to the Republic of Korea, Côte d'Ivoire, and Mozambique, respectively accounting for 34.0%, 22.6%, and 10.8% of exported rice.

Maize

China imported 306.6 thousand tons of maize in the first quarter, 52.5% less than the year before. The main sources of imports were Ukraine and the United States, respectively accounting for 93.6% and 5% of the total. The imports amounted to US$ 67 million in total. Exports were 1,344.85 tons (US$ 0.2978 million), of which most went to the Democratic People's Republic of Korea (94.5% of total exports).

Soybean

In the first quarter, soybean imports were 19.520 million tons, up 20.0%, mainly from the United States and Brazil (79.0% and 13.8%). The value of imports amounted to US$ 8,453 billion. Soybean exports were 32,500 tons, up 7.3%.

2017 prospects for imported food staples in China

The projections below are based on 2016-2017 global crop monitoring based on remote sensing data and a simulation model that takes into account major shocks and policies (based on the standard GTAP model).

- *Wheat.* China's wheat imports are estimated to grow 4.5%, while wheat exports will fall 10.2% in 2017. Domestic high-quality wheat production prospects were positively influenced by structural changes on the supply side. Overall, wheat imports are stable with a slight increase in 2017.
- *Rice.* In 2017, rice imports are expected to increase 8.7%, and exports will increase 1.5%. At present, domestic and foreign price differentials continue to exist; as a result, rice imports are predicted to continue an increase, but still within the quotas.
- *Maize.* Imports of the crop are expected to drop 30.6%, while exports of maize will increase 12.6%. The supply and demand situation of domestic maize is still loose, and maize imports are restricted.
- *Soybean.* In 2017, soybean imports are expected to increase 1.2%, while exports decrease 2.8%. Due to planting structure adjustment policies and low maize production, a growth in soybean import seems unlikely and soybean imports are expected to remain low in 2017.

4.5 Regional analysis

Figures 4.11 through 4.17 present crop condition information for each of China's seven agricultural regions. The provided information is as follows: (a) Crop condition development graph based on NDVI, comparing the current season up to April 2017 to the previous season, to the five-year average (5YA), and to the five-year maximum; (b) Spatial NDVI patterns for January to April 2017 (compared to the (5YA); (c) NDVI profiles associated with the spatial patterns under (b); (d) maximum VCI (over arable land mask); and (e) biomass for January-April 2017. Additional information about agroclimatic indicators and BIOMSS for China is provided in Annex A, table A.11.

Northeast region

Agroclimatic conditions were favorable over the recent monitoring period of January-April, which covers the sowing period of crops in Northeast China. CropWatch agroclimatic indicators show average rainfall (RAIN, -1%) and slightly below average sunshine (RADPAR, -1%) associated with a significant positive temperature anomaly (TEMP, +1.9°C). The favorable agroclimatic conditions resulted in a 9% above average biomass potential (BIOMSS) in the region.

Crops have just been sowed in the region, and so far crop conditions are favorable for the early growing period of the crop.

Figure 4.11. Crop condition China Northeast region, January-April 2017

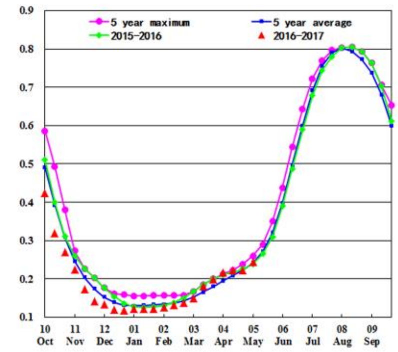

(a) Crop condition development graph based on NDVI

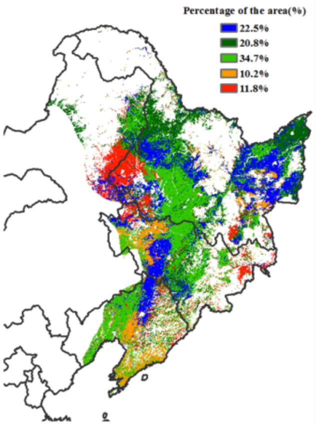

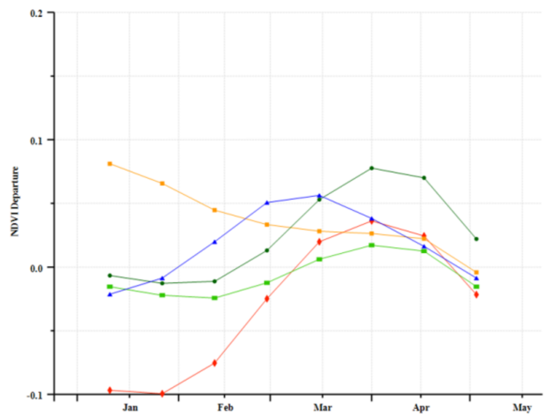

(b) Spatial NDVI patterns compared to 5YA (c) NDVI profiles

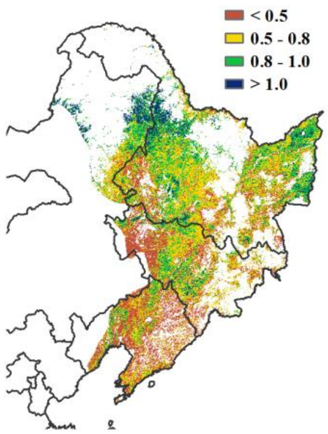

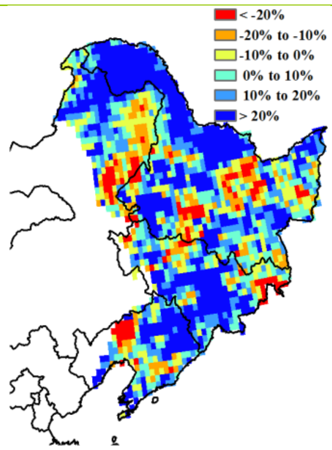

(d) Maximum VCI (e) Biomass

Inner Mongolia

No crops were cultivated in Inner Mongolia between January and April due to the seasonally low temperatures. The NDVI index in the crop condition development graph was very low before April. Along with gradually increasing temperatures, crops are starting to be sowed from April on. For the first four months of the calendar year, CropWatch rainfall and temperature indices were well above average (RAIN, +60% and TEMP, +1.5°C), while PAR accumulation was average. The resulting biomass increase measured by the BIOMSS indicator reaches 48%, with increases especially in central and northern areas. A record VCIx is observed in the north of the region. If favorable conditions continue over the whole crop cycle, the outcome may be an exceptionally good season.

Figure 4.12. Crop condition China Inner Mongolia, January-April 2017

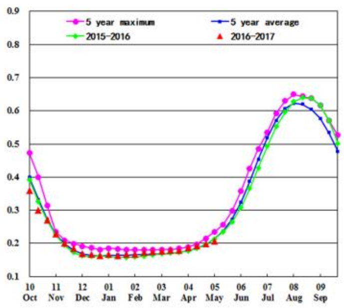

(a) Crop condition development graph based on NDVI

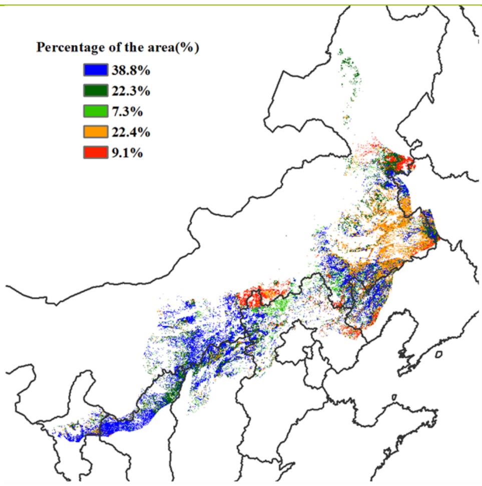

(b) Spatial NDVI patterns compared to 5YA

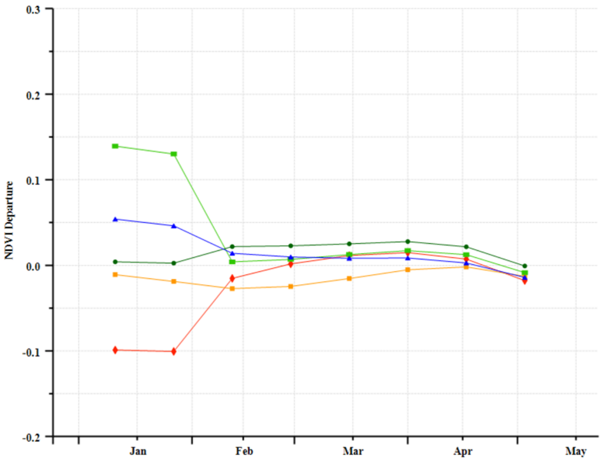

(c) NDVI profiles

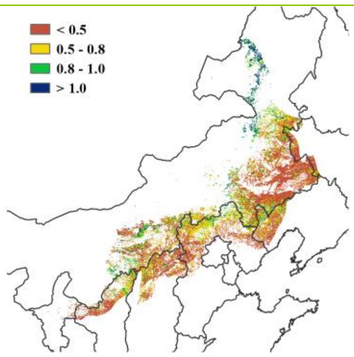

(d) Maximum VCI

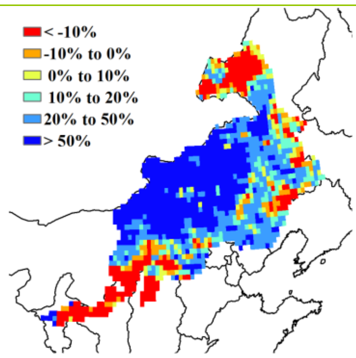

(e) Biomass

Huanghuaihai

In Huanghuaihai, the harvesting of winter wheat will start in two months, while summer maize is going to be sowed immediately after. As shown by the NDVI development graph, crop condition was generally above the five-year average during the monitoring period and even better than the five-year maximum before March. According to the spatial NDVI patterns and profiles, the overall situation appears to be above average in most of the region, with the exception of some southern provinces (eastern Henan, northern Anhui, and Jiangsu) where crop condition was below average. Spatial NDVI patterns and the map indicating biomass production potential agree in showing below average conditions in the south. Satisfactory crop condition can be inferred also from the prevailing agroclimatic conditions in Huanghuaihai: 15% above average rainfall (RAIN), 0.9°C above average temperature (TEMP), and -3% below average PAR, resulting in a large improvement in the biomass production potential (BIOMSS, +19%) compared to the recent five-year average. The maximum VCI presents high values in almost the entire region, while low values occur in eastern Hebei. Overall, favorable climatic conditions will greatly benefit the development of winter wheat and the sowing of the forthcoming summer crop.

Figure 4.13. Crop condition China Huanghuaihai, January-April 2017

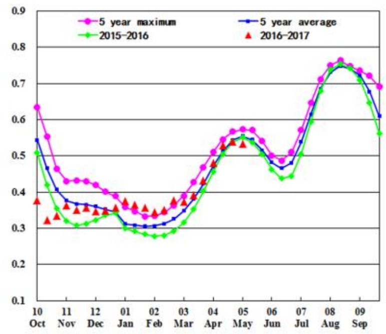

(a) Crop condition development graph based on NDVI

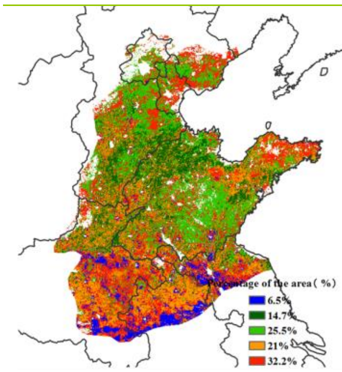

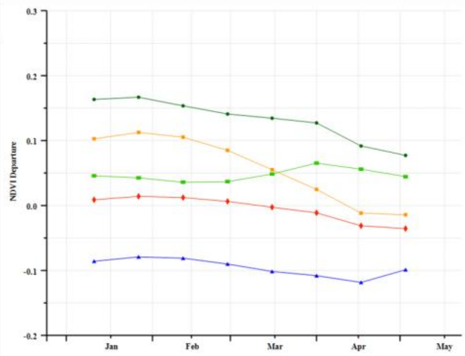

(b) Spatial NDVI patterns compared to 5YA

(c) NDVI profiles

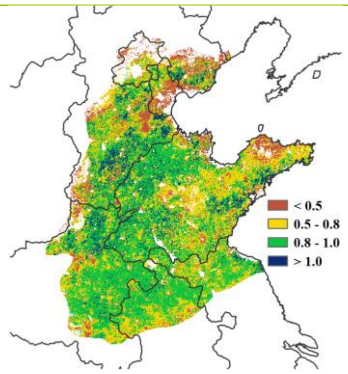

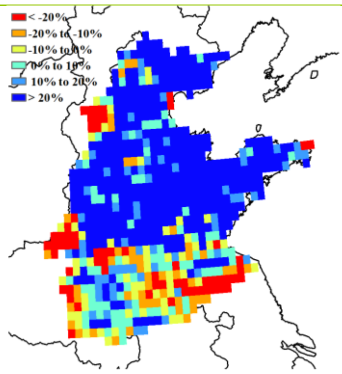

(d) Maximum VCI

(e) Biomass

Loess region

According to the crop condition development graph based on NDVI, crop condition was generally better than last year's in the Loess region except during the second half of April. The main crops in the region are spring wheat and winter wheat. Spring wheat was sowed during late March to early April, while winter wheat was sowed in October and will be harvested in early June. During the monitoring period, rainfall (RAIN) exceeded average by 23%, while temperature (TEMP) was 0.4°C above. Radiation (RADPAR) was 5% below average, which is consistent with the excess precipitation. The additional detail provided by the NDVI clusters and profiles shows that crop condition was close to average in most parts of the region until mid-April. It then deteriorated, and at the end of the monitoring period, crop condition was below average, especially in the middle and east of Gansu province. The fraction of cropped arable land (CALF) for the region decreased 7 percentage points when compared with the five-year average, which indicates less land is cropped. The potential biomass indicator (BIOMSS) was 16% above average, with above average values in particular reported in the south of Shanxi and eastern Shaanxi province. According to the VCIx map, with the exception of central Shaanxi, current crop condition in the region is unfavorable but deserves close monitoring.

Figure 4.14. Crop condition China Loess region, January-April 2017

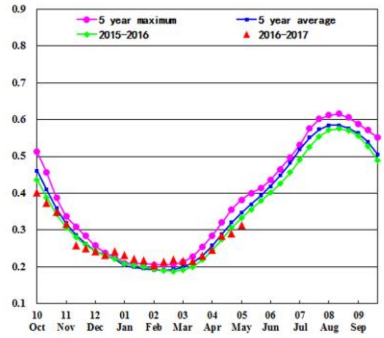

(a) Crop condition development graph based on NDVI

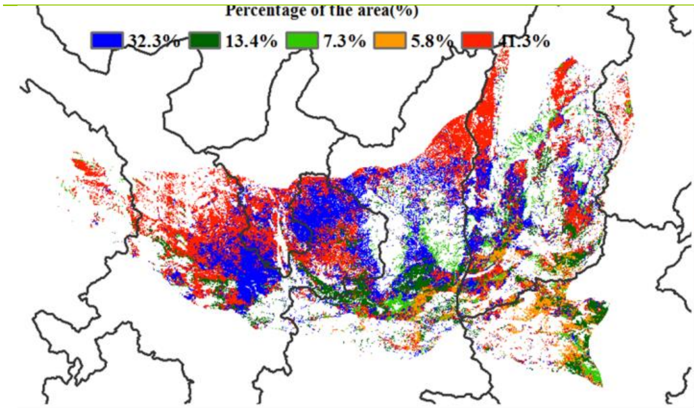

(b) Spatial NDVI patterns compared to 5YA

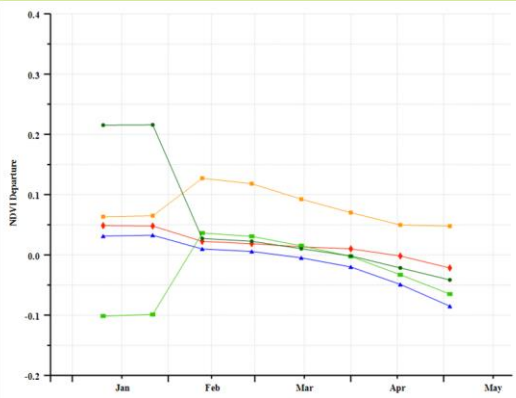

(c) NDVI profiles

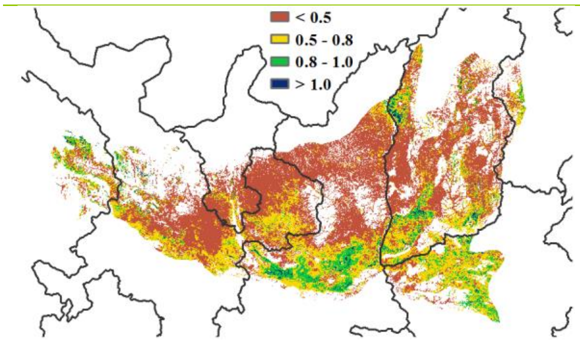

(d) Maximum VCI

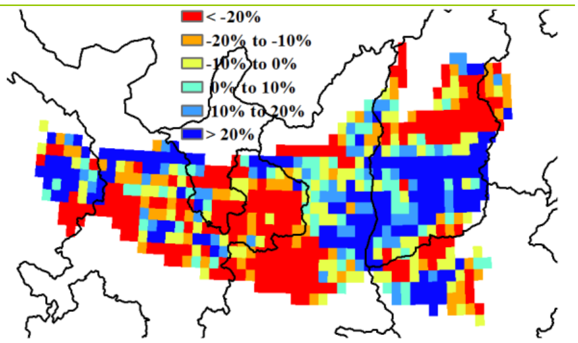

(e) Biomass

Lower Yangtze region

In the north of the region, winter wheat has reached the flowering stage, while in the south early rice was at transplanting. The harvest of rapeseed was completed in early April. Overall, crop condition in the region was below the five-year average, according to the crop condition development graph based on NDVI. As for the agroclimatic indicators, rainfall (RAIN, -21%) and radiation (RADPAR, -7%) were below average, while temperature was about average (+0.4°C). As a result, the BIOMSS index dropped 6% compared to the average for this region and period, and even as much as 20% in middle and southwest Jiangsu, middle of Jiangxi and Hubei, and in the east of Hunan. Considering that the fraction of cropped arable land (CALF) was 2 percentage points below the average of recent years, crop production is anticipated to be mostly unfavorable.

Figure 4.15. Crop condition Lower Yangtze region, January-April 2017

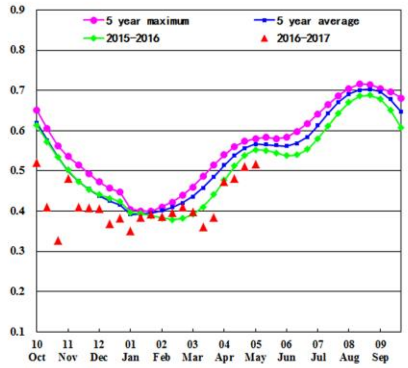

(a) Crop condition development graph based on NDVI

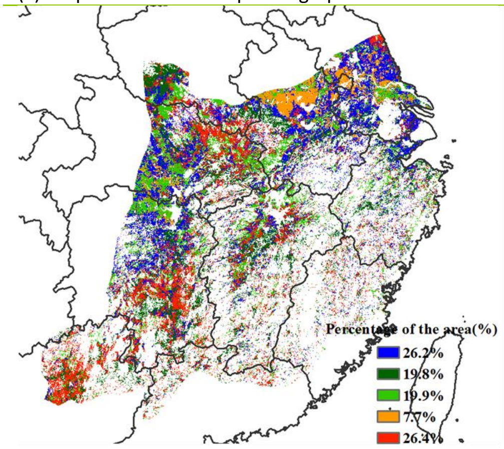

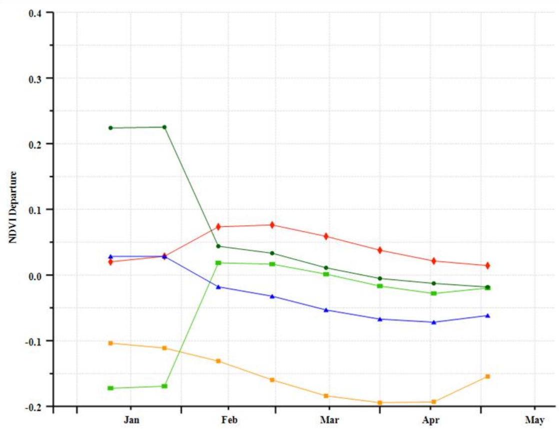

(b) Spatial NDVI patterns compared to 5YA

(c) NDVI profiles

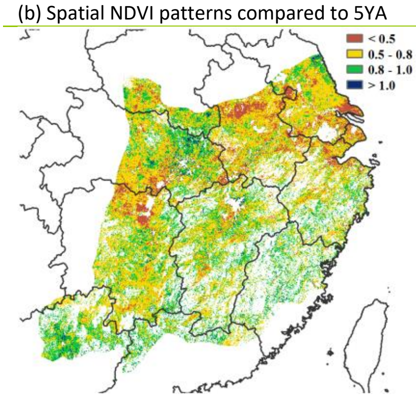

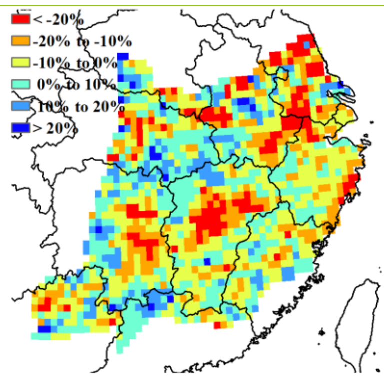

(d) Maximum VCI

(e) Biomass

Southwest China

The monitoring period covers the planting of maize and single rice, as well as the growth of winter wheat in this region. Conditions were generally below average in January and March and close to average in February and April. Rainfall (RAIN, -17%) and radiation (RADPAR, -13%) indicators were below average for this monitoring period, while temperature was about normal (TEMP, -0.1°C).

The maximum VCI for Southwest China (0.69) is just fair, and the fraction of cropped arable land (CALF) underwent a slight drop of 1 percentage point. The map of spatial NDVI patterns and associated profiles adds some spatial detail: below average conditions occurred in (i) parts of east Sichuan and west Guizhou in February and March, and also in (ii) parts of north and west Chongqing and east Sichuan in January. Compared to average, 37% and 30% below average rainfall were observed in Chongqing and Guizhou respectively. As this will probably negatively influence the outcome of the cropping season, close monitoring is required.

Figure 4.16. Crop condition Southwest China region, January-April 2017

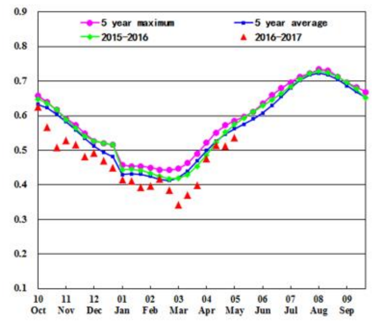

(a) Crop condition development graph based on NDVI

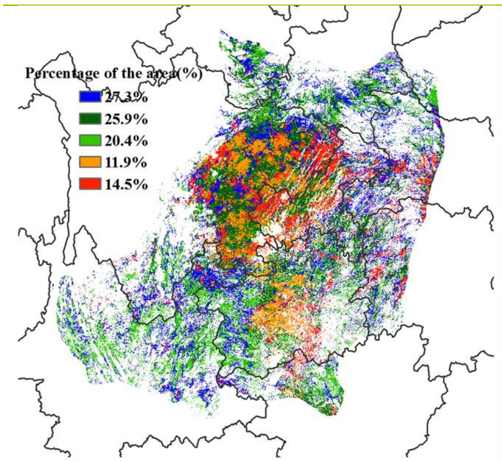

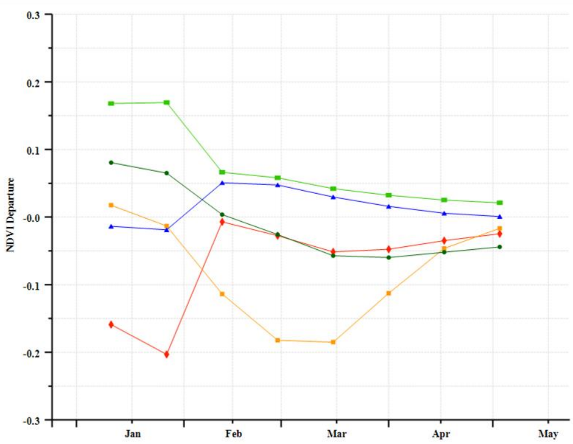

(b) Spatial NDVI patterns compared to 5YA

(c) NDVI profiles

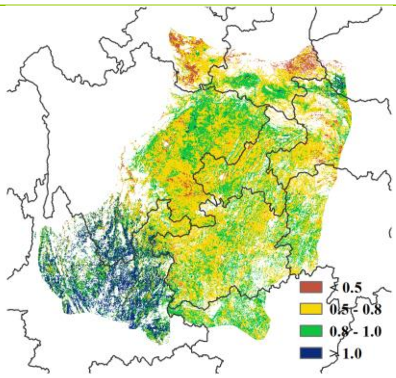

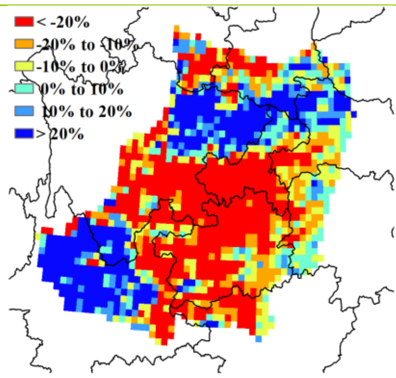

(d) Maximum VCI

(e) Biomass

Southern China

This reporting period mainly covers the planting of early rice and the growing season of winter wheat in Southern China. Crop condition was mixed, with condition generally above average between January and February, then below average from March to April—possibly due to heavy rain and low temperature, and average again at the end of April. For the period as a whole, rainfall was almost double the average (RAIN, +99%), while the temperature departure was negative (TEMP, -1.1°C). Parts of southern Fujian and central Guangxi provinces showed below average crop condition in March and April according to the spatial NDVI patterns. This was brought about by the excess rain (+96% in Guangxi and +85% in Fujian), and the area will need close monitoring. Other areas in the region shows above average condition but with a mix of average and anomalous climate variables between provinces: in Yunnan, rain was below average (-10%) and TEMP and RADPAR were relatively low (-1°C and -8%, respectively); in Guangdong, rainfall and TEMP were average (RAIN, 0% and TEMP, 0%), while RADPAR was below average (-6%). Southern Yunnan and Guangxi also showed a significant drop in the biomass production potential (BIOMSS, -20%), further underlining the need for continued close monitoring. The excess precipitation is likely to negatively influence the current winter crops. Summer crops are likely to benefit from abundant soil moisture.

Figure 4.17. Crop condition Southern China region, January-April 2017

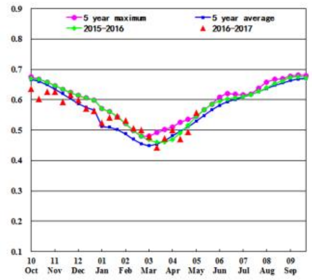

(a) Crop condition development graph based on NDVI

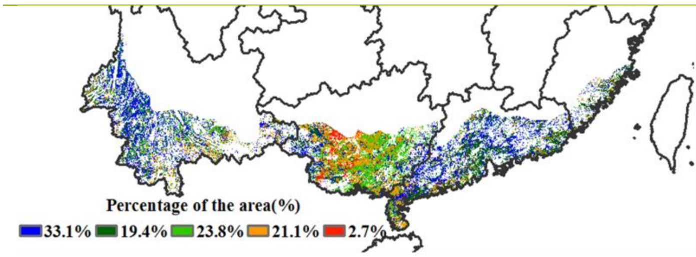

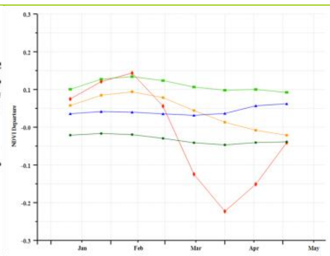

(b) Spatial NDVI patterns compared to 5YA

(c) NDVI profiles

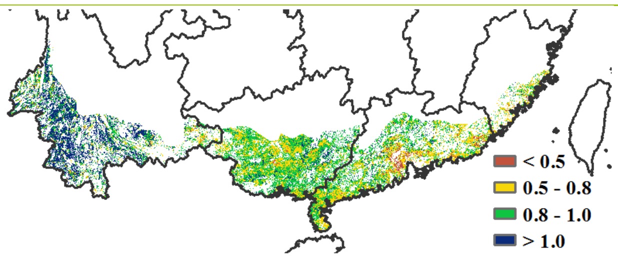

(d) Maximum VCI

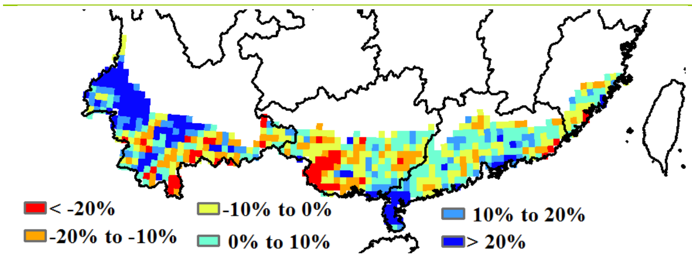

(e) Biomass

Chapter 5. Focus and perspectives

Building on the CropWatch analyses presented in chapters 1 through 4, this chapter presents initial CropWatch food production estimates for 2017 (section 5.1), as well as sections on recent disaster events (section 5.2), and an update on El Niño (5.3).

5.1 CropWatch food production estimates

Methodological introduction

Table 5.1 presents the first estimate by the CropWatch team of global maize, rice, wheat, and soybeans production in 2017. It is issued at a time when many winter crops in the northern hemisphere are still growing and summer crops are in very early stages, or even to be planted; in the southern hemisphere the harvest of the summer season/monsoon season was completed. The estimate is based on a combination of remote-sensing models (used for major commodities at the national level and presented in red in table 5.1) and statistical trend-based projections, which are used for minor producers and for those countries which will harvest their crops later during 2017 and for which no directly monitored crop condition information is currently available. The percentage of modeled production varies by crop: 24% for maize, 65% for rice, 98% of wheat (most of it being winter wheat) and 52% for soybeans.

For China and the 30 countries described in chapters 3 and 4 and listed by name (the "major producers"), the quantitative estimates in this chapter are calibrated against national agricultural statistics (as opposed to FAOSTAT). This means that (i) sub-national statistics are used at least for the largest countries and (ii) 2016 information in included in the calibration. It is also stressed that the calibration is crop-specific, which means it is based on different crop masks for each crop and that, for each crop, both yield variation and cultivated area variation are taken into account when deriving the production estimates. The major producers represent at least 80% of production and 80% of exports. "Others"[3] and the countries shown in black in the production table were extrapolated to 2017 based on the linear trend from 2010 to 2016, with FAOSTAT data up to 2014 (the last year available) and CropWatch final estimates for 2015 and 2016.

CropWatch production estimates differ from other global estimates by the use of geophysical data in addition to statistical and other reference information such as detailed crop distribution maps.

Production estimates

CropWatch estimates the global 2017 production of the major commodities at 730 million tons of wheat (a 1% drop below 2016), 761 million tons of rice (up 3%), 305 million tons of soybeans (down 3%), and 1056 million tons of maize, up 5% over 2016. The major producers contribute 622 million tons of wheat (-1%), 685 million tons of rice (+3%), 282 million tons of soybeans (-4%), and 936 million tons of maize (+6%). The share of the "minor producers" (shown as "others" in the table) to the global production is 8% (soybean) to 15% (maize) of the global production, and about 10% for rice and wheat. With the exception of wheat and soybeans, the group of the major producers outperforms the bulk of the remaining nations, with the largest increases over 2016.

[3] "Minor producers" include the 151 countries from Afghanistan and Angola to Zambia and Zimbabwe.

Table 5.1. CropWatch estimated maize, rice, wheat and soybean production for 2017 (thousands tons)

	Maize		Rice		Wheat		Soybean	
	Production (ktons)	% change from 2016	Production (ktons)	% change from 2016	Production (ktons)	% change from 2016	Production (ktons)	% change from 2016
Argentina	29946	16	1769	4	11338	-3	51116	0
Australia	759	61	1864	24	32066	1	92	-7
Bangladesh	2751	16	50365	6	1471	12	64	
Brazil	79243	13	11177	1	7771	3	96726	5
Cambodia	811	4	8880	3			147	-11
Canada	12198	4			32589	-2	5829	8
China	212114	6	204744	2	120611	2	12842	-3
Egypt	5628	-1	6109	-3	9947	-3	33	18
Ethiopia	6806	-5	173	29	5066	7	72	-28
France	14518	-1	380	387	37460	-1	129	-38
Germany	4351	-5			27566	-2	8	
India	19522	5	167735	7	100777	17	13873	14
Indonesia	17627	-4	70000	1			900	2
Iran	2535	-6	2690	-3	11884	-26	173	0
Kazakhstan	722	5	392	-5	15607	-14	207	-24
Mexico	22779	-4	158	-11	3542	0	278	-30
Myanmar	1841	5	27752	9	190	1	178	40
Nigeria	10392	-4	5248	14	84	-27	517	-22
Pakistan	4216	-7	9302	2	24239	-2	0	
Philippines	8519	13	19103	-5			1	
Poland	4703	28			10017	-6	1	
Romania	10105	-12	39	-18	6184	-19	141	-32
Russian Federation	15199	23	996	-2	47379	-18	2025	-4
South Africa	12370	37	3	0	1776	4	912	-17
Thailand	5037	-1	41732	5	1	18	144	-38
Turkey	6632	12	949	1	16916	-11	180	-17
Ukraine	35535	15	98	-8	25254	5	3183	-16
U. Kingdom					12691	-11		
United States	383410	4	10030	-5	54375	-4	92351	-16
Uzbekistan	490	15	496	13	6037	-6		
Vietnam	5434	4	42643	0			172	
Sub-total	**936194**	**6**	**684828**	**3**	**622838**	**-1**	**282296**	**-4**
Others	119762	2	75997	2	106946	4	23027	5
Global	**1055956**	**5**	**760825**	**3**	**729784**	**-1**	**305322**	**-3**

Note: Numbers in red are based on remote-sensing models, while other numbers are statistical trend-based projections.

Maize

In the southern hemisphere, a large increase in maize production is listed for South Africa (+37%), as the country recovers from the 2016 El Niño drought. Both Brazil and Argentina did well with 79 million tons (+13%) and 30 million tons (+16%), respectively; the tables in Annex B show additional detail. In both countries, "others" are catching up with the main producing areas, illustrating the fact that production areas are diversifying, which can only be beneficial in the long term for the stability of output, especially in Argentina which has recently suffered from large production variability. The provinces of Cordoba and Buenos Aires still account for 25% of production each, but "others" is now reaching the same percentage. Moreover, while the two leading provinces experience a drop in the production of maize (-3% and -2%), "others" increased 7%. In Brazil, the states of Mato Grosso, Parana, and Goias still lead: they make up 24%, 19%, and 10% of the national production, respectively. The first, however, grew over 2016 at a rate of 5% to 6%, while Goias progressed 27%, and "others" 47%, describing the same picture of spatial diversification as in Argentina.

In the northern hemisphere, Poland (+28%), Russia (+23%), and Ukraine (+15%) showed increases that result from the trend of the previous seasons. Among the major producers in the northern hemisphere, CropWatch puts China at 212 million tons (+6%) and the United States at 383 million ton (+4%).

Rice

Among the major Asian producers, most are assessed to be doing well in 2017, including Bangladesh (50 million tons and a +6% increase over 2016), India (167 million tons, +7%) in spite of very mixed weather conditions in late 2016, Indonesia (70 million tons, +1%), and Myanmar (28 million tons, +9%). Among the major exporters, Thailand (41 million tons, +5%) did well, but less favorable outputs are projected for Vietnam (43 million tons, 0%). The Philippines are the only major Asian producer that is projected to undergo a decrease (-5%). All negative impacts are more or less directly the result of El Niño, and the current situation of the phenomenon (see section 5.4) raises the fear that it may repeat itself in 2017. The main producers in Latin America, while their rice outputs are sizeable, are dwarfed in comparison with Asia. CropWatch covers Brazil with some detail (see also annex B2), and the country is projected to increase this year's rice production. Argentina, which is listed in table 5.1 with 2 million tons of rice output (+4%) actually comes after Peru and Colombia in terms of production. Among the largest non-trend based production estimates, the largest decrease in rice production is listed for Egypt (-3%), along with decreases for all its cereals (maize, -1% and wheat, -3%). CropWatch puts rice production for China at 205 million tons (+2%) and for Pakistan at 9 million tons (+2%).

Wheat

Table 5.1 lists few countries with an improved production over 2016, resulting in the above-mentioned global production decrease of 1%. Positive values for winter wheat in the northern hemisphere, which makes up the bulk of wheat production, are estimated at 12% for Bangladesh, where the crop is gaining popularity, 2% for China, 17% for India (the Rabi crop), and 5% for Ukraine, which contradicts the generally mixed qualitative assessment in Chapter 3 and thus requires special attention in the next monitoring period. Large negative values are given for Iran (-26%) and Kazakhstan (-14%), Romania (-19%), the Russian Federation (-18%), and Turkey (-11%). Many of the areas suffered from an unusually large shortage of sunshine, but this occurred at late dormancy and early spring growth. Better estimates will become available at the time of harvest. The CropWatch estimate for the United States stands at -4%, which will probably need to be revised upward according to the qualitative assessment (see also the detailed estimates by state in annex B). All the major wheat producing states with a drop in production compared with 2016 also recorded very low sunshine and very abundant rainfall that may have affected crop development through water logging. These include Kansas (-8% wheat production, -7% RADPAR), North Dakota (-20%, -4%), South Dakota (-19%, -5%), Colorado (-5%, -4%), Idaho (-18%, -9%), and Nebraska (-15%, -8%).

Soybean

Only two estimates based on remote sensing are currently available after the South American summer crop harvest, for which details are given in annex B. Argentina remained at the same level as in 2016, and Brazil is up 5% for soybean production. In Argentina, the production drop recorded by the two main provinces (-3% in Buenos Aires and -2% in Córdoba) that together provide about half the national output, is compensated by increases in Entre Rios (+6%) and by "others" (+7%). In Brazil, all states did well, including the two major producers (Mato Grosso +5% and Parana +6%), but with the exception of Minas Gerais (-3%).

Major importers and Exporters

Table 5.2 provides some information about the likely impact on trade of the production variations outlined above. Both maize importers and exporters increased their production by approximately the same percentage between 5% and 7%. For rice, however, the output of the two major importers was low: Philippines (-5%, modelled) and Iran (-3%, trend-based). Nigeria, the top importer in Africa, which produces about 5 million ton of rice, will do well (+14%) if the recent trend continues into 2017.

Table 5.2. 2017 production (million tons) and difference from 2016 of major importing and exporting countries

	Maize		Rice		Wheat		Soybean	
	Prod. (million tons)	% change from 2016	Prod. (million tons)	% change from 2016	Prod. (million tons)	% change from 2016	Prod. (million tons)	% change from 2016
Top 5 importers	241	5	28	-1	30	1	13	-4
Top 10 importers	252	5	306	2	38	1	14	-11
Top 5 exporters	543	7	271	5	204	-6	246	-9
Top 10 exporters	809	6	315	5	290	-6	432	3

Wheat importers did relatively well (+1%), but exporters are assessed as generally poor, with negative changes among 4 of the top 5 exporters (United States -4%, France -1%, Canada -2%, and Russia -18%) and 8 of the top 10 (including also Germany -2%, Argentina -3%, Kazakhstan -14%, and Romania -19%).

For soybean, top importers produce typically only a fraction of their consumption, so that the negative 2017 trend compared with 2016 is of little significance; it is, however, an illustration of ever increasing demand. Among the top 5 exporters of the crop actual data are available for Latin America, where the total output remained stable in Argentina but increased in Brazil.

5.2 Disaster events

This section focuses on disasters that occurred between February and the end of April 2017, a relatively quiet period in comparison with previous ones in terms of the number of events to be reported on. The period is characterized mainly by the aftermath of El Niño, i.e., floods in north-western South America in March (excess rain started last year in December); the difficult recovery from the impact of El Niño in the Horn of Africa where drought drags on in large areas; and the recovery from hurricane Matthew, which befell the Caribbean and adjacent areas in September 2016, causing damage now estimated to be in excess of US$ 15 billion. Haiti was badly affected because of the prevailing poverty and resulting lack of resilience against disasters, and 400,000 people are still in need of food aid.

Fall Armyworm

At the end of April, Reliefweb released an updated report about a new pest called the Fall Armyworm (*Spodoptera frugiperda*), which continues spreading in southern, east and west Africa (Figure 5.1). The insect is native to Central

Figure 5.1. Fall Armyworm situation as of 26 April 2017

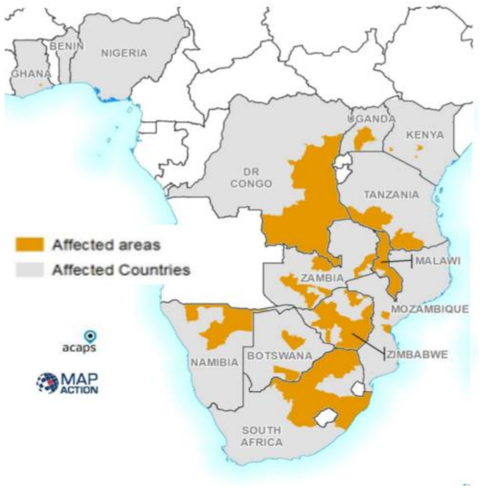

Source: ACAPS thematic report, http://reliefweb.int/sites/reliefweb.int/files/resources/20170425_acaps_thematic_report_southern_africa_armyworms_update.pdf and South America, and it is not known how it reached Africa where another armyworm (*S. exempta*) is a native species. According to a recent note in the journal Nature, even if the Fall Armyworm is currently causing limited damage in Africa, it is very likely that it will eventually spread to Europe and Asia as well.

Temperature excesses

With few exceptions (such as a heat wave in Australia), no excessive temperature situations (cold or warm waves) were flagged by the entities monitoring disasters (Reliefweb, ACAPS, and Recent Natural Disasters, among others.)

Cyclones

Several cyclones with limited impact on agriculture were recorded in Oceania and the Indian Ocean. These include for example Debbie (in late March in east and northeast Australia) and, in April, Cook (New Zealand) and Maarutha (Myanmar). None of these, however, created significant damage in the agricultural sector, unlike two African storms.

In mid-February, tropical storm Dineo killed at least seven people in Mozambique and destroyed thousands of homes and buildings. Strong winds of up to 160 km/h affected 550,000 people as well as crops mainly in Inhambane province. Impacted crops included cereals and fruits, which are important local cash crops (cashew, coconut).

Figure 5.2. Track of cyclone Enawo

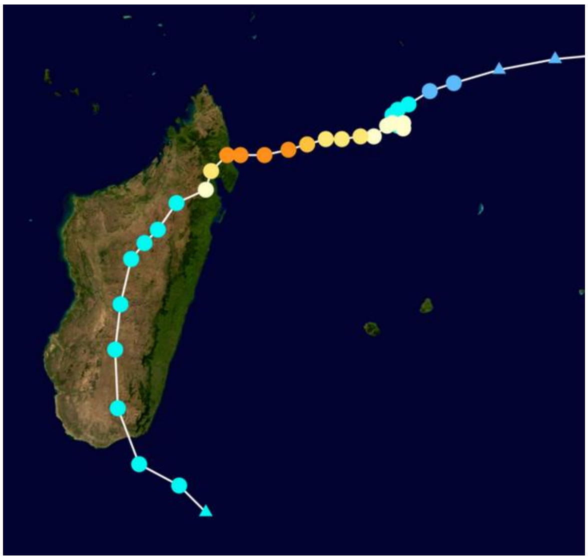

Source: https://en.wikipedia.org/wiki/Cyclone_Enawo#/media/File:Enawo_2017_track.png

One month later, on March 7, tropical cyclone Enawo (Figure 5.2) hit land in the northeastern district of Antalaha in Madagascar, the strongest cyclone in about 15 years. Heavy rain and strong wind that reached 230 km/h were recorded. After landfall, the cyclone turned left and crossed the island from north to south in two days, affecting the whole country, though mostly eastern and central areas. At least 80 people were killed and 183 wounded, mainly in Analanjirofo and Sava regions. Moreover, all crops and rice fields in Antalaha and Sambava were submerged and have been destroyed. Village food reserves were also destroyed by the floods, and food prices in local markets are increasing. More importantly, the impact on cash crops such as vanilla will be felt well after the situation returns to normal. According to World Bank estimates, losses in the agricultural sector reach about US$ 200 million.

Droughts

Drought situations are mainly reported from the Horn of Africa and Pakistan.

For the Horn of Africa, El Niño related droughts have been described in previous CropWatch bulletins. While the situation seems to have improved significantly in southern Africa, where floods were recorded (see below), the drought continued in areas of Somalia, Kenya, and Ethiopia. In the whole region, if the situation continues to deteriorate, cattle will die or herders will not be able to sell them. In contrast, maize prices went up, for example by 30% in Ethiopia, where prices currently are 43% above those for the same period last year. The price of milk and eggs has increased by 50% over the middle of last year.

Somalia experienced a bad dry Jilaal season (January-March). The river Shabelle, the main river, dried up, triggering movements into cities and Ethiopia. Half the population of the country currently needs food assistance (involving more than 6 million people, of which 50% in IPC phases 3 and 4). In just the last three weeks of April, the number of people displaced by drought increased 16%, bringing the total number of people in the country driven from their home areas by unrest and lack of water to more than 600,000, mostly in Baidoa (+34,700) and Mogadishu (+18,000). No new refugee movements were reported. Half the population of the country currently needs food assistance (involving more than 6 million people, of which 50% in IPC phases 3 and 4). At the beginning of the reporting period (January and February), the number of malnourished children had increased 24% over August last year. Somalia needs more international social attention to avoid that the unrests of Syria reappear.

In Ethiopia, about 120,000 people in the Somali region alone have been displaced since the beginning of the year, due to a combination of drought and unrest in neighboring Somalia. Food insecurity is largest mostly in the east, affecting Afar, the Sitti zone of Somali region, and parts of Amhara, Oromia, and SNNPR. In the east and south, about 6 million need humanitarian assistance.

In Kenya, just short of 40,000 displaced persons were reported in Isiolo and Baringo. Even if some relief was brought by March and April rainfall in some drought affected areas, the IGAD[4] Climate Prediction and Applications Centre (ICPAC) predicts a second consecutive poor rainy season in the semi-arid, pastoral areas, which will also affect Belg crops in Ethiopia that are normally harvested before August. The main rainy season in Kenya ("long rains", between March and May) was late in many areas already tried by last year's drought.

Altogether, the current situation in the Horn of Africa raises the risks that displaced persons may not be able to go back to their home areas (in spite of the fact that a few thousands were already supported by international aid organizations to return) and that the currently tense situation is bound to continue for months.

In Pakistan, a drought was reported for Sindh province in April by the EC Humanitarian Aid and Civil Protection (ECHO). About a quarter of the population is assessed as being moderately to acutely food insecure, mostly due to limited access to safe drinking water for people and animals. Waterborne diseases and malnutrition are increasing.

Floods and landslides

Heavy rainfall, often resulting in landslides, is reported from Indonesia (Java Island) and Bangladesh at the beginning of April, and in Afghanistan in March. Other continents were affected as well, especially the south of Africa and northwest Latin America.

In Bangladesh, rain started at the end of March, and low-lying areas, including croplands, have been inundated in the northeast (districts of Sylhet, Moulavibazar, Sunamganj, Habiganj, Netrokona, and Kishoreganj) as a result of rising waters and breached embankments (figure 5.3). The floods have caused 150,000 hectares of Boro rice to be destroyed just

Figure 5.3. Broken embankment in Tahirpur district, Northeast Bangladesh

Source: https://elispiritweaver.wordpress.com/category/storms/page/2/

[4] The Intergovernmental Authority on Development is a regional development community covering eight countries in the Horn of Africa.

before harvest, a production loss close to 800,000 tons according to the Ministry of Agriculture. Heavy March rains in Afghanistan led to floods in the provinces of Nimroz (especially Chakhansur district) and Khashrod; In total, 20,000 hectares of arable land were submerged in 23 villages, with the population made extremely vulnerable and in need of assistance.

South African floods, while providing a welcome relief after the 2015-16 drought, affected Mozambique (in relation with the above-mentioned cyclone Dineo), Zimbabwe (in early March), and northern Angola (late March). In Angola, 11 people died and thousands were made homeless. The most serious situation is reported from Zimbabwe, where about 250 people died, and the sudden afflux of water led to about 70 dams bursting.

The South American floods were severe both by their duration (they started in December 2016) and the number of people affected: 1.1 million in Peru and 180,000 in Ecuador and Colombia combined. Problems were first reported from Peru, but later moved into adjacent areas in the other two countries. The floods were brought about by an unusual phenomenon described as a "Coastal El Niño" (see section 5.4), and the whole array of phenomena linked with excess water occurred—landslides, floods, flash floods, and mud flows (figure 5.4). Throughout the region, relief operations were extremely difficult because of destroyed bridges and roads (6000 km in Peru alone); local food stocks were affected as well.

Figure 5.4. Devastation after a mudslide in Trujillo, northern Peru

Source: https://globalrumblings.blogspot.com/2017/04/floodsmudslides-disasters-death-toll.html

In Peru specifically, out of its 25 regions, 24 were affected by the floods and landslides and 12 declared a state of emergency, including the most affected regions of Piura and Lambayeque in the northwest, and Ica and Arequipa in the southwest. Infrastructure damage was most serious in Piura, Lambayeque, Lima, Ica, and Arequipa, with damages to dams and sewage and drainage systems. Food and water shortages are even reported in supermarkets in Lima. Food prices are rising in markets, even as only about 200 hectares of agricultural lands were destroyed as of March 20.[5]

The international media widely reported about the massive mudslide near Mocoa in Colombia (in the Department of Putumayo), which killed 254 people and injured 203 on March 31. The death toll is even expected to increase by at least 200 people. A state of emergency was declared in Putumayo, which borders Ecuador and Peru. In Ecuador, 47,000 people were affected, 21 people have died, and 1,410 were displaced throughout the country due to floods.

In the agricultural sector, the damage of the recent Peruvian floods is estimated to have reached US$ 645 million. The total cost of reconstruction (US$ 2-3 billion) could cancel out the planned GDP growth for the country for 2017.

5.3 Update on El Niño

El Niño conditions have strengthened across the Pacific Ocean during the first quarter of 2017 with an increasing probability (around 50% chance) that the phenomenon may develop again in the coming

[5] INDECI 20/03/2017.

months. The sea surface temperatures in the tropical Pacific Ocean have warmed since the start of 2017, especially in the west coastal regions of Peru with a 6°C above normal temperature, according to the Peruvian Government Multisectoral Committee on the El Niño Phenomenon (ENFEN). In the current season, the Southern Oscillation Index (SOI) has decreased from +1.3 in January to -2.2 in February, after which it rose to 5.1 in March and then again decreased to -6.3 in April (figure 5.5). The Australian BOM reports an El Niño watch, and CropWatch will continue paying attention to the risk of a renewed El Niño in 2017.

The average sea surface temperature anomalies are depicted in the NOAA image in figure 5.6, showing a different phenomenon referred to as a "Coastal El Niño," as only the sea waters in the coastal areas of Peru and Ecuador warmed up significantly. As a result, severe rains have been ongoing since December 2016 in Peru and neighboring countries (see also section 5.2), which have intensified in the past few weeks, causing landslides, floods, flash floods, and mud flows.

Figure 5.5. Behavior of the standard Southern Oscillation Index (SOI) of the Australian Bureau of Meteorology (BOM), April 2016 to April 2017

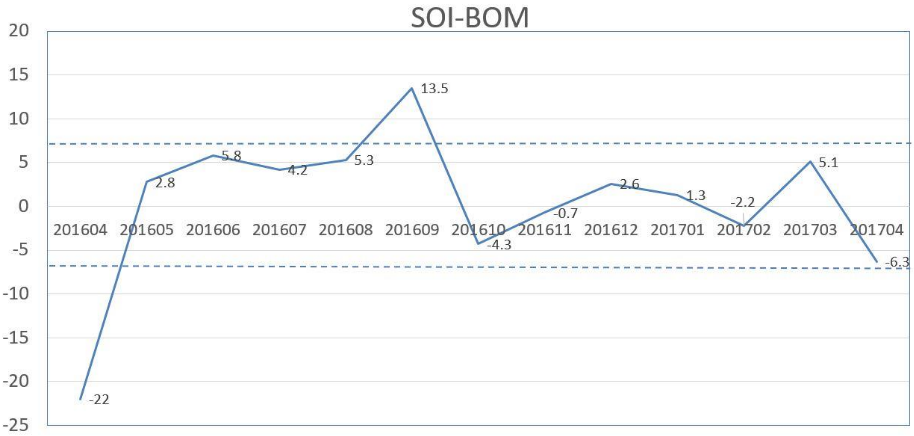

Source: http://www.bom.gov.au/climate/current/soi2.shtml.

Figure 5.6. Average sea surface temperature (SST) anomalies (°C), April 2017

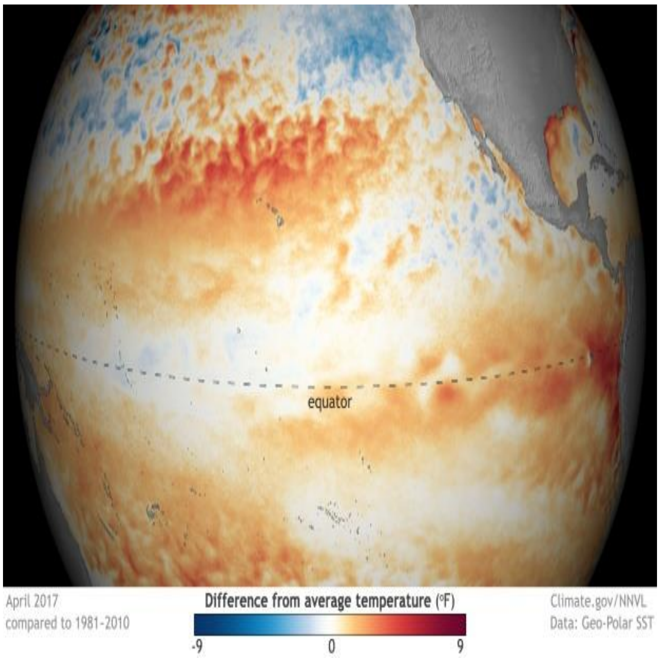

Note: Anomalies are computed with respect to the monthly means for the 1981 to 2010 period.
Source: NOAA, https://www.climate.gov/maps-data/data-snapshots/data-source-sst-anomaly-enso-monitoring-region

Annex A. Agroclimatic indicators and BIOMSS

Table A.1. January-April 2017 agroclimatic indicators and biomass by global Monitoring and Reporting Unit

	65 Global MRUs	RAIN		TEMP		RADPAR		BIOMSS	
		Current (mm)	15YA dep. (%)	Current (°C)	15YA dep. (°C)	Current (MJ/m^2)	15YA dep. (%)	Current (gDM/m^2)	5YA dep. (%)
1	Equatorial central Africa	512	-1	25.8	-0.1	1196	5	1518	-1
2	East African highlands	165	-27	20.7	-0.3	1332	4	630	-18
3	Gulf of Guinea	201	5	28.8	-0.3	1217	0	631	-1
4	Horn of Africa	253	-30	24.7	-0.7	1314	4	821	-22
5	Madagascar (main)	978	-3	24.8	-0.5	1125	4	1924	-1
6	Southwest Madagascar	427	-16	25.6	-0.5	1225	2	1263	-5
7	North Africa-Mediterranean	126	-20	12.3	0.1	981	2	449	-17
8	Sahel	25	-4	29.4	-0.7	1364	0	84	-4
9	Southern Africa	557	12	23.4	-1.2	1138	-3	1434	8
10	Western Cape (South Africa)	78	-30	19.6	0.1	1296	1	349	-22
11	British Columbia to Colorado	284	38	-3.3	-0.3	737	-6	508	8
12	Northern Great Plains	233	37	1.6	1.7	733	-8	669	20
13	Corn Belt	433	25	2.8	2.3	663	-9	829	17
14	Cotton Belt to Mexican Nordeste	426	15	14.4	2.2	870	-3	1145	11
15	Sub-boreal America	158	21	-7.5	1.6	575	-4	373	8
16	West Coast (North America)	406	43	6.5	-0.5	715	-12	866	22
17	Sierra Madre	62	-12	16.3	0.2	1284	2	260	-8
18	SW U.S. and N. Mex.highlands	133	71	10.0	0.9	1046	-3	449	32
19	Northern S. and Central America	270	10	26.3	-0.4	1124	4	681	1
20	Caribbean	243	26	23.9	-0.8	1056	-3	673	6
21	Central-northern Andes	781	26	16.6	-0.2	1042	1	1474	10
22	Nordeste (Brazil)	328	-30	28.3	0.9	1203	-1	1001	-21
23	Central eastern Brazil	734	-4	26.0	-0.5	1131	2	1781	-3
24	Amazon	1345	23	26.9	-0.8	949	-1	2409	7
25	Central-north Argentina	679	44	24.6	-0.7	1098	2	1676	23
26	Pampas	768	34	23.0	-0.5	1121	-2	1745	15
27	Western Patagonia	84	-39	14.1	0.1	1116	-4	384	-18
28	Semi-arid Southern Cone	189	21	18.7	-0.1	1206	2	618	20
29	Caucasus	200	-28	2.1	-0.7	838	3	650	-14
30	Pamir area	236	-3	2.6	-0.6	952	-2	619	-3
31	Western Asia	168	4	6.9	-0.4	903	-1	561	0
32	Gansu-Xinjiang (China)	83	78	-1.6	0.2	858	-5	352	85
33	Hainan (China)	206	52	21.7	-0.2	865	-5	716	55
34	Huanghuaihai (China)	108	15	7.6	0.9	872	-3	463	19
35	Inner Mongolia (China)	77	60	-2.7	1.5	865	0	336	48
36	Loess region (China)	76	23	3.5	0.4	883	-5	333	16
37	Lower Yangtze (China)	349	-21	11.5	0.4	724	-7	1101	-6
38	Northeast China	78	-1	-4.8	1.9	792	1	349	9
39	Qinghai-Tibet (China)	164	-5	2.3	0.2	1047	-1	408	-2
40	Southern China	219	-7	16.4	0.0	790	-8	766	7
41	Southwest China	134	-17	10.1	-0.1	675	-13	539	-6
42	Taiwan (China)	215	9	17.0	-0.4	894	1	840	21
43	East Asia	103	-43	-1.0	1.0	799	1	411	-18
44	Southern Himalayas	158	-6	19.7	0.2	1061	-2	435	-14

	65 Global MRUs	RAIN		TEMP		RADPAR		BIOMSS	
		Current (mm)	15YA dep. (%)	Current (°C)	15YA dep. (°C)	Current (MJ/m²)	15YA dep. (%)	Current (gDM/m²)	5YA dep. (%)
45	Southern Asia	93	-9	26.6	0.0	1260	2	240	-28
46	Southern Japan and Korea	283	-27	6.9	-0.1	816	0	927	-11
47	Southern Mongolia	109	309	-6.3	2.1	816	-4	427	209
48	Punjab to Gujarat	43	-19	23.3	0.0	1192	1	189	-12
49	Maritime Southeast Asia	1212	13	25.4	-0.7	951	-5	2237	5
50	Mainland Southeast Asia	228	49	26.3	-0.5	1139	-2	633	18
51	Eastern Siberia	122	-2	-8.7	2.3	596	-3	332	11
52	Eastern Central Asia	47	-4	-11.7	2.3	703	1	226	8
53	Northern Australia	941	15	26.5	-0.7	1056	-4	1783	6
54	Queensland to Victoria	242	7	21.8	0.3	1208	-1	765	5
55	Nullarbor to Darling	119	19	20.3	-1.3	1254	-4	488	16
56	New Zealand	242	-8	14.7	-0.3	962	-7	881	-1
57	Boreal Eurasia	224	17	-3.9	1.0	414	-3	466	4
58	Ukraine to Ural mountains	194	17	-1.3	0.7	468	-7	630	4
59	Med. Europe and Turkey	170	-34	7.8	0.0	823	3	618	-26
60	W. Europe (non Mediterranean)	207	-10	4.7	-0.3	563	-3	777	-6
61	Boreal America	171	-27	-9.4	-0.5	498	3	302	-4
62	Ural to Altai mountains	105	-4	-7.0	1.0	602	0	420	5
63	Australian desert	134	39	22.1	-0.8	1268	-3	558	36
64	Sahara to Afghan deserts	113	44	17.7	-0.5	1138	-3	355	27
65	Sub-arctic America	101	128	-20.0	3.9	205	2	67	140

Table A.2. January-April 2017 agroclimatic indicators and biomass by country

31 Countries	RAIN		TEMP		RADPAR		BIOMSS	
	Current (mm)	15YA Departure (%)	Current (°C)	15YA Departure (°C)	Current (MJ/m²)	15YA Departure (%)	Current (gDM/m²)	5YA Departure (%)
Argentina	696	40	22.3	-0.6	1124	-1	1587	19
Australia	296	14	22.1	0.0	1208	-2	762	7
Bangladesh	367	76	22.9	-1.1	1050	-5	900	48
Brazil	903	6	26.0	-0.4	1079	1	1861	-2
Cambodia	208	30	28.0	-1.0	1180	0	744	26
Canada	230	17	-5.6	1.4	597	-6	425	11
China	186	-13	7.8	0.5	775	-6	556	5
Egypt	46	-18	15.4	-0.9	1055	-1	221	27
Ethiopia	171	-9	21.2	-0.4	1317	4	642	-5
France	149	-36	6.6	-0.8	622	0	586	-31
Germany	202	-4	4.1	-0.2	493	-5	866	2
India	86	-16	24.5	0.2	1215	1	226	-28
Indonesia	1236	7	25.5	-0.7	940	-4	2326	2
Iran	185	-9	6.9	-0.6	975	-2	612	-7
Kazakhstan	111	-2	-5.7	0.4	662	-1	450	2
Mexico	80	-9	20.3	0.4	1220	3	299	-3
Myanmar	96	5	24.0	-0.2	1159	-3	368	5
Nigeria	147	-1	29.0	-0.4	1292	0	361	-10
Pakistan	142	-15	16.0	-0.1	1066	-1	382	-8
Philippines	880	69	25.2	-0.9	1014	-5	1527	33
Poland	213	23	2.2	-0.2	437	-13	817	6
Romania	267	33	2.8	-0.4	640	1	822	12

31 Countries	RAIN		TEMP		RADPAR		BIOMSS	
	Current (mm)	15YA Departure (%)	Current (°C)	15YA Departure (°C)	Current (MJ/m^2)	15YA Departure (%)	Current (gDM/m^2)	5YA Departure (%)
Russian F.	152	6	-4.5	1.2	529	-3	479	5
South Africa	284	-11	20.2	-0.7	1188	-2	975	-7
Thailand	302	61	26.6	-0.7	1144	-1	681	9
Turkey	239	-22	3.6	-0.5	860	3	753	-11
Ukraine	211	20	1.9	0.3	544	-3	784	10
United Kingdom	279	-1	6.2	-0.2	420	-9	966	-1
United States	368	25	7.1	1.8	782	-6	835	17
Uzbekistan	248	21	4.9	-1.2	813	0	727	11
Vietnam	186	14	22.6	-0.1	892	-8	668	17

See note table A.1.

Table A.3. Argentina, January-April 2017 agroclimatic indicators and biomass (by province)

	RAIN		TEMP		RADPAR		BIOMSS	
	Current (mm)	15YA Departure (%)	Current (°C)	15YA Departure (°C)	Current (MJ/m^2)	15YA Departure (%)	Current (gDM/m^2)	5YA Departure (%)
Buenos Aires	532	22	20.4	-0.1	1132	-4	1475	15
Chaco	1010	70	24.8	-1.2	1130	-2	2054	34
Cordoba	493	7	21.8	-0.4	1159	1	1438	2
Corrientes	1155	81	24.2	-1.2	1123	-4	2121	33
Entre Rios	789	28	22.6	-0.8	1132	-3	1686	11
La Pampa	652	73	21.1	-0.2	1192	-2	1594	35
Misiones	1106	58	24.2	-0.8	1107	-1	2078	21
Santiago Del Estero	668	45	24.6	-0.7	1092	0	1681	23
San Luis	500	24	20.9	-0.4	1202	3	1569	20
Salta	757	41	23.4	-0.5	1056	4	1684	19
Santa Fe	750	32	23.2	-0.7	1132	-3	1747	15
Tucuman	566	13	22.9	-0.4	1075	7	1607	14

See note table A.1.

Table A.4. Australia, January-April 2017 agroclimatic indicators and biomass (by state)

	RAIN		TEMP		RADPAR		BIOMSS	
	Current (mm)	15YA Departure (%)	Current (°C)	15YA Departure (°C)	Current (MJ/m^2)	15YA Departure (%)	Current (gDM/m^2)	5YA Departure (%)
New South Wales	212	-6	22.5	0.4	1226	-1	701	-5
South Australia	149	47	20.1	0.0	1207	-4	608	38
Victoria	173	1	19.0	0.2	1170	-3	735	13
W. Australia	172	29	20.9	-1.3	1249	-4	541	18

See note table A.1.

Table A.5. Brazil, January-April 2017 agroclimatic indicators and biomass (by state)

	RAIN		TEMP		RADPAR		BIOMSS	
	Current (mm)	15YA Departure (%)	Current (°C)	15YA Departure (°C)	Current (MJ/m^2)	15YA Departure (%)	Current (gDM/m^2)	5YA Departure (%)
Ceara	556	-15	28.0	0.2	1099	-5	1549	-6
Goias	694	-18	25.4	-0.5	1205	6	1866	-8
Mato Grosso Do Sul	756	9	26.2	-1.3	1163	2	2037	12
Mato Grosso	1112	7	26.7	-0.7	1069	3	2376	5
Minas Gerais	444	-32	24.9	0.1	1196	4	1267	-22
Parana	643	-4	23.6	-0.5	1099	2	1856	4
Rio Grande Do Sul	951	57	23.5	-0.2	1090	-3	1959	19
Santa Catarina	616	-13	22.5	0.4	1022	-3	1671	-9
Sao Paulo	736	-2	24.6	-0.5	1125	3	1876	-1

See note table A.1.

Table A.6. Canada, January-April 2017 agroclimatic indicators and biomass (by province)

	RAIN		TEMP		RADPAR		BIOMSS	
	Current (mm)	15YA Departure (%)	Current (°C)	15YA Departure (°C)	Current (MJ/m^2)	15YA Departure (%)	Current (gDM/m^2)	5YA Departure (%)
Alberta	125	13	-5.8	0.6	573	-6	437	7
Manitoba	117	10	-6.9	2.4	650	-3	405	14
Saskatchewan	104	3	-6.6	1.9	623	-4	412	11

See note table A.1.

Table A.7. India, January-April 2017 agroclimatic indicators and biomass (by state)

	RAIN		TEMP		RADPAR		BIOMSS	
	Current (mm)	15YA Departure (%)	Current (°C)	15YA Departure (°C)	Current (MJ/m^2)	15YA Departure (%)	Current (gDM/m^2)	5YA Departure (%)
Arunachal Pradesh	478	-12	15.4	0.1	849	-4	1162	-2
Andhra Pradesh	33	-41	28.1	-0.2	1285	2	146	-34
Assam	503	31	22.3	0.3	918	-4	1159	16
Bihar	38	-47	23.5	-0.6	1148	-2	174	-45
Chhattisgarh	15	-81	25.9	0.2	1268	5	77	-77
Daman and Diu	7	36	25.5	-0.7	1314	1	35	35
Delhi	82	-7	22.1	0.3	1144	1	303	-20
Gujarat	7	8	26.3	0.2	1291	1	43	19
Goa	1	-95	25.9	0.2	1344	2	8	-93
Himachal Pradesh	271	4	5.3	0.8	1055	-3	553	-12
Haryana	130	21	20.8	0.1	1121	1	416	-2
Jharkhand	36	-54	24.2	0.2	1208	1	159	-54
Kerala	242	1	26.7	-0.3	1223	-3	692	-6
Karnataka	47	-39	26.8	-0.1	1338	3	185	-35
Meghalaya	687	43	19.4	0.7	973	-6	1225	27
Maharashtra	5	-86	27.1	0.4	1326	5	26	-85
Manipur	317	18	17.2	-0.1	1040	-4	904	24
Madhya Pradesh	21	-63	24.9	0.4	1254	3	97	-58
Mizoram	295	21	19.0	-0.8	1089	-4	902	34
Nagaland	355	13	16.8	0.7	953	-4	1030	9
Orissa	31	-65	26.3	0.2	1247	4	148	-60
Puducherry	77	729	27.9	-0.3	1258	0	277	407

	RAIN		TEMP		RADPAR		BIOMSS	
	Current (mm)	15YA Departure (%)	Current (°C)	15YA Departure (°C)	Current (MJ/m^2)	15YA Departure (%)	Current (gDM/m^2)	5YA Departure (%)
Punjab	149	-1	19.2	0.3	1055	0	491	-12
Rajasthan	27	-8	23.5	-0.2	1211	1	123	-11
Sikkim	252	17	5.9	0.5	1095	-1	540	3
Tamil Nadu	121	12	28.0	-0.3	1265	-1	417	10
Tripura	484	61	22.3	-0.8	1018	-5	1121	48
Uttarakhand	178	-16	11.7	1.9	1092	-2	510	-14
Uttar Pradesh	40	-52	23.3	0.5	1174	1	173	-51
West Bengal	107	-17	24.6	0.0	1127	-2	405	-16

See note table A.1.

Table A.8. Kazakhstan, January-April 2017 agroclimatic indicators and biomass (by Oblast)

	RAIN		TEMP		RADPAR		BIOMSS	
	Current (mm)	15YA Departure (%)	Current (°C)	15YA Departure (°C)	Current (MJ/m^2)	15YA Departure (%)	Current (gDM/m^2)	5YA Departure (%)
Akmolinskaya	84	-6	-7.6	0.8	622	0	400	1
Karagandinskaya	107	12	-7.5	0.2	677	-2	427	3
Kustanayskaya	104	1	-7.2	0.3	613	3	443	2
Pavlodarskaya	73	6	-7.0	1.1	617	-1	392	13
Severo kazachstanskaya	91	-3	-7.5	1.0	585	3	404	3
Vostochno kazachstanskaya	109	-11	-8.2	0.9	711	-2	363	-1
Zapadno kazachstanskaya	124	-1	-3.5	0.1	597	-1	578	5

See note table A.1.

Table A.9. Russia, January-April 2017 agroclimatic indicators and biomass (by Oblast, Kray and Republic)

	RAIN		TEMP		RADPAR		BIOMSS	
	Current (mm)	15YA Departure (%)	Current (°C)	15YA Departure (°C)	Current (MJ/m^2)	15YA Departure (%)	Current (gDM/m^2)	5YA Departure (%)
Bashkortostan Rep.	175	13	-6.4	0.3	520	-1	431	-2
Chelyabinskaya Oblast	99	-11	-6.4	0.8	554	3	441	5
Gorodovikovsk	331	27	3.3	0.2	609	0	916	9
Krasnodarskiy Kray	133	-33	-1.7	1.6	599	2	512	-4
Kurganskaya Oblast	94	-3	-7.2	0.5	560	6	439	6
Kirovskaya Oblast	217	31	-5.5	0.5	399	-8	451	-1
Kurskaya Oblast	133	-21	0.1	1.0	524	-2	669	0
Lipetskaya Oblast	164	-3	-0.8	1.3	501	-6	671	9
Mordoviya Rep.	191	19	-2.6	1.3	490	-1	576	5
Novosibirskaya Oblast	108	8	-8.0	1.7	534	-2	412	13
Nizhegorodskaya Oblast	190	19	-3.1	0.9	431	-6	557	4
Orenburgskaya Oblast	143	0	-5.8	0.0	583	0	471	-3
Omskaya Oblast	102	4	-8.1	1.3	532	0	411	10

	RAIN		TEMP		RADPAR		BIOMSS	
	Current (mm)	15YA Departure (%)	Current (°C)	15YA Departure (°C)	Current (MJ/m^2)	15YA Departure (%)	Current (gDM/m^2)	5YA Departure (%)
Permskaya Oblast	180	14	-7.0	0.3	425	-4	410	-1
Penzenskaya Oblast	189	16	-2.6	1.3	502	-5	577	4
Rostovskaya Oblast	178	-15	1.9	0.6	576	-2	711	-3
Ryazanskaya Oblast	183	9	-1.6	1.4	454	-7	624	7
Stavropolskiy Kray	210	7	3.4	0.1	642	1	792	4
Sverdlovskaya Oblast	99	-14	-6.8	0.7	488	4	438	6
Samarskaya Oblast	183	26	-4.5	0.5	532	-3	508	-2
Saratovskaya Oblast	174	17	-2.3	1.0	544	-6	604	4
Tambovskaya Oblast	186	10	-1.5	1.4	504	-6	639	7
Tyumenskaya Oblast	101	3	-7.9	0.8	526	3	424	8
Tatarstan Rep.	172	19	-4.9	0.5	487	-4	480	-2
Ulyanovskaya Oblast	172	21	-3.7	1.1	507	-4	532	2
Udmurtiya Rep.	193	25	-5.9	0.4	428	-6	438	-2
Volgogradskaya Oblast	197	21	0.0	0.8	557	-5	726	9
Voronezhskaya Oblast	181	10	-0.1	1.3	514	-7	722	12

See note table A.1.

Table A.10. United States, January-April 2017 agroclimatic indicators and biomass (by state)

	RAIN		TEMP		RADPAR		BIOMSS	
	Current (mm)	15YA Departure (%)	Current (°C)	15YA Departure (°C)	Current (MJ/m^2)	15YA Departure (%)	Current (gDM/m^2)	5YA Departure (%)
Arkansas	622	28	12.7	2.5	783	-7	1542	17
California	389	76	8.0	-0.1	834	-10	827	37
Idaho	321	76	-2.0	-0.8	729	-9	619	14
Indiana	481	24	6.8	3.0	694	-10	1151	22
Illinois	419	21	6.5	2.9	688	-12	1080	17
Iowa	313	23	2.9	2.3	668	-16	881	17
Kansas	322	67	7.2	1.8	820	-7	801	17
Michigan	364	23	1.0	2.3	599	-15	737	20
Minnesota	242	38	-1.9	2.1	673	-8	617	17
Missouri	633	71	8.6	2.7	725	-10	1243	19
Montana	215	74	-2.0	-0.3	723	-5	632	32
Nebraska	205	28	3.6	1.5	781	-8	710	12
North Dakota	152	29	-3.6	1.2	717	-4	545	27
Ohio	494	38	6.3	3.2	682	-8	1121	24
Oklahoma	420	48	11.1	1.7	845	-6	1050	19
Oregon	373	42	2.5	-1.4	621	-13	807	13
South Dakota	214	49	0.6	1.4	759	-5	736	31
Texas	318	35	15.8	2.0	933	-2	873	23
Washington	368	43	1.2	-1.9	577	-11	769	15
Wisconsin	388	48	-0.2	2.1	632	-12	695	14

See note table A.1.

Table A.11. China, January-April 2017 agroclimatic indicators and biomass (by province)

	RAIN		TEMP		RADPAR		BIOMSS	
	Current (mm)	15YA Departure (%)	Current (°C)	15YA Departure (°C)	Current (MJ/m^2)	15YA Departure (%)	Current (gDM/m^2)	5YA Departure (%)
Anhui	251	-27	10.0	0.5	813	-3	913	-9
Chongqing	126	-37	9.4	-0.1	544	-17	519	-29
Fujian	358	-24	13.0	0.3	754	-6	1150	-4
Gansu	64	18	2.1	0.2	908	-5	278	21
Guangdong	355	0	16.5	0.1	727	-6	1092	15
Guangxi	249	-16	15.8	0.3	616	-12	840	-3
Guizhou	137	-30	10.7	0.2	528	-23	562	-18
Hebei	78	59	3.0	1.1	877	-2	347	45
Heilongjiang	68	-7	-6.5	2.2	753	0	329	7
Henan	126	-3	8.7	0.6	833	-6	525	1
Hubei	256	-11	9.5	0.3	713	-9	880	-2
Hunan	358	-18	10.9	0.1	613	-13	1147	-6
Jiangsu	151	-26	9.1	0.8	857	-1	640	-16
Jiangxi	419	-26	12.3	0.5	713	-7	1265	-8
Jilin	91	9	-3.8	1.6	827	2	400	18
Liaoning	103	13	0.3	1.5	871	2	439	16
Inner Mongolia	71	50	-4.8	1.9	830	0	314	47
Ningxia	34	8	1.8	0.5	933	-3	169	7
Shaanxi	94	18	5.1	0.2	803	-7	380	11
Shandong	117	45	7.1	1.0	880	-3	517	41
Shanxi	77	32	2.0	0.8	890	-4	351	23
Sichuan	107	-1	8.9	-0.2	746	-9	441	0
Yunnan	108	-10	12.9	-0.5	945	-8	467	4
Zhejiang	329	-28	10.5	0.6	768	-3	1119	-7

See note table A.1.

Annex B. 2017 production estimates

Tables B.1-B.3 present 2017 CropWatch production estimates for Argentina, Brazil, and the United States.

Table B.1. Argentina, 2017 maize and soybean production, by province (thousand tons)

	Maize		Soybean	
	2017	Δ%	2017	Δ%
Buenos Aires	7651	8	13660	-3
Córdoba	7387	5	11911	-2
Entre Rios	1269	11	3806	6
San Luis	1085	-3		
Santa Fe	4264	-1	10218	-3
Santiago Del Estero	1210	0		
Sub total	22866	4	39596	-2
Others	7080	87	11521	7
Argentina	29947	16	51117	0

Δ% indicates percentage difference with 2016.

Table B.2. Brazil, 2017 maize, rice, and soybean production, by state (thousand tons)

	Maize		Rice		Soybean	
	2017	Δ%	2017	Δ%	2017	Δ%
Goias	8080	27			10327	5
Mato Grosso	18864	5			28146	5
Mato Grosso Do Sul	7735	17			6816	7
Minas Gerais	6157	2			3422	-3
Parana	15388	6			18327	6
Rio Grande Do Sul	4641	1	8770	3	13684	1
Santa Catarina	2957	5	1130	11	1790	5
Sao Paulo	3629	1			2195	1
Sub total	67452	8	9899	4	84708	4
Others	11791	47	1278	-17	12018	13
Brazil	79243	13	11177	1	96726	5

Δ% indicates percentage difference with 2016.

Table B.3. United States, 2017 wheat production, by state (thousand tons)

	Wheat				
	2017	Δ%		2017	Δ%
Arkansas	703	9	Nebraska	1795	-15
California	664	0	New York	186	14
Colorado	2319	-5	North Carolina	1307	8
Georgia	299	-4	North Dakota	7581	-20
Idaho	2202	-18	Ohio	1299	8
Illinois	1211	-1	Oklahoma	1447	5
Indiana	812	9	Oregon	1069	9
Kansas	7752	-8	Pennsylvania	284	7
Kentucky	1097	10	South Carolina	289	3
Maryland	521	10	South Dakota	3011	-19
Michigan	886	-16	Tennessee	825	8
Minnesota	721	-59	Texas	2107	-1
Mississippi	347	1	Virginia	544	11
Missouri	1196	0	Washington	2940	1
Montana	7240	33	Wisconsin	361	-20
Sub total	53014	-5			
Other states	1361	57			
United States	54376	-4			

Δ% indicates percentage difference with 2016.

Annex C. Quick reference to CropWatch indicators, spatial units and methodologies

The following sections give a brief overview of CropWatch indicators and spatial units, along with a description of the CropWatch production estimation methodology. For more information about CropWatch methodologies, visit CropWatch online at www.cropwatch.com.cn**.**

CropWatch indicators

The CropWatch indicators are designed to assess the condition of crops and the environment in which they grow and develop; the indicators—RAIN (for rainfall), TEMP (temperature), and RADPAR (photosynthetically active radiation, PAR)—are not identical to the weather variables, but instead are value-added indicators computed only over crop growing areas (thus for example excluding deserts and rangelands) and spatially weighted according to the agricultural production potential, with marginal areas receiving less weight than productive ones. The indicators are expressed using the usual physical units (e.g., mm for rainfall) and were thoroughly tested for their coherence over space and time. CWSU are the CropWatch Spatial Units, including MRUs, MPZ, and countries (including first-level administrative districts in select large countries). For all indicators, high values indicate "good" or "positive."

INDICATOR			
BIOMSS			
Biomass accumulation potential			
Crop/ Ground and satellite	Grams dry matter/m^2, pixel or CWSU	An estimate of biomass that could potentially be accumulated over the reference period given the prevailing rainfall and temperature conditions.	Biomass is presented as maps by pixels, maps showing average pixels values over CropWatch spatial units (CWSU), or tables giving average values for the CWSU. Values are compared to the average value for the last five years (2012-16), with departures expressed in percentage.
CALF			
Cropped arable land and cropped arable land fraction			
Crop/ Satellite	[0,1] number, pixel or CWSU average	The area of cropped arable land as fraction of total (cropped and uncropped) arable land. Whether a pixel is cropped or not is decided based on NDVI twice a month. (For each four-month reporting period, each pixel thus has 8 cropped/ uncropped values).	The value shown in tables is the maximum value of the 8 values available for each pixel; maps show an area as cropped if at least one of the 8 observations is categorized as "cropped." Uncropped means that no crops were detected over the whole reporting period. Values are compared to the average value for the last five years (2012-16), with departures expressed in percentage.
CROPPING INTENSITY			
Cropping intensity Index			
Crop/ Satellite	Number of crops growing over a year for each pixel	Cropping intensity index describes the number of times the same hectare is used over a year. It is the ratio of the total crop area of all planting seasons in a year to the total area of arable land. It can be expressed as a dimensionless number (e.g., 1.85) or percentage (185%).	Cropping intensity is presented as maps by pixels or spatial average pixels values for MPZs, 31 countries, and 7 regions for China. Values are compared to the average of the previous five years, with departures expressed in percentage.
NDVI			
Normalized Difference Vegetation Index			

INDICATOR			
Crop/ Satellite	[0.12-0.90] number, pixel or CWSU average	An estimate of the density of living green biomass.	NDVI is shown as average profiles over time at the national level (cropland only) in crop condition development graphs, compared with previous year and recent five-year average (2012-16), and as spatial patterns compared to the average showing the time profiles, where they occur, and the percentage of pixels concerned by each profile.
RADPAR			
CropWatch indicator for Photosynthetically Active Radiation (PAR), based on pixel based PAR			
Weather /Satellite	W/m^2, CWSU	The spatial average (for a CWSU) of PAR accumulation over agricultural pixels, weighted by the production potential.	RADPAR is shown as the percent departure of the RADPAR value for the reporting period compared to the recent fifteen-year average (2002-16), per CWSU. For the MPZs, regular PAR is shown as typical time profiles over the spatial unit, with a map showing where the profiles occur and the percentage of pixels concerned by each profile.
RAIN			
CropWatch indicator for rainfall, based on pixel-based rainfall			
Weather /Ground and satellite	$Liters/m^2$, CWSU	The spatial average (for a CWSU) of rainfall accumulation over agricultural pixels, weighted by the production potential.	RAIN is shown as the percent departure of the RAIN value for the reporting period, compared to the recent fifteen-year average (2002-16), per CWSU. For the MPZs, regular rainfall is shown as typical time profiles over the spatial unit, with a map showing where the profiles occur and the percentage of pixels concerned by each profile.
TEMP			
CropWatch indicator for air temperature, based on pixel-based temperature			
Weather /Ground	°C, CWSU	The spatial average (for a CWSU) of the temperature time average over agricultural pixels, weighted by the production potential.	TEMP is shown as the departure of the average TEMP value (in degrees Centigrade) over the reporting period compared with the average of the recent fifteen years (2002-16), per CWSU. For the MPZs, regular temperature is illustrated as typical time profiles over the spatial unit, with a map showing where the profiles occur and the percentage of pixels concerned by each profile.
VCIx			
Maximum vegetation condition index			
Crop/ Satellite	Number, pixel to CWSU	Vegetation condition of the current season compared with historical data. Values usually are [0,1], where 0 is "NDVI as bad as the worst recent year" and 1 is "NDVI as good as the best recent year." Values can exceed the range if the current year is the best or the worst.	VCIx is based on NDVI and two VCI values are computed every month. VCIx is the highest VCI value recorded for every pixel over the reporting period. A low value of VCIx means that no VCI value was high over the reporting period. A high value means that at least one VCI value was high. VCI is shown as pixel-based maps and as average value by CWSU.
VHI			
Vegetation health index			
Crop/ Satellite	Number, pixel to CWSU	The average of VCI and the temperature condition index (TCI), with TCI defined like VCI but for temperature. VHI is based on the assumption that "high temperature is	Low VHI values indicate unusually poor crop condition, but high values, when due to low temperature, may be difficult to interpret. VHI is shown as typical time profiles over Major Production Zones (MPZ), where they occur, and

INDICATOR			
		bad" (due to moisture stress), but ignores the fact that low temperature may be equally "bad" (crops develop and grow slowly, or even suffer from frost).	the percentage of pixels concerned by each profile.
VHIn			
Minimum Vegetation health index			
Crop/ Satellite	Number, pixel to CWSU	VHIn is the lowest VHI value for every pixel over the reporting period. Values usually are [0, 100]. Normally, values lower than 35 indicate poor crop condition.	Low VHIn values indicate the occurrence of water stress in the monitoring period, often combined with lower than average rainfall. The spatial/time resolution of CropWatch VHIn is 16km/week for MPZs and 1km/dekad for China.

Note: Type is either "Weather" or "Crop"; source specifies if the indicator is obtained from ground data, satellite readings, or a combination; units: in the case of ratios, no unit is used; scale is either pixels or large scale CropWatch spatial units (CWSU). Many indicators are computed for pixels but represented in the CropWatch bulletin at the CWSU scale.

CropWatch spatial units (CWSU)

CropWatch analyses are applied to four kinds of CropWatch spatial units (CWSU): Countries, China, Major Production Zones (MPZ), and global crop Monitoring and Reporting Units (MRU). The tables below summarize the key aspects of each spatial unit and show their relation to each other. For more details about these spatial units and their boundaries, see the CropWatch bulletin online resources.

SPATIAL LUNITS	
CHINA	
Overview	*Description*
Seven monitoring regions	The seven regions in China are agro-economic/agro-ecological regions that together cover the bulk of national maize, rice, wheat, and soybean production. Provinces that are entirely or partially included in one of the monitoring regions are indicated in color on the map below.

Countries (and first-level administrative districts, e.g., states and provinces)	
Overview	*Description*
"Thirty plus one" countries to represent main producers/exporters and other key countries.	CropWatch monitored countries together represent more than 80% of the production of maize, rice, wheat and soybean, as well as 80% of exports. Some countries were included in the list based on criteria of proximity to China (Uzbekistan, Cambodia), regional importance, or global geopolitical relevance (e.g., four of five most populous countries in Africa). The total number of countries monitored is "thirty plus one," referring to thirty countries and China itself. For the nine largest countries—, United States, Brazil, Argentina, Russia, Kazakhstan, India, China, and Australia, maps and analyses may also present results for the first-level administrative subdivision. The CropWatch agroclimatic indicators are computed for all countries and included in the analyses when abnormal conditions occur. Background information about the countries' agriculture and trade is available on the CropWatch Website, **www.cropwatch.com.cn**.

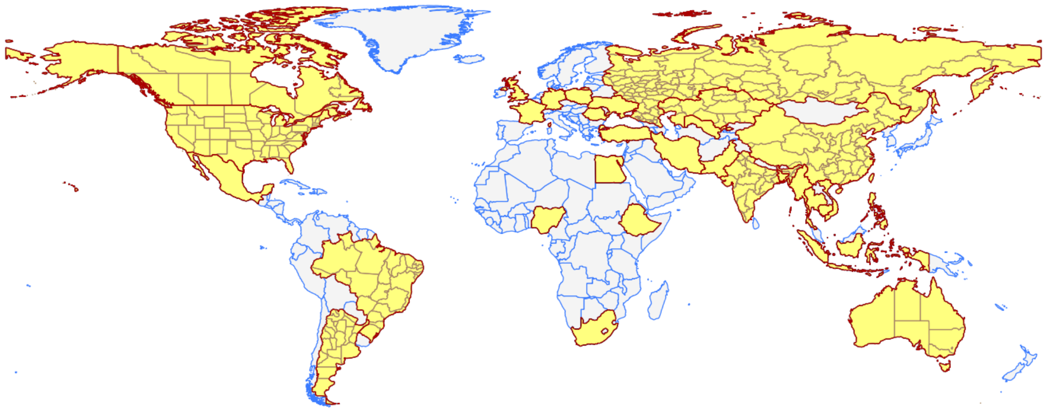

Major Production Zones (MPZ)	
Overview	*Description*
Seven globally important areas of agricultural production	The six MPZs include West Africa, South America, North America, South and Southeast Asia, Western Europe and Central Europe to Western Russia. The MPZs are not necessarily the main production zones for the four crops (maize, rice, soybean, wheat) currently monitored by CropWatch, but they are globally or regionally important areas of agricultural production. The seven zones were identified based mainly on production statistics and distribution of the combined cultivation area of maize, rice, wheat and soybean.

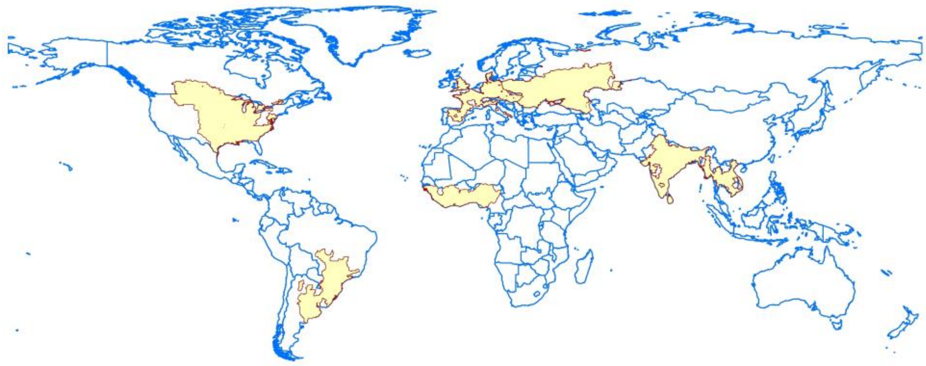

Global Monitoring and Reporting Unit (MRU)	
Overview	*Description*
65 agro-ecological/agro-economic units across the world	MRUs are reasonably homogeneous agro-ecological/agro-economic units spanning the globe, selected to capture major variations in worldwide farming and crops patterns while at the same time providing a manageable (limited) number of spatial units to be used as the basis for the analysis of environmental factors affecting crops. Unit numbers and names are shown in the figure below. A limited number of units (e.g., MRU-63 to 65) are not relevant for the crops currently monitored by CropWatch but are included to allow for more complete coverage of global production. Additional information about the MRUs is provided online under **www.cropwatch.com.cn** .

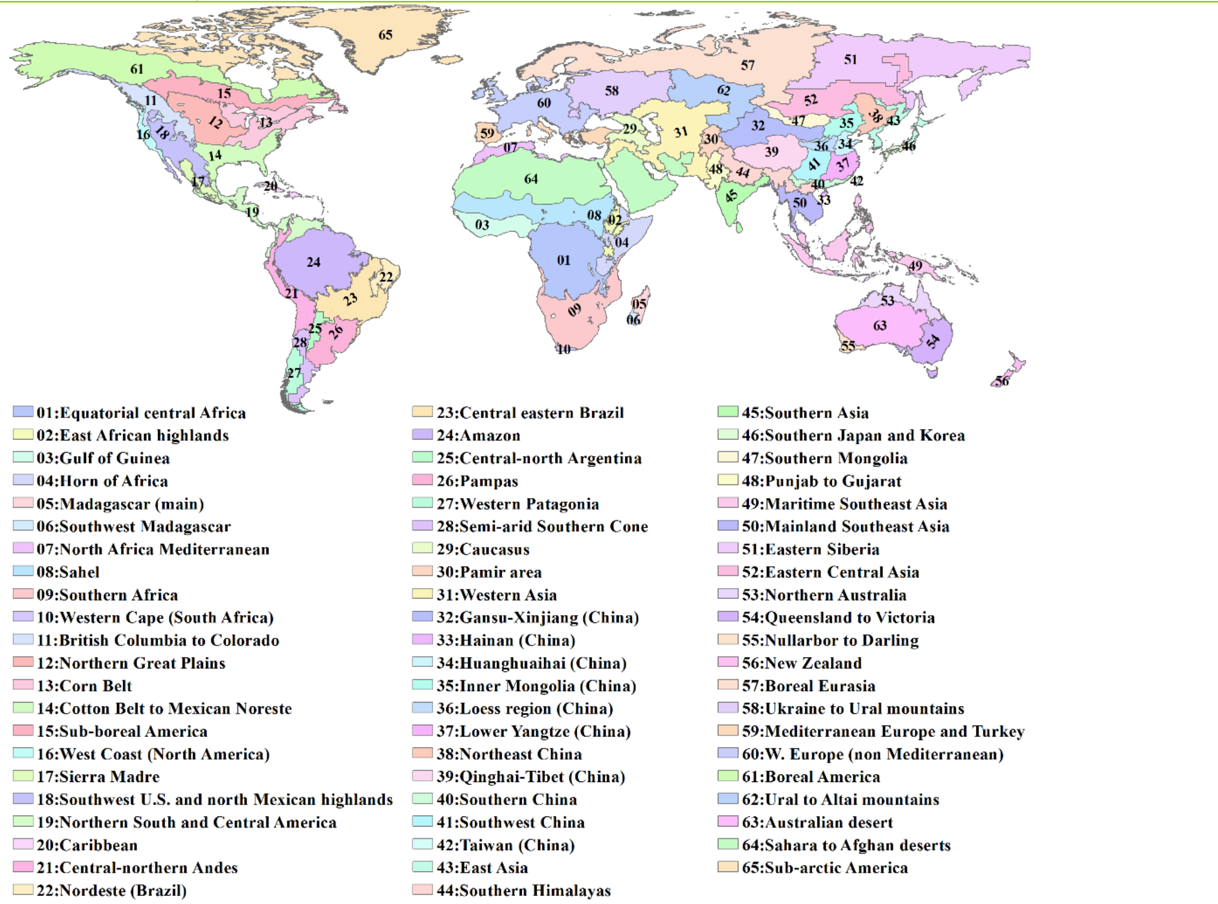

Production estimation methodology

The main concept of the CropWatch methodology for estimating production is the calculation of current year production based on information about last year's production and the variations in crop yield and cultivated area compared with the previous year. The equation for production estimation is as follows:

$$Production_i = Production_{i-1} * (1 + \Delta Yield_i) * (1 + \Delta Area_i)$$

Where i is the current year, $\Delta Yield_i$ and $\Delta Area_i$ are the variations in crop yield and cultivated area compared with the previous year; the values of $\Delta Yield_i$ and $\Delta Area_i$ can be above or below zero.

For the 31 countries monitored by CropWatch, yield variation for each crop is calibrated against NDVI time series, using the following equation:

$$\Delta Yield_i = f(NDVI_i, NDVI_{i-1})$$

Where $NDVI_i$ and $NDVI_{i-1}$ are taken from the time series of the spatial average of NDVI over the crop specific mask for the current year and the previous year. For NDVI values that correspond to periods after the current monitoring period, average NDVI values of the previous five years are used as an average expectation. $\Delta Yield_i$ is calculated by regression against average or peak NDVI (whichever yields the best regression), considering the crop phenology of each crop for each individual country.

A different method is used for areas. For China, CropWatch combines remote-sensing based estimates of the crop planting proportion (cropped area to arable land) with a crop type proportion (specific type area to total cropped area). The planting proportion is estimated based on an unsupervised classification of high resolution satellite images from HJ-1 CCD and GF-1 images. The crop-type proportion for China is obtained by the GVG instrument from field transects. The area of a specific crop is computed by multiplying farmland area, planting proportion, and crop-type proportion of the crop.

To estimate crop area for wheat, soybean, maize, and rice outside China, CropWatch relies on the regression of crop area against cropped arable land fraction of each individual country (paying due attention to phenology):

$$Area_i = a + b * CALF_i$$

where a and b are the coefficients generated by linear regression with area from FAOSTAT or national sources and CALF the Cropped Arable Land Fraction from CropWatch estimates. $\Delta Area_i$ can then be calculated from the area of current and the previous years.

The production for "other countries" (outside the 31 CropWatch monitored countries) was estimated as the linear trend projection for 2014 of aggregated FAOSTAT data (using aggregated world production minus the sum of production by the 31 CropWatch monitored countries).

Classification of pests and diseases

The criteria for the classification of pests and diseases in this report are based on industry standards and plant protection survey and evaluation specifications issued by the Chinese Ministry of Agriculture, combined with crop growth information and conditions obtained through remote sensing.

Table C.1 presents the criteria for determining the level of wheat yellow rust occurrence, which is based on the “Rules for the investigation and forecast of wheat yellow rust” (GB/T15795-2011). Based on this standard, a disease index model was established, integrating the remote sensing disease data and in-field survey disease data. The term “mildly severe” used in this report to describe the occurrence of wheat yellow rust corresponds with levels 1 and 2, while “moderately severe” refers to level 3, and “severe” comprises levels 4 and 5.

Table C.1. Criteria for wheat yellow rust occurrence level

Index	Level				
	1	2	3	4	5
Disease index	$0.001<Y\leq5$	$5<Y\leq 10$	$10<Y\leq20$	$20<Y\leq30$	$Y>30$
Disease field rate/%	$1<R\leq5$	$5<R\leq10$	$10<R\leq20$	$20<R\leq30$	$R>30$

Note: In the table, Y is the disease index; it shows the impact of the disease and is defined as: Y=F*D*100, in which F is the rate of disease leaves and D is the average of the severity level of disease leaves. R is the disease field rate, which means the rate of disease field in the whole region.
Source: Standardization Administration of China, Rules for the investigation and forecast of wheat yellow rust (GB/T 15795-2011), 2011. http://doc.mbalib.com/view/2e0ae53c7f397af70deb37edb07c5a12.html

Tables C.2 and C.3 respectively list the criteria for wheat sheath blight (table C.2 and based on the “Rules for the investigation and forecast of wheat sheath blight” (NY/T614-2002)) and wheat aphid (table C.3, following “Rules for the investigation and forecast of wheat aphid” (NY/T612-2002)). The terms mildly severe, moderately severe, and severe—as used in this report—again refer to levels 1-2, 3, and 4-5 in the table.

Table C.2. Criteria for wheat sheath blight occurrence level

Index	Level				
	1	2	3	4	5
Disease index	Y≤5	5＜Y≤15	15＜Y≤25	25＜Y≤35	Y＞35

Source: Standardization Administration of China, Rules for the investigation and forecast of wheat sheath blight (NY/T614-2002), 2002. http://doc.mbalib.com/view/4c9d23d380f36d038af855fcdf089f93.html

Table C.3. Criteria for wheat aphid occurrence level

Index	Level				
	1	2	3	4	5
Aphid (heads/ hundred plants, Y)	Y≤500	500＜Y≤1500	1500＜Y≤2500	2500＜Y≤3500	Y＞3500

Source: Standardization Administration of China, Rules for the investigation and forecast of wheat aphid (NY/T612-2002), 2002. http://www.doc88.com/p-7708315673411.html

Data notes and bibliography

ACAPS, https://www.acaps.org/country/pakistan/special-reports#container-872; https://www.acaps.org/country/peru/special-reports#container-859; https://www.acaps.org/country/south-sudan/scenarios; https://www.acaps.org/sites/acaps/files/products/files/20170302_acaps_start_briefing_note_afghanistan_floods_0.pdf; https://www.acaps.org/sites/acaps/files/products/files/20170411_acaps_start_briefing_note_colombia_floods_and_mudslides_update.pdf; https://www.acaps.org/sites/acaps/files/products/files/20170425_acaps_thematic_report_southern_africa_armyworms_update.pdf; https://www.acaps.org/sites/acaps/files/products/files/middle_east_eu_migration_scenarios_mmp_acaps.pdf

Africa News, http://www.africanews.com/2017/02/17/cyclone-dineo-ravages-mozambique//; http://www.africanews.com/2017/03/03/zimbabwe-seeks-100m-in-aid-as-floods-kill-246-displaced-1000s

Andina, http://www.andina.com.pe/ingles/noticia-peru-president-announces-reconstruction-and-construction-works-after-disaster-661940.aspx

Barton B and S E Clark 2014 Water & climate risks facing U.S. corn production. How companies & investors can cultivate sustainability. A Ceres Report. Boston, USA. 71 pp.

Ben-Ari T and D Makowski 2014 Decomposing global crop yield variability. Environ. Res. Lett. 9 114011

Carr J A, P D'Odorico, S Suweis, D A Seekell 2016 What commodities and countries impact inequality in the global food system? Environ. Res. Lett. 11:095013

Dhaka Tribune, http://www.dhakatribune.com/bangladesh/nation/2017/04/08/paddy-production-hit-flood-haors/

Disaster-report, http://www.disaster-report.com; http://www.disaster-report.com/2017/04/recent-natural-disasters-list-may-1-2017.html

DMK 2014 chapter http://www.davidmckee.org/2014/03/20/government-global-grain-reserves/

FAO 1986. The ICS users' manual. Interlinked computer storage and processing system of food and agricultural commodity data. Rome, Italy.

FAO 2011, Policy options to address price volatility and high prices, in : The state of food insecurity in the world 2011. FAO, Rome, Italy. http://www.fao.org/docrep/014/i2330e/i2330e.pdf

FAO 2015. Guidelines on the collection of information on food processing through food consumption surveys. FAO, Rome, Italy.

FAO, 2017. Global Administrative Units Layers (GAUL). http://www.fao.org/geonetwork/srv/en/metadata.show?currTab=simple&id=12691.

FAOSTAT, http://faostat3.fao.org/faostat-gateway/go/to/home/E.

FSNAU/FEWS, fsnau.org/downloads/FSNAU-FEWS-NET-Post-Deyr-2016-Presentation-2-February-2017.pdf

G20 2011 Cannes summit final declaration "building our common future: renewed collective action for the benefit of all" http://worldjpn.grips.ac.jp/documents/texts/G20/20111104.D2E.html

Gilbert C L 2011 Food Reserves in Developing Countries: Trade Policy Options for Improved Food Security. International Centre for Trade and Sustainable Development (ICTSD) Issue Paper N.37. Geneva, Switzerland

Gilbert C L, C W Morgan 2010 Review Food price volatility. Phil. Trans. R. Soc. B 365:3023-3034

Gouel C 2014 Food Price Volatility and Domestic Stabilization Policies in Developing Countries. National Bureau of Economic Research (NBER) Working Paper series, Paper 18934, Cambridge (MA), USA. https://www.nber.org/papers/w18934.pdf

Guardian, the, https://www.theguardian.com/australia-news/2017/feb/10/australias-heatwave-continues-with-record-temperatures-expected

Hanson J 1985 Procedures for Handling Seeds in Genebanks, IBPGR, Practical manuals for genebanks N. 1. Bioversity international. Rome, Italy.

Humanitarian Response, https://www.humanitarianresponse.info/system/files/documents/files/flash_mira_mocoa_04.04.17.pdf

IATP 2012 Grain Reserves and the Food Price Crisis: Selected Writings from 2008–2012

Institute for Agriculture and Trade Policy. Institute for agriculture and trade policy, Minneapolis (MI), USA. http://www19.iadb.org/intal/intalcdi/PE/2012/10324.pdf http://www19.iadb.org/intal/intalcdi/PE/2012/10324.pdf http://www19.iadb.org/intal/intalcdi/PE/2012/10324.pdf

IPC, http://www.ipcinfo.org/ipcinfo-detail-forms/ipcinfo-news-detail/en/c/854362/

Kornher L 2015 Food price volatility: the role of stocks and trade. Zentrum für Entwicklungsforschung, Rheinische Friedrich-Wilhelms-Universität, Bonn. hss.ulb.uni-bonn.de/2015/4121/4121.pdf

Kornher L, M Kalkuhl 2013 Food price volatility in developing countries and its determinants. Zentrum für Entwicklungsforschung, Universität Bonn http://ageconsearch.tind.io//bitstream/156132/2/B4-Kornher-Food_c.pdf

Laio F, L Ridolfi, P D'Odorico 2016 The past and future of food stocks. Environ. Res. Lett. 11:1748-9326.

Lynton-Evans J 1997 Strategic grain reserves - Guidelines for their establishment, management and operation. FAO Agricultural Services Bulletin N.126, FAO, Rome, Italy.

Marchand P, J A Carr, J Dell'Angelo, M Fader, J A Gephart, M Kummu, N R Magliocca, M Porkka, M J Puma, Z Ratajczak 2016 Reserves and trade jointly determine exposure to food supply shocks Environ. Res. Lett. 11:095009

Prakash A (Ed) 2011 Safeguarding food security in volatile global markets. FAO, Rome, Italy. http://www.fao.org/docrep/013/i2107e/i2107e25.pdf

Proctor D L (Ed) 1994 Grain storage techniques, evolution and trends in developing countries. FAO agricultural services bulletin N. 109. FAO and GASCA, Rome, Italy.

Rao N K, J Hanson, M E Dulloo, K Ghosh, D Nowell, M Larinde 2006 Manual of Seed Handling in Genebanks. Handbooks for Genebanks N. 8. Bioversity international with ILRI, FAO and CTA. Rome, Italy.

Redhum, http://www.redhum.org/mapas

Reliefweb, http://reliefweb.int/report/bangladesh/flash-flood-situation-april-09-2017

Sarris A Food Security Stocks and Emergency Reserves from a European Union CAP Perspective Vestnik of Saint-Peterburg University. Series 5 ECONOMICS Issue 1, 2015 pp. 37-68

Schmidhuber J 2015 Comparing and reconciling food consumption from household surveys and food balance sheets, FAO/Statistics Division. Beijing, AMIS workshop, July 2015

Seekell D, J Carr, J Dell'Angelo, P D'Odorico, M Fader, J Gephart, M Kummu, N Magliocca, M Porkka, M Puma 2017 Resilience in the global food system. Environ. Res. Lett. 12:025010

TelesurTV, http://www.telesurtv.net/english/news/Peru-Floods-Cause-US645-million-in-Agriculture-Losses-20170411-0002.html

UNOCHA, https://vosocc.unocha.org/GetFile.aspx?xml=4467tkwa_l1.html&tid=4467&laid=1; https://vosocc.unocha.org/GetFile.aspx?xml=4490wqeb_l1.html&tid=4490&laid=1

USDA 2017 World Agricultural Supply and Demand Estimates. https://www.usda.gov/oce/commodity/wasde/latest.pdf

Wikipedia, https://en.wikipedia.org/wiki/Cyclone_Enawo

Wild, S 2017 Invasive pest hits Africa: As hungry caterpillar eats its way through 12 countries, researchers begin to fight back. Nature 543:13-14

Wright B D 2012 International grain reserves and other instruments to address volatility in grain markets http://libcatalog.cimmyt.org/download/reprints/97072.pdf

Acknowledgments

This bulletin is produced by the CropWatch research team at the Institute of Remote Sensing and Digital Earth (RADI), at the Chinese Academy of Sciences in Beijing, China. The team gratefully acknowledges the active support of a range of organizations and individuals, both in China and elsewhere.

Financial and programmatic support is provided by the Ministry of Science and Technology of the People's Republic of China, National Natural Science Foundation of China, State Administration of Grain, and the Chinese Academy of Sciences. We specifically would like to acknowledge the financial support through China Grains Administration Special Fund for Public Interest, Grant No. 201313009-02, 201413003-7; The National Key Research and Development Program of China, Grant No:2016YFA0600300;National Natural Science Foundation, Grant No: 41561144013; the National High Technology Research and Development Program of China (863 program), Grant No. 2012AA12A307; and RADI funding in the form of the "Global Spatial Information System for Environment and Resources" project, Grant No: Y6SG0300CX.

The following contributions by national organizations and individuals are greatly appreciated: China Center for Resources Satellite Data and Application for providing the HJ-1 CCD data; China Meteorological Satellite Center for providing FY-2/3 data; China Meteorological Data Sharing Service System for providing the agro-meteorological data; and Chia Tai Group (China) for providing GVG (GPS, Video, and GIS) field sampling data.

The following contributions by international organizations and individuals are also recognized: François Kayitakire at FOODSEC/JRC for making available and allowing use of their crop masks; Ferdinando Urbano also at FOODSEC/JRC for his help with data; Herman Eerens, Dominique Haesen, and Antoine Royer at VITO, for providing the JRC/MARS SPIRITS software, Spot Vegetation imagery and growing season masks, together with generous advice; Patrizia Monteduro and Pasquale Steduto for providing technical details on GeoNetwork products; and IIASA and Steffen Fritz for their land use map.

Online resources

Online Resources posted on www.cropwatch.com.cn

This bulletin is only part of the CropWatch resources available. Visit www.cropwatch.com.cnfor access to additional resources, including the methods behind CropWatch, country profiles, and other CropWatch publications. For additional information or to access specific data or high-resolution graphs, simply contact the CropWatch team at cropwatch@radi.ac.cn.

CropWatch bulletins introduce the use of several new and experimental indicators. We would be very interested in receiving feedback about their performance in other countries. With feedback on the contents of this report and the applicability of the new indicators to global areas, please contact:

Professor Bingfang Wu
Institute of Remote Sensing and Digital Earth
Chinese Academy of Sciences, Beijing, China
E-mail: cropwatch@radi.ac.cn, wubf@radi.ac.cn